

MECHANISMS OF *VIBRIO CHOLERAE* ADAPTATION TO ZINC-STARVED
ENVIRONMENTS

A Dissertation

Presented to the Faculty of the Graduate School
of Cornell University

In Partial Fulfillment of the Requirements for the Degree of
Doctor of Philosophy

by

Shannon Grace Murphy

May 2021

© 2021 Shannon Grace Murphy

MECHANISMS OF *VIBRIO CHOLERAE* ADAPTATION TO ZINC-STARVED
ENVIRONMENTS

Shannon Grace Murphy

Cornell University 2021

Vibrio cholerae is the causative agent of cholera, a notorious diarrheal disease that is typically transmitted via contaminated drinking water. The current pandemic agent, the El Tor biotype, has undergone several genetic changes that include horizontal acquisition of two genomic islands. The VSP-II island is 26-kb of mystery; most of its contents are not expressed under standard laboratory conditions, suggesting that its induction requires an unknown signal from the host or environment. In this work, we identify zinc starvation as one such cue. Bacteria must acquire trace metal cofactors, like zinc, from their surrounding environment for protein folding and catalysis. When zinc is scarce, bacteria employ a set of genes known as the “zinc starvation response.” This regulon is transcriptionally repressed by Zur when zinc is abundant. Using a variety of molecular approaches — including transposon mutagenesis, RNA-seq, and *lacZ* transcriptional reporters — we show that VSP-II encodes several novel members of the zinc starvation response. These novel Zur targets include a cell wall hydrolase (ShyB) and a transcriptional activator (VerA). ShyB is one of *V. cholerae*’s numerous endopeptidases, which cleave peptide crosslinks within the cell wall sacculus to allow for elongation. ShyB is sufficient to sustain cell elongation during zinc starvation; however, it appears to overlap in function with other *V. cholerae* endopeptidases. Unlike

these other Zn²⁺-dependent endopeptidases, ShyB activity is uniquely resistance to metal chelators *in vitro*, suggesting it is well-adapted to metal-limited environments. The other Zur-regulated genes identified on VSP-II include a three gene operon encoding an AraC-family transcriptional activator. VerA induces expression of nearby chemotaxis receptor on VSP-II (AerB). AerB is a putative energy taxis receptor, which is predicted to sense cell metabolic status and relay a signal to chemotaxis proteins that effect flagellar rotation. We show that AerB causes *V. cholerae* cells to congregate in nutrient poor medium away from the air-liquid interface in an oxygen-dependent manner, suggesting it might enable *V. cholerae* to migrate towards more anoxic microenvironments. Collectively, we identify four Zur-regulated genes and one secondary target on VSP-II that are novel additions to the El Tor zinc starvation response. These data suggest that VSP-II may serve a role in a zinc-starved environment, such as within the human host or during colonization of chitinous surfaces in aquatic reservoirs.

BIOGRAPHICAL SKETCH

Shannon G. Murphy earned a Bachelor of Science in Biochemistry with Summa Cum Laude honors from the State University New York (SUNY) at Geneseo. During her undergraduate studies, her passion for scientific inquiry bloomed in an unconventional laboratory – the Audubon Community Nature Center in her hometown, Jamestown, NY. After interning as a nature educator and volunteering for ecology-based research programs, she sought a career advancing biological sciences through research and communication. She went on to conduct research in algal biofuels and plant genetics, which sparked her interest in microscopy and molecular biology. After graduating from SUNY Geneseo in 2016, she entered the microbiology Ph.D. program at Cornell University and joined the lab of Dr. Tobias Dörr. She initially set out to study cell wall homeostasis in the Gram-negative bacterium *Vibrio cholerae*; however, her project quickly expanded to include metal ion homeostasis and investigating the role of *V. cholerae*'s genomic islands. While at Cornell, Shannon engaged in scientific communication and outreach. In 2021, she was selected as New York State's Young Ambassador for the American Society of Microbiology. She is also a three-time fellow and the current President of Cornell's Graduate Student School Outreach Program, which teaches hands-on science lessons to K-12 students in the greater Ithaca Community. Shannon advanced to candidacy in 2018 and presents her work here in fulfillment of the degree of Doctor of Philosophy in microbiology.

I dedicate this work to my family.

To my dad, Kevin Murphy, for instilling the value of hard work.

To my mom, Laurie Murphy, for reminding me to take care of myself.

To my big sister, Elise Murphy, for always looking out for me.

To my partner, David Brunette, for his endless support and encouragement.

I owe you each more than I can express.

ACKNOWLEDGMENTS

“It takes a village.”

This work could not have been accomplished without the guidance and support of many scientific mentors, collaborators, and friends.

Thank you to my advisor, Dr. Tobi Dörr, for his immense support of all of my endeavors, both in and outside the laboratory. I am grateful to have worked alongside fellow graduate students Anna Weaver, Trevor Cross, Andy Murtha, Manuela Alvarado Obando, Kelly Rosch, and Megan Keller, along with my three very hardworking undergraduate mentees, Shuning Liu, Brianna Johnson, and Camille Ledoux.

Thank you to my committee members, Dr. Joshua Chappie and Dr. Ilana Brito, for guiding my graduate school experience. Thank you to my collaborators near and far: Myfanwy Adams and Dr. Chappie (Cornell University); Dr. Laura Alvarez and Dr. Felipe Cava (Umeå University, Sweden).

Thank you to the Cornell microbiology department and field, for its generosity with time, resources, and feedback. I would especially like to acknowledge labs of Dr. John Helmann, Dr. Dan Buckley, and Dr. Joe Peters for their assistance over the years. Thank you to the staff and community at the Weill Institute for Cell and Molecular Biology for their support.

Thank you to the funding sources that made this work possible: Cornell University, the Cornell Institute of Host-Microbe Interactions and Disease (CIHMID), and the NIH National Institute of General Medical Sciences (Award # R01GM130971 to TD).

TABLE OF CONTENTS

1. Introduction	1
a. <i>V. cholerae</i> is a notorious diarrheal pathogen	2
b. <i>V. cholerae</i> is an inhabitant of estuarine environments	4
c. <i>V. cholerae</i> is a potentially lethal pathogen in the host intestine	5
d. The seventh pandemic cholera agent acquired two large genomic islands	6
e. The Zur-regulated zinc starvation response	9
f. References	11
2. Endopeptidase Regulation as a Novel Function of the Zur-Dependent Zinc Starvation Response	20
a. <i>Published in mBio</i> Feb 2019, 10 (1) e02620-18	
b. Title and Abstract	21
c. Introduction	23
d. Results	26
e. Discussion	43
f. Experimental Procedures	46
g. References	54
h. Supplementary Data	60

3. <i>Vibrio cholerae</i> 's mysterious Seventh Pandemic island (VSP-II) encodes novel Zur-regulated zinc starvation genes involved in chemotaxis and cell congregation	70
a. Preprint on <i>Biorxiv</i> (doi: 10.1101/2021.03.09.434465)	
b. Title and Abstract	71
c. Introduction	73
d. Results	76
e. Discussion	100
f. Experimental Procedures	105
g. References	113
h. Supplementary Data	125
4. Concluding Remarks and Future Directions	141
a. Concluding Remarks	142
b. Future Directions	143

Chapter 1. Introduction

***V. CHOLERAE* IS A NOTORIOUS DIARRHEAL PATHOGEN**

Vibrio cholerae is the Gram-negative bacterium that causes the notorious diarrheal disease cholera (1). This bacterium is a native inhabitant of estuarine environments and a frequent colonizer of crustaceans and other biotic surfaces (2). *V. cholerae* enters the host via ingestion of contaminated seafood or drinking water, colonizes the small intestine, and secretes a potent diarrheal toxin (2). Cholera rapidly transmits when drinking water is contaminated with wastewater; thus, outbreaks tend to occur in regions where sanitation infrastructure is insufficient or damaged. Early scientific inquiries into cholera were foundational to modern epidemiology and infectious disease; however, despite its intensive study, *V. cholerae* still poses a major threat to global health. Cholera remains endemic in 69 countries, causes an estimated 1.4-2.3 million cases and 21,000-143,000 deaths annually, and is currently in its seventh pandemic wave (3).

The first six cholera pandemics (1817-1923) were caused by the “classical” O1 serovar of *V. cholerae* (4) (**Fig. 1**), but it wasn’t until the late 1800’s that a bacterium was correctly identified as the causative agent (5, 6). The idea that “miasma”, or foul air, caused illness was the predominant disease theory of the era, while the competing “germ theory” had not yet garnered widespread support. This paradigm began to shift in the mid-to-late 1800s with several cholera-related discoveries. A deadly cholera outbreak devastated London’s Soho district in 1854. In response, a physician named John Snow gathered resident data and generated a map that traced the source of the outbreak to a single, contaminated water pump (7, 8). The outbreak quelled soon after the pump handle was removed, and Snow’s detective work serves as a founding example

of modern epidemiological approaches to tracking disease. Snow suspected that a “germ” caused the cholera, but it was not until 1883 when Robert Koch isolated the bacterium from cholera patients that germ theory became more widely accepted (9). This comma shaped rod Vibriion described by Koch (and by Filippo Pacini in 1854) and tracked by John Snow was likely the “classical” O1 serovar.

Intriguingly, “classical” infections dwindled in the early 1900s and there was a brief period where cholera was no longer considered pandemic (**Fig. 1**). In the 1960s, however, a new O1 serovar known as “El Tor” emerged and initiated the ongoing seventh pandemic (10, 11). El Tor globally outcompeted the classical biotype, co-existing only in Bangladesh from 1963-1991 (12). El Tor harbors a number of distinguishing features that are suspected to confer a competitive advantage over other *V. cholerae* strains; however, the contribution of these features to pathogenicity and environmental persistence are incompletely understood. This chapter herein will review the environmental and pathogenic lifestyles of *V. cholerae* and focus on the unique and mysterious elements associated with the El Tor seventh pandemic agent.

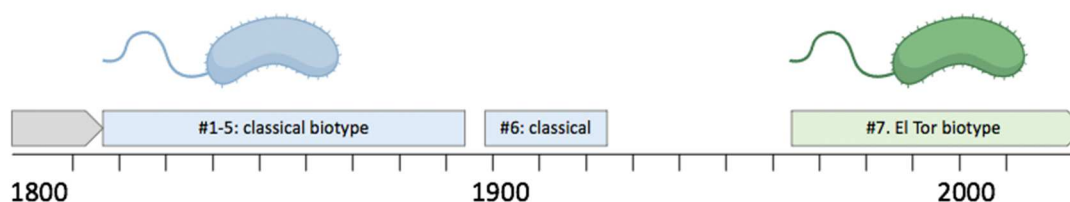


Figure 1. **Timeline of *V. cholerae* pandemics.** The first six pandemics from (1817-1923) were caused by the classical O1 serovar (blue). The seventh pandemic began in the 1960’s following the emergence of the El Tor biotype (green).

***V. CHOLERAE* IS AN INHABITANT OF ESTUARINE ENVIRONMENTS**

V. cholerae is a native resident of estuarine environments and can inhabit a wide range of water salinities (13). Planktonic *V. cholerae* cells are detected at low abundance within the water column (14) but these bacteria preferentially colonize biotic surfaces such as copepods and crustaceans (15), arthropods (16, 17), cyanobacteria (18, 19), shellfish (20), waterfowl (21), and fish (22). This surface attachment is mediated by the flagellum and a type IV pili (the mannose-sensitive hemagglutinin), while the formation of cell monolayers, microcolonies, or three-dimensional biofilms is mediated by exopolysaccharide synthesis (19). These cell-dense configurations, both within the human host and in environment reservoirs, offer protection against a variety of environmental insults (23). Colonization of chitinous exoskeletons provides additional benefits: chitin oligosaccharides serve as a carbon source and as well as a signaling molecule that regulates chitin uptake and catabolism (24-27), type VI secretion systems (28), and genetic competence programs (29). The latter enables *V. cholerae* to acquire naked DNA from its surroundings (30, 31). Importantly, biofilm formation induces a hyper-infectious state that primes *V. cholerae* to adapt to the human host (30).

***V. CHOLERAE* IS A POTENTIALLY LETHAL PATHOGEN IN THE HOST INTESTINE**

Of the more than 200 serovars of *V. cholerae* that exist in nature, only the O1 and O139 serovars are associated with cholera disease (22). Pathogenic varieties of *V. cholerae* acquired two key virulence factors -- the cholera toxin (CTX) and the toxin co-regulated attachment pilus (TCP) -- via bacteriophage infection. The cholera toxin is encoded by a lysogenic, filamentous phage CTX ϕ integrated within the *V. cholerae* chromosome (32-39). Toxin secretion leads to constitutive activation of the host adenylate cyclase. This increased cyclic AMP synthesis opens CFTR channels, driving water and salts from the intestinal epithelium and into the lumen (32). This toxin causes *V. cholerae*'s signature symptom: diarrhea with a rice-watery appearance (38). The other major virulence factor, TCP, is encoded on Vibrio pathogenicity island 1 (VPI-1) acquired via a filamentous phage (40). TCP facilitates small intestine colonization in both animal models and human volunteers (29). More specifically, this pili mediates attachment to the intestinal epithelial cells (41), aids in microcolony formation (42), and its matrices protect *V. cholerae* from host bile (43, 44). The TCP additionally functions as a receptor for the CTX phage (45). Both CTX and TCP are components of the toxR regulon and versions of these virulence factors are present in both the "classical" and "El Tor" biotypes (30).

THE SEVENTH PANDEMIC CHOLERA AGENT ACQUIRED TWO LARGE GENOMIC ISLANDS

The El Tor biotype arose from a non-pathogenic pre-cursor via acquisition of TCP and CTX virulence factors (46-63) and largely outcompeted its classical predecessor. Although both of these *V. cholerae* isolates are O1 serovars, they are considered biotypes due to number of distinguishing biochemical criteria (64); these include differences in hemolysis (65-68), hemagglutination, phage susceptibility, and resistance to polymyxin B (69-71). The Classical and El Tor biotypes are genetically very similar; however, a large portion of the genome (13.5%) is differentially expressed under virulence-inducing conditions (72). Nearly a fifth of this difference is explained by the *VieA* regulator that primarily alters expression of virulence factors, exopolysaccharide biosynthesis, and flagellum production in the classical biotype (73). Genomic comparisons identified two large genomic islands present in El Tor (74) that are referred to as the Vibrio Seventh Pandemic (VSP) islands -I and -II (75) (**Fig. 2**). VSP islands bare all the hallmarks of horizontal acquisition: below average G+C-content (VSP-I, 40%; VSP-II, 43%) relative to the rest of the genome (47%), presence of mobile genetic elements (e.g. integrases and transposases), and positioning between repeat sequences (76). Further, these islands retain the ability to excise into circular intermediates (77). It has long been suspected that these VSP islands confer El Tor a competitive edge over other biotypes (78).

The presence of VSP islands is strongly correlated with pandemicity; however, surprisingly little is known about their contents. Most efforts have focused on the role of VSP-I. This 16-kb island encompasses eleven open reading frames (*vc0175–vc0185*)

and appears to encode a conserved cyclic-oligonucleotide-based anti-phage signaling system (CBASS) (79). *dncV* (*vc0179*) encodes a dinucleotide cyclase that synthesizes 3'-cyclic GMP-AMP (cGAMP). This DncV-synthesized signaling molecule down-regulates chemotactic (chemical-sensing) motility and enhances intestinal colonization in a mouse-model (80). Other work has shown that cGAMP activates the nearby phospholipase CapV (encoded by *vc0178*), resulting in growth inhibition, degradation of cell membrane phospholipids, and possibly abortive replication to protect the bacterial population from phage infection. DcdV (encoded by *vc0175*) is a deoxycytidylate deaminase that corrupts cellular nucleotide concentrations and protects a naïve bacterial system against phage infection(81).

By comparison, even less is known about VSP-II. This 26-kb island encodes 30 ORFs (*vc0490-vc0516*) predicted to encode transcriptional regulators (*vc0497*, *vc0513*), ribonuclease H (*vc0498*), type IV pilin (*vc0502*), a cell wall endopeptidase (*vc0503*), a DNA repair protein (*vc0510*), methyl-accepting chemotaxis proteins (*vc0512*, *vc0514*), and a cyclic di-GMP phosphodiesterase (*vc0515*) (82). Prior to this work, only the excision-mediating integrase encoded by *vc0516* was characterized (78, 83, 84). It is unclear if (or how) El Tor's VSP-II contents contribute to pathogenicity or environmental persistence.

The primary barrier to investigating the role of VSP-II is a lack of knowledge about the stimuli that favor expression of its contents. Transcriptomic analyses have shown that *V. cholerae* grown under standard laboratory conditions (LB medium) exhibit little to no expression of VSP-II encoded genes (85). VSP-II contents may be transcriptionally regulated and only induced in response to a particular set of host or

environmental variables that necessitate their function. The work described here identifies a signal that induces a substantial portion of the VSP-II island: zinc starvation.

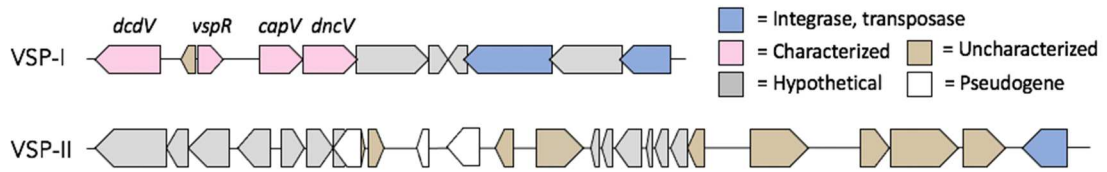


Figure 2. Most genes on the Vibrio Seventh Pandemic (VSP) -I and -II islands encode hypothetical or uncharacterized proteins. The VSP-I island spans *vc0175*–*vc0185* and the VSP-II island spans *vc0490*–*vc0516*. Open reading frames encoding integrases or transposases (blue), characterized proteins (pink), uncharacterized proteins (beige), hypothetical proteins (gray), pseudogenes (white), and are indicated.

THE ZUR-REGULATED ZINC STARVATION RESPONSE

We have found that segments of the VSP-II island are induced as part of the zinc starvation response. Divalent cation zinc, and other transition metals, are required in trace amounts as structural ligands and enzymatic cofactors. These metal ions must be acquired from the bacterium's environment and may be in limited supply. For example, bacteria growing in cell-dense communities (e.g. within a biofilm) experience metal deficiency (86). Metals are also a limiting micronutrient within the host, since many vertebrates sequester desirable metal cofactors within their tissues to restrict the growth of potentially harmful bacteria (i.e., nutritional immunity, (80, 83)). For this reason, mutations to zinc uptake systems in various pathogens – including *V. cholerae* (83) – resulted in colonization defects *in vivo* (80), possibly because these mutants are unable to effectively compete against the microbiota for sparse metal cofactors (79, 81).

Bacteria encode a variety of adaptations to cope with zinc limitation. These adaptations are collectively referred to as the “zinc starvation response” and they comprise a regulon controlled by the zinc uptake regulator, Zur (19, 82, 87, 88). Zur is a Fur-family transcriptional repressor that senses zinc availability (24-27). When zinc is abundant, a Zur-Zn complex binds with high affinity to conserved promoter sequences (**Fig. 3**). These so called “Zur boxes” contain an AT-rich inverted repeat sequence and typically overlap key promoter elements, such as the minus 35 region (29, 89-96). Thus, Zur represses transcription of downstream genes when zinc ions are abundant.

In low zinc environments, the Zur-Zn complex dissociates and the full Zur regulon is expressed (**Fig. 3**). These Zur targets typically encode (1) zinc acquisition

systems and (2) non-zinc binding protein alternatives that maintain cellular functions (97). *V. cholerae*'s Zur regulon, for example, encodes two zinc importers (ZnuABC and ZrgABCDE) (23) and two non-zinc binding ribosomal proteins (rpmE2, rpmJ2) (29). The full regulon has not been comprehensively studied through transcriptomics as in other bacteria (98). In this work, we use a variety of molecular approaches to characterize the Zur regulon in the *V. cholerae* El Tor strain, which we expand to include several VSP-II genes involved in cell wall homeostasis (in Chapter 2) and chemotaxis regulation (in Chapter 3).

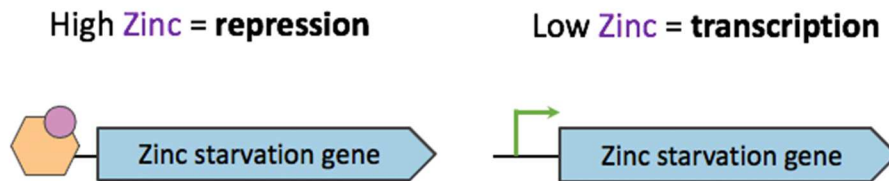


Figure 3. Zur-regulated zinc starvation response. Zur (orange) forms a complex with zinc (purple) and binds with high affinity to conserved promoter sequences, thereby repressing transcription of downstream genes (blue). Zur dissociates from the promoter in low zinc environments, thereby allowing transcription of zinc starvation response genes.

REFERENCES

1. **Harris JB, LaRocque RC, Qadri F, Ryan ET, Calderwood SB.** 2012. Cholera. *The Lancet* **379**:2466–2476.
2. **Reidl J, Klose KE.** 2002. *Vibrio cholerae* and cholera: out of the water and into the host. *FEMS Microbiol Rev* **26**:125–139.
3. **Ali M, Nelson AR, Lopez AL, Sack DA.** 2015. Updated Global Burden of Cholera in Endemic Countries. *PLOS Neglected Tropical Diseases* **9**:e0003832.
4. **Siddique AK, Cash R.** 2013. Cholera Outbreaks in the Classical Biotype Era, pp. 1–16. *In Cholera Outbreaks*. Springer, Berlin, Heidelberg, Berlin.
5. **Purdy AE, Watnick PI.** 2011. Spatially selective colonization of the arthropod intestine through activation of *Vibrio cholerae* biofilm formation. *Proc Natl Acad Sci USA* **108**:19737–19742.
6. **Broza M, Halpern M.** 2001. Chironomid egg masses and *Vibrio cholerae*. *Nature* **412**:40–40.
7. **DePAOLA A.** 1981. *Vibrio cholerae* in Marine Foods and Environmental Waters: A Literature Review. *Journal of Food Science* **46**:66–70.
8. **Kaysner CA, Hill WE.** 1994. *Vibrio cholerae and Cholera: Molecular to Global Perspectives*. John Wiley & Sons, Ltd, Washington, DC, USA.
9. **Chatterjee SN, Chaudhuri K.** 2003. Lipopolysaccharides of *Vibrio cholerae*: I. Physical and chemical characterization. *Biochimica et Biophysica Acta (BBA) - Molecular Basis of Disease* **1639**:65–79.
10. **Thelin KH, Taylor RK.** 1996. Toxin-coregulated pilus, but not mannose-sensitive hemagglutinin, is required for colonization by *Vibrio cholerae* O1 El Tor biotype and O139 strains. *Infection and Immunity* **64**:2853–2856.
11. **Krebs SJ, Taylor RK.** 2011. Protection and Attachment of *Vibrio cholerae* Mediated by the Toxin-Coregulated Pilus in the Infant Mouse Model. *Journal of Bacteriology* **193**:5260–5270.
12. **Sanchez J, Holmgren J.** 2008. Cholera toxin structure, gene regulation and pathophysiological and immunological aspects. *Cell Mol Life Sci* **65**:1347–1360.
13. **Rivera-Chávez F, Mekalanos JJ.** 2019. Cholera toxin promotes pathogen acquisition of host-derived nutrients. *Nature* **572**:244–248.

14. **Hu D, Liu B, Feng L, Ding P, Guo X, Wang M, Cao B, Reeves PR, Wang L.** 2016. Origins of the current seventh cholera pandemic. *Proc Natl Acad Sci USA* **113**:E7730–E7739.
15. **Son MS, Megli CJ, Kovacikova G, Qadri F, Taylor RK.** 2011. Characterization of *Vibrio cholerae* O1 El Tor biotype variant clinical isolates from Bangladesh and Haiti, including a molecular genetic analysis of virulence genes. *J Clin Microbiol* **49**:3739–3749.
16. **Henderson JC, Herrera CM, Trent MS.** 2017. AlmG, responsible for polymyxin resistance in pandemic *Vibrio cholerae*, is a glycytransferase distantly related to lipid A late acyltransferases. *J Biol Chem* **292**:21205–21215.
17. **Hankins JV, Madsen JA, Giles DK, Brodbelt JS, Trent MS.** 2012. Amino acid addition to *Vibrio cholerae* LPS establishes a link between surface remodeling in Gram-positive and Gram-negative bacteria. *Proc Natl Acad Sci USA* **109**:8722–8727.
18. **Dziejman M, Balon E, Boyd D, Fraser CM, Heidelberg JF, Mekalanos JJ.** 2002. Comparative genomic analysis of *Vibrio cholerae*: Genes that correlate with cholera endemic and pandemic disease. *Proc Natl Acad Sci USA* **99**:1556–1561.
19. **O'Shea YA, Finnan S, Reen JF, Morrissey JP, OGara F, Boyd EF.** 2004. The *Vibrio* seventh pandemic island-II is a 26.9 kb genomic island present in *Vibrio cholerae* El Tor and O139 serogroup isolates that shows homology to a 43.4 kb genomic island in *V. vulnificus*. *Microbiology* **150**:4053–4063.
20. **Davies BW, Bogard RW, Young TS, Mekalanos JJ.** 2012. Coordinated Regulation of Accessory Genetic Elements Produces Cyclic Di-Nucleotides for *V. cholerae* Virulence. *Cell* **149**:358–370.
21. **Murphy RA, Boyd EF.** 2008. Three Pathogenicity Islands of *Vibrio cholerae* Can Excise from the Chromosome and Form Circular Intermediates. *Journal of Bacteriology* **190**:636–647.
22. **Murphy SG, Alvarez L, Adams MC, Liu S, Chappie JS, Cava F, Dörr T.** 2019. Endopeptidase Regulation as a Novel Function of the Zur-Dependent Zinc Starvation Response. *mBio* **10**:e02620–18.
23. **Mandlik A, Livny J, Robins WP, Ritchie JM, Mekalanos JJ, Waldor MK.** 2011. RNA-Seq-Based Monitoring of Infection-Linked Changes in *Vibrio cholerae* Gene Expression. *Cell Host & Microbe* **10**:165–174.
24. **Palmer LD, Skaar EP.** 2016. Transition Metals and Virulence in Bacteria. *Annu Rev Genet* **50**:67–91.

25. **Kehl-Fie TE, Skaar EP.** 2010. Nutritional immunity beyond iron: a role for manganese and zinc. *Current Opinion in Chemical Biology* **14**:218–224.
26. **Hood MI, Skaar EP.** 2012. Nutritional immunity: transition metals at the pathogen–host interface. *Nat Rev Microbiol* **10**:525–537.
27. **Hennigar SR, McClung JP.** 2016. Nutritional Immunity: Starving Pathogens of Trace Minerals. *American Journal of Lifestyle Medicine* **10**:170–173.
28. **Meibom KL, Li XB, Nielsen AT, Wu C-Y, Roseman S, Schoolnik GK.** 2004. The *Vibrio cholerae* chitin utilization program. *Proc Natl Acad Sci USA* **101**:2524–2529.
29. **Sheng Y, Fan F, Jensen O, Zhong Z, Kan B, Wang H, Zhu J.** 2015. Dual Zinc Transporter Systems in *Vibrio cholerae* Promote Competitive Advantages over Gut Microbiome. *Infection and Immunity* **83**:3902–3908.
30. **Novichkov PS, Kazakov AE, Ravcheev DA, Leyn SA, Kovaleva GY, Sutormin RA, Kazanov MD, Riehl W, Arkin AP, Dubchak I, Rodionov DA.** 2013. RegPrecise 3.0 – A resource for genome-scale exploration of transcriptional regulation in bacteria. *BMC Genomics* **14**:745.
31. **Panina EM, Mironov AA, Gelfand MS.** 2011. Comparative genomics of bacterial zinc regulons: Enhanced ion transport, pathogenesis, and rearrangement of ribosomal proteins. *Proc Natl Acad Sci USA* **100**:9912–9917.
32. **Jemielita M, Wingreen NS, Bassler BL.** 2018. Quorum sensing controls *Vibrio cholerae* multicellular aggregate formation. *eLife* **7**:e1002210.
33. **Taylor RK, Miller VL, Furlong DB, Mekalanos JJ.** 1987. Use of *phoA* gene fusions to identify a pilus colonization factor coordinately regulated with cholera toxin. *Proc Natl Acad Sci USA* **84**:2833–2837.
34. **Sun D, Lafferty MJ, Peek JA, Taylor RK.** 1997. Domains within the *Vibrio cholerae* toxin coregulated pilin subunit that mediate bacterial colonization. *Gene* **192**:79–85.
35. **Kirn TJ, Lafferty MJ, Sandoe CMP, Taylor RK.** 2000. Delineation of pilin domains required for bacterial association into microcolonies and intestinal colonization by *Vibrio cholerae*. *Molecular Microbiology* **35**:896–910.
36. **Adams DW, Stutzmann S, Stoudmann C, Blokesch M.** 2019. DNA-uptake pili of *Vibrio cholerae* are required for chitin colonization and capable of kin recognition via sequence-specific self-interaction **4**:1545–1557.
37. **Trunk T, Khalil HS, Leo JC.** 2018. Bacterial autoaggregation. *AIMS Microbiology* **4**:140–164.

38. **Perez-Soto N, Creese O, Fernandez-Trillo F, Krachler A-M.** 2018. Aggregation of *Vibrio cholerae* by Cationic Polymers Enhances Quorum Sensing but Overrides Biofilm Dissipation in Response to Autoinduction. *ACS Chemical Biology* **13**:3021–3029.
39. **Zamorano-Sánchez D, Xian W, Lee CK, Salinas M, Thongsomboon W, Cegelski L, Wong GCL, Yildiz FH.** 2019. Functional Specialization in *Vibrio cholerae* Diguanylate Cyclases: Distinct Modes of Motility Suppression and c-di-GMP Production. *mBio* **10**.
40. **Struempfer AW.** 2002. Adsorption characteristics of silver, lead, cadmium, zinc, and nickel on borosilicate glass, polyethylene, and polypropylene container surfaces. *Anal Chem* **45**:2251–2254.
41. **O'Toole GA, Pratt LA, Watnick PI, Newman DK, Weaver VB, Kolter R.** 1999. Genetic approaches to study of biofilms. *Methods Enzymol* **310**:91–109.
42. **Nakao R, Ramstedt M, Wai SN, Uhlin BE.** 2012. Enhanced Biofilm Formation by *Escherichia coli* LPS Mutants Defective in Hep Biosynthesis. *PLOS ONE* **7**:e51241.
43. **Heidelberg JF, Eisen JA, Nelson WC, Clayton RA, Gwinn ML, Dodson RJ, Haft DH, Hickey EK, Peterson JD, Umayam L, Gill SR, Nelson KE, Read TD, Tettelin H, Richardson D, Ermolaeva MD, Vamathevan J, Bass S, Qin H, Dragoi I, Sellers P, McDonald L, Utterback T, Fleischmann RD, Nierman WC, White O, Salzberg SL, Smith HO, Colwell RR, Mekalanos JJ, Venter JC, Fraser CM.** 2000. DNA sequence of both chromosomes of the cholera pathogen *Vibrio cholerae*. *Nature* **406**:477–483.
44. **Joelsson A, Liu Z, Zhu J.** 2006. Genetic and Phenotypic Diversity of Quorum-Sensing Systems in Clinical and Environmental Isolates of *Vibrio cholerae*. *Infection and Immunity* **74**:1141–1147.
45. **Stutzmann S, Blokesch M, D'Orazio SEF.** 2016. Circulation of a Quorum-Sensing-Impaired Variant of *Vibrio cholerae* Strain C6706 Masks Important Phenotypes. *mSphere* **1**:e00098–16.
46. **Hensley MP, Gunasekera TS, Easton JA, Sigdel TK, Sugarbaker SA, Klingbeil L, Breece RM, Tierney DL, Crowder MW.** 2012. Characterization of Zn(II)-responsive ribosomal proteins YkgM and L31 in *E. coli*. *Journal of Inorganic Biochemistry* **111**:164–172.
47. **Sigdel TK, Easton JA, Crowder MW.** 2006. Transcriptional response of *Escherichia coli* to TPEN. *Journal of Bacteriology* **188**:6709–6713.
48. **Kallifidas D, Ben Pascoe, Owen GA, Strain-Damerell CM, Hong H-J, Paget MSB.** 2010. The Zinc-Responsive Regulator Zur Controls Expression of

- the Coelibactin Gene Cluster in *Streptomyces coelicolor*. *Journal of Bacteriology* **192**:608–611.
49. **Gaballa A, Wang T, Ye RW, Helmann JD.** 2002. Functional analysis of the *Bacillus subtilis* Zur regulon. *Journal of Bacteriology* **184**:6508–6514.
 50. **Büttof L, Schmidt-Vogler C, Herzberg M, Große C, Nies DH, DiRita VJ.** 2017. The Components of the Unique Zur Regulon of *Cupriavidus metallidurans* Mediate Cytoplasmic Zinc Handling. *Journal of Bacteriology* **199**:e00372–17.
 51. **Pawlik M-C, Hubert K, Joseph B, Claus H, Schoen C, Vogel U.** 2012. The zinc-responsive regulon of *Neisseria meningitidis* comprises seventeen genes under control of a Zur element. *Journal of Bacteriology* **194**:6594–6603.
 52. **Neupane DP, Jacquez B, Sundararajan A, Ramaraj T, Schilkey FD, Yukl ET.** 2017. Zinc-Dependent Transcriptional Regulation in *Paracoccus denitrificans*. *Front Microbiol* **8**:123.
 53. **Mazzon RR, Braz VS, da Silva Neto JF, do Valle Marques M.** 2014. Analysis of the *Caulobacter crescentus* Zur regulon reveals novel insights in zinc acquisition by TonB-dependent outer membrane proteins. *BMC Genomics* **15**:1–14.
 54. **Moreau GB, Qin A, Mann BJ, Stock AM.** 2018. Zinc Acquisition Mechanisms Differ between Environmental and Virulent *Francisella* Species. *Journal of Bacteriology* **200**:e00587–17.
 55. **Mortensen BL, Rathi S, Chazin WJ, Skaar EP.** 2014. *Acinetobacter baumannii* Response to Host-Mediated Zinc Limitation Requires the Transcriptional Regulator Zur. *Journal of Bacteriology* **196**:2616–2626.
 56. **Li Y, Qiu Y, Gao H, Guo Z, Han Y, Song Y, Du Z, Wang X, Zhou D, Yang R.** 2009. Characterization of Zur-dependent genes and direct Zur targets in *Yersinia pestis*. *BMC Microbiol* **9**:1–13.
 57. **Lim CK, Hassan KA, Penesyan A, Loper JE, Paulsen IT.** 2013. The effect of zinc limitation on the transcriptome of *Pseudomonas protegens* Pf-5. *Environmental Microbiology* **15**:702–715.
 58. **Pederick VG, Eijkelkamp BA, Begg SL, Ween MP, McAllister LJ, Paton JC, McDevitt CA.** 2015. ZnuA and zinc homeostasis in *Pseudomonas aeruginosa*. *Scientific Reports* 2015 **5**:1–14.
 59. **Mastropasqua MC, D'Orazio M, Cerasi M, Pacello F, Gismondi A, Canini A, Canuti L, Consalvo A, Ciavardelli D, Chirullo B, Pasquali P, Battistoni A.** 2017. Growth of *Pseudomonas aeruginosa* in zinc poor environments is

- promoted by a nicotianamine-related metallophore. *Molecular Microbiology* **106**:543–561.
60. **Latorre M, Low M, Gárate E, Reyes-Jara A, Murray BE, Cambiazo V, González M.** 2015. Interplay between copper and zinc homeostasis through the transcriptional regulator Zur in *Enterococcus faecalis*. *Metallomics* **7**:1137–1145.
 61. **Schröder J, Jochmann N, Rodionov DA, Tauch A.** 2010. The Zur regulon of *Corynebacterium glutamicum* ATCC 13032. *BMC Genomics* **11**:1–18.
 62. **Eckelt E, Jarek M, Frömke C, Meens J, Goethe R.** 2014. Identification of a lineage specific zinc responsive genomic island in *Mycobacterium avium* ssp. paratuberculosis. *BMC Genomics* **15**:1–15.
 63. **Owen GA, Pascoe B, Kallifidas D, Paget MSB.** 2007. Zinc-responsive regulation of alternative ribosomal protein genes in *Streptomyces coelicolor* involves *zur* and *sigmaR*. *Journal of Bacteriology* **189**:4078–4086.
 64. **Fong JCN, Syed KA, Klose KE, Yildiz FH.** 2010. Role of *Vibrio* polysaccharide (*vps*) genes in VPS production, biofilm formation and *Vibrio cholerae* pathogenesis. *Microbiology* **156**:2757–2769.
 65. **DiRita VJ.** 1992. Co-ordinate expression of virulence genes by ToxR in *Vibrio cholerae*. *Molecular Microbiology* **6**:451–458.
 66. **DiRita VJ, Parsot C, Jander G, Mekalanos JJ.** 1991. Regulatory cascade controls virulence in *Vibrio cholerae*. *Proc Natl Acad Sci USA* **88**:5403–5407.
 67. **Higgins DE, Nazareno E, DiRita VJ.** 1992. The virulence gene activator ToxT from *Vibrio cholerae* is a member of the AraC family of transcriptional activators. *Journal of Bacteriology* **174**:6974–6980.
 68. **Weber GG, Klose KE.** 2011. The complexity of ToxT-dependent transcription in *Vibrio cholerae*. *The Indian Journal of Medical Research* **133**:201–206.
 69. **Metzger LC, Blokesch M.** 2016. Regulation of competence-mediated horizontal gene transfer in the natural habitat of *Vibrio cholerae*. *Current Opinion in Microbiology* **30**:1–7.
 70. **Yamamoto S, Mitobe J, Ishikawa T, Wai SN, Ohnishi M, Watanabe H, Izumiya H.** 2014. Regulation of natural competence by the orphan two-component system sensor kinase ChiS involves a non-canonical transmembrane regulator in *Vibrio cholerae*. *Molecular Microbiology* **91**:326–347.

71. **Dalia AB, Lazinski DW, Camilli A.** 2014. Identification of a membrane-bound transcriptional regulator that links chitin and natural competence in *Vibrio cholerae*. *mBio* **5**:e01028–13.
72. **Ud-Din AIMS, Roujeinikova A.** 2017. Methyl-accepting chemotaxis proteins: a core sensing element in prokaryotes and archaea. *Cell Mol Life Sci* **74**:3293–3303.
73. **Ringgaard S, Yang W, Alvarado A, Schirner K, Briegel A, DiRita VJ.** 2018. Chemotaxis Arrays in *Vibrio* Species and Their Intracellular Positioning by the ParC/ParP System. *Journal of Bacteriology* **200**:267–17.
74. **Alexander RP, Zhulin IB.** 2007. Evolutionary genomics reveals conserved structural determinants of signaling and adaptation in microbial chemoreceptors. *Proc Natl Acad Sci USA* **104**:2885–2890.
75. **Matthew D Coleman, Randal B Bass, Ryan S Mehan A, Falke JJ.** 2005. Conserved Glycine Residues in the Cytoplasmic Domain of the Aspartate Receptor Play Essential Roles in Kinase Coupling and On–Off Switching. *Biochemistry* **44**:7687–7695.
76. **Boin MA, Austin MJ, Häse CC.** 2004. Chemotaxis in *Vibrio cholerae*. *FEMS Microbiology Letters* **239**:1–8.
77. **Kanehisa M, Goto S, Kawashima S, Okuno Y, Hattori M.** 2004. The KEGG resource for deciphering the genome. *Nucleic Acids Res* **32**:D277–D280.
78. **Taylor BL.** 2007. Aer on the inside looking out: paradigm for a PAS–HAMP role in sensing oxygen, redox and energy. *Molecular Microbiology* **65**:1415–1424.
79. **Cohen D, Melamed S, Millman A, Shulman G, Oppenheimer-Shaanan Y, Kacen A, Doron S, Amitai G, Sorek R.** 2019. Cyclic GMP–AMP signalling protects bacteria against viral infection. *Nature* **574**:691–695.
80. **Boin MA, Häse CC.** 2007. Characterization of *Vibrio cholerae* aerotaxis. *FEMS Microbiology Letters* **276**:193–201.
81. **Severin GB, Hsueh BY, Elg CA, Dover JA, Rhoades CR, Wessel AJ, Ridenhour BJ, Top EM, Ravi J, Parent KN, Waters CM.** 2021. A Broadly Conserved Deoxycytidine Deaminase Protects Bacteria from Phage Infection. *bioRxiv* 2021.03.31.437871.
82. **Taviani E, Grim CJ, Choi J, Chun J, Haley BJ, Hasan NA, Hug A, Colwell RR.** 2010. Discovery of novel *Vibrio cholerae* VSP-II genomic islands using comparative genomic analysis. *FEMS Microbiology Letters* **308**:130–137.

83. **Bibikov SI, Biran R, Rudd KE, Parkinson JS.** 1997. A signal transducer for aerotaxis in *Escherichia coli*. *Journal of Bacteriology* **179**:4075–4079.
84. **Bibikov SI, Barnes LA, Gitin Y, Parkinson JS.** 2000. Domain organization and flavin adenine dinucleotide-binding determinants in the aerotaxis signal transducer Aer of *Escherichia coli*. *Proc Natl Acad Sci USA* **97**:5830–5835.
85. **Xie Z, Ulrich LE, Zhulin IB, Alexandre G.** 2010. PAS domain containing chemoreceptor couples dynamic changes in metabolism with chemotaxis. *Proc Natl Acad Sci USA* **107**:2235–2240.
86. **Harris HW, El-Naggar MY, Neilson KH.** 2012. *Shewanella oneidensis* MR-1 chemotaxis proteins and electron-transport chain components essential for congregation near insoluble electron acceptors. *Biochemical Society Transactions* **40**:1167–1177.
87. **Sakib SN, Reddi G, Almagro-Moreno S, DiRita VJ.** 2018. Environmental Role of Pathogenic Traits in *Vibrio cholerae*. *Journal of Bacteriology* **200**:2123–17.
88. **Pant A, Bag S, Saha B, Verma J, Kumar P, Banerjee S, Kumar B, Yashwant Kumar, Desigamani A, Suhrid Maiti, Tushar K Maiti, Sanjay K Banerjee, Rupak K Bhadra, Hemanta Koley, Dutta S, G Balakrish Nair, Ramamurthy T, Das B.** 2020. Molecular insights into the genome dynamics and interactions between core and acquired genomes of *Vibrio cholerae*. *Proc Natl Acad Sci USA* **117**:23762–23773.
89. **Davis LM, Kakuda T, DiRita VJ.** 2009. A *Campylobacter jejuni* *znuA* Orthologue Is Essential for Growth in Low-Zinc Environments and Chick Colonization. *Journal of Bacteriology* **191**:1631–1640.
90. **Ammendola S, Pasquali P, Pistoia C, Petrucci P, Petrarca P, Rotilio G, Battistoni A.** 2007. High-Affinity Zn²⁺ Uptake System ZnuABC Is Required for Bacterial Zinc Homeostasis in Intracellular Environments and Contributes to the Virulence of *Salmonella enterica*. *Infection and Immunity* **75**:5867–5876.
91. **Campoy S, Jara M, Busquets N, de Rozas AMP, Badiola I, Barbé J.** 2002. Role of the High-Affinity Zinc Uptake znuABC System in *Salmonella enterica* Serovar Typhimurium Virulence. *Infection and Immunity* **70**:4721–4725.
92. **Bobrov AG, Kirillina O, Fosso MY, Fetherston JD, Miller MC, VanCleave TT, Burlison JA, Arnold WK, Lawrenz MB, Garneau-Tsodikova S, Perry RD.** 2017. Zinc transporters YbtX and ZnuABC are required for the virulence of *Yersinia pestis* in bubonic and pneumonic plague in mice. *Metallomics* **9**:757–772.

93. **Nielubowicz GR, Smith SN, Mobley HLT.** 2010. Zinc uptake contributes to motility and provides a competitive advantage to *Proteus mirabilis* during experimental urinary tract infection. *Infection and Immunity* **78**:2823–2833.
94. **Sabri M, Houle S, Dozois CM.** 2009. Roles of the extraintestinal pathogenic *Escherichia coli* ZnuACB and ZupT zinc transporters during urinary tract infection. *Infection and Immunity* **77**:1155–1164.
95. **Corbett D, Wang J, Schuler S, Lopez-Castejon G, Glenn S, Brough D, Andrew PW, Cavet JS, Roberts IS, Bäumler AJ.** 2012. Two Zinc Uptake Systems Contribute to the Full Virulence of *Listeria monocytogenes* during Growth *In Vitro* and *In Vivo*. *Infection and Immunity* **80**:14–21.
96. **Hood MI, Mortensen BL, Moore JL, Zhang Y, Kehl-Fie TE, Sugitani N, Chazin WJ, Caprioli RM, Skaar EP.** 2012. Identification of an *Acinetobacter baumannii* Zinc Acquisition System that Facilitates Resistance to Calprotectin-mediated Zinc Sequestration. *PLoS Pathog* **8**:e1003068.
97. **Gielda LM, DiRita VJ.** 2012. Zinc competition among the intestinal microbiota. *mBio* **3**:e00171–12.
98. **Kamp HD, Patimalla-Dipali B, Lazinski DW, Wallace-Gadsden F, Camilli A.** 2013. Gene Fitness Landscapes of *Vibrio cholerae* at Important Stages of Its Life Cycle. *PLoS Pathog* **9**:e1003800.

Chapter 2. Endopeptidase regulation as a novel function of the Zur-dependent zinc
starvation response

Endopeptidase regulation as a novel function of the Zur-dependent zinc starvation response

Shannon G. Murphy^{1,2}, Laura Alvarez³, Myfanwy C. Adams⁴, Shuning Liu^{1,2}, Joshua S. Chappie⁴, Felipe Cava³, Tobias Dörr^{1,2}#

¹ Department of Microbiology, Cornell University, Ithaca, New York, USA.

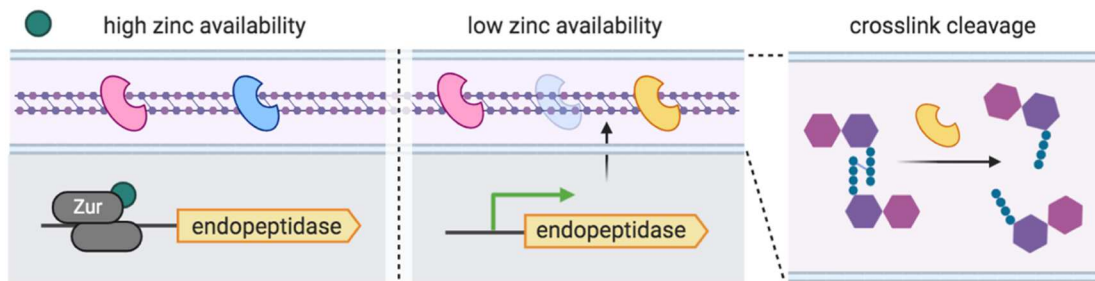
² Weill Institute for Cell and Molecular Biology, Cornell University, Ithaca, New York, USA.

³ Laboratory for Molecular Infection Medicine, Department of Molecular Biology, Umeå University, Umeå, Sweden.

⁴ Department of Molecular Medicine, College of Veterinary Medicine, Cornell University, Ithaca, NY, USA.

To whom correspondence should be addressed: Tobias Dörr, tdoerr@cornell.edu.

GRAPHICAL SUMMARY



ABSTRACT

The cell wall is a strong, yet flexible, meshwork of peptidoglycan (PG) that gives a bacterium structural integrity. To accommodate a growing cell, the wall is remodeled by both PG synthesis and degradation. *Vibrio cholerae* encodes a group of three nearly identical zinc-dependent endopeptidases (EPs) that are predicted to hydrolyze PG to facilitate cell growth. Two of these (ShyA and ShyC) are conditionally essential housekeeping EPs, while the third (ShyB) is not expressed under standard laboratory conditions. To investigate the role of ShyB, we conducted a transposon screen to identify mutations that activate *shyB* transcription. We found that *shyB* is induced as

part of the Zur-mediated zinc starvation response, a mode of regulation not previously reported for cell wall lytic enzymes. *In vivo*, ShyB alone was sufficient to sustain cell growth in low-zinc environments. *In vitro*, ShyB retained its D,D-endopeptidase activity against purified sacculi in the presence of the metal chelator EDTA at concentrations that inhibit ShyA and ShyC. This insensitivity to metal chelation is likely what enables ShyB to substitute for other EPs during zinc starvation. Our survey of transcriptomic data from diverse bacteria identified other candidate Zur-regulated EPs, suggesting that this adaptation to zinc starvation is employed by other Gram-negative bacteria.

IMPORTANCE

Bacteria encode a variety of adaptations that enable them to survive during zinc starvation, a condition which is encountered both in natural environments and inside the human host. In *Vibrio cholerae*, the causative agent of the diarrheal disease cholera, we have identified a novel member of this zinc starvation response: a cell wall hydrolase that retains function, and is conditionally essential for cell growth, in low-zinc environments. Other Gram-negative bacteria contain homologs that appear to be under similar regulatory control. These findings are significant because they represent, to our knowledge, the first evidence that zinc homeostasis influences cell wall turnover. Anti-infective therapies commonly target the bacterial cell wall and, therefore, an improved understanding of how the cell wall adapts to host-induced zinc starvation could lead to new antibiotic development. Such therapeutic interventions are required to combat the rising threat of drug resistant infections.

INTRODUCTION

The cell wall provides a bacterium with structural integrity and serves as a protective layer guarding against a wide range of environmental insults. Due to its importance for bacterial survival, the cell wall is a powerful and long-standing target for antibiotics (1). The wall is composed primarily of peptidoglycan (PG), a polymer of β -(1,4) linked N-acetylglucosamine (NAG) and N-acetylmuramic acid (NAM) sugar strands (2) (**Fig. 1A**). Adjacent PG strands are linked to each other via peptide side chains, enabling the PG to assemble into a meshlike structure called the sacculus (3). In Gram-negative bacteria, the sacculus is a single PG layer that is sandwiched between an inner and an outer membrane (4). This thin wall must be rigid enough to maintain cell shape and to contain high intracellular pressure (3, 5); however, the wall must also be flexible enough to accommodate cell elongation, cell division, and the insertion of *trans*-envelope protein complexes (6). This requirement for both rigidity and flexibility necessitates continuous remodeling of the cell wall, which is accomplished by a delicate interplay between PG synthesis and degradation. Inhibition or dysregulation of either process can cause growth cessation or cell lysis, rendering the mechanisms of cell wall turnover an attractive target for new antibiotic development (7, 8).

PG synthesis is mediated by Penicillin Binding Proteins (PBPs, the targets for beta-lactam antibiotics) and SEDS proteins (9). These proteins collectively catalyze cell wall synthesis through two main reactions: glycosyltransfer (GT) to add new PG monomers to the glycan strand and transpeptidation (TP) to crosslink the peptides of adjacent strands (2). Cell wall turnover is mediated by “autolysins”, a collective term for diverse and often redundant enzymes (amidases, lytic transglycosylases and

endopeptidases) that are able to cleave PG at almost any chemical bond (6). Endopeptidases (EPs), for example, hydrolyze the peptide crosslinks that covalently link adjacent PG strands. EPs are crucial for cell elongation in several well-studied Gram-positive and Gram-negative rod-shaped bacteria (10-12), presumably because EPs create gaps in the PG meshwork to allow for the insertion of new cell wall material. Consistent with this proposed role, EP overexpression promotes aPBP activity in *Escherichia coli*, likely through the generation of initiation sites for PG synthesis (13).

While EPs are essential for growth, they are also main drivers of PG degradation after inhibition of PBPs (14, 15). Thus, EP activity must be tightly controlled under normal growth conditions. EPs in two divergent bacterial species (*E. coli* and *Pseudomonas aeruginosa*) are proteolytically degraded to adapt to conditions that require changes in PG cleavage activity (16, 17), such as the transition into stationary phase. In *Bacillus subtilis*, EP expression is regulated by growth-phase dependent sigma factors (18-21). However, it is not known how EP expression is modified in response to specific environmental stresses.

In this study, we investigate the genetic regulation of specialized EPs in *Vibrio cholerae*, the causative agent of the diarrheal disease cholera. *V. cholerae* encodes three nearly identical EPs that are homologous to the well-characterized D,D-endopeptidase MepM in *E. coli* (10). Each EP contains a LysM domain that likely binds PG (22) and a putatively Zn²⁺-dependent M23 catalytic domain that hydrolyzes peptide cross links (23) (**Fig. 1B**). We previously showed that two of these homologs (ShyA and ShyC) are housekeeping EPs that are collectively essential for *V. cholerae* growth (12). The gene encoding the third EP, *shyB*, is not transcribed under standard laboratory conditions (LB

medium) and thus little is known about its biological function. To elucidate the role of ShyB, we conducted a transposon screen to identify mutations that promote *shyB* expression in LB. We found that *shyB* is induced by zinc starvation and, unlike the other two M23 EPs, ShyB enzymatic activity is resistant to treatment with the metal chelator EDTA. These data suggest that ShyB acts as an alternative EP to ensure proper PG maintenance during zinc starvation. Importantly, this represents the first characterization of an autolysin that is controlled by Zur-mediated zinc homeostasis and provides insight into how other Gram-negative bacteria might alter EP activity in zinc-limited environments.

RESULTS

shyB is repressed in LB, but transcribed in minimal medium.

The hydrolytic activity of EPs needs to be carefully controlled to maintain cell wall integrity. We therefore considered it likely that specialized EPs are transcriptionally regulated and only induced when required. To test this hypothesis, we examined expression patterns of *V.cholerae*'s LysM/M23 endopeptidases using *lacZ* transcriptional fusions. We first compared promoter activity on LB and M9 agar, as our previous work had shown that a $\Delta shyB$ mutation exacerbates a $\Delta shyA$ growth defect in M9 minimal medium (12). The $P_{shyA}:lacZ$ and $P_{shyC}:lacZ$ reporters generated a blue colony color on both LB and M9 agar (**Fig. 1C**); thus, these promoters are actively transcribed in either media. Quantification of β -galactosidase (LacZ) activity in liquid culture showed that P_{shyA} transcription does not vary between LB and M9 media, whereas P_{shyC} promoter activity was slightly lower, yet still robust, in M9 minimal medium (**Fig. S1**). These data are consistent with ShyA and ShyC's role as the predominant growth-promoting EPs (12). In contrast, $P_{shyB}:lacZ$ yielded blue colonies and produced detectable levels of β -Galactosidase activity in M9 minimal medium only, indicating that the *shyB* promoter is induced in M9 but tightly repressed in LB (**Fig. 1C, Fig. S1**).

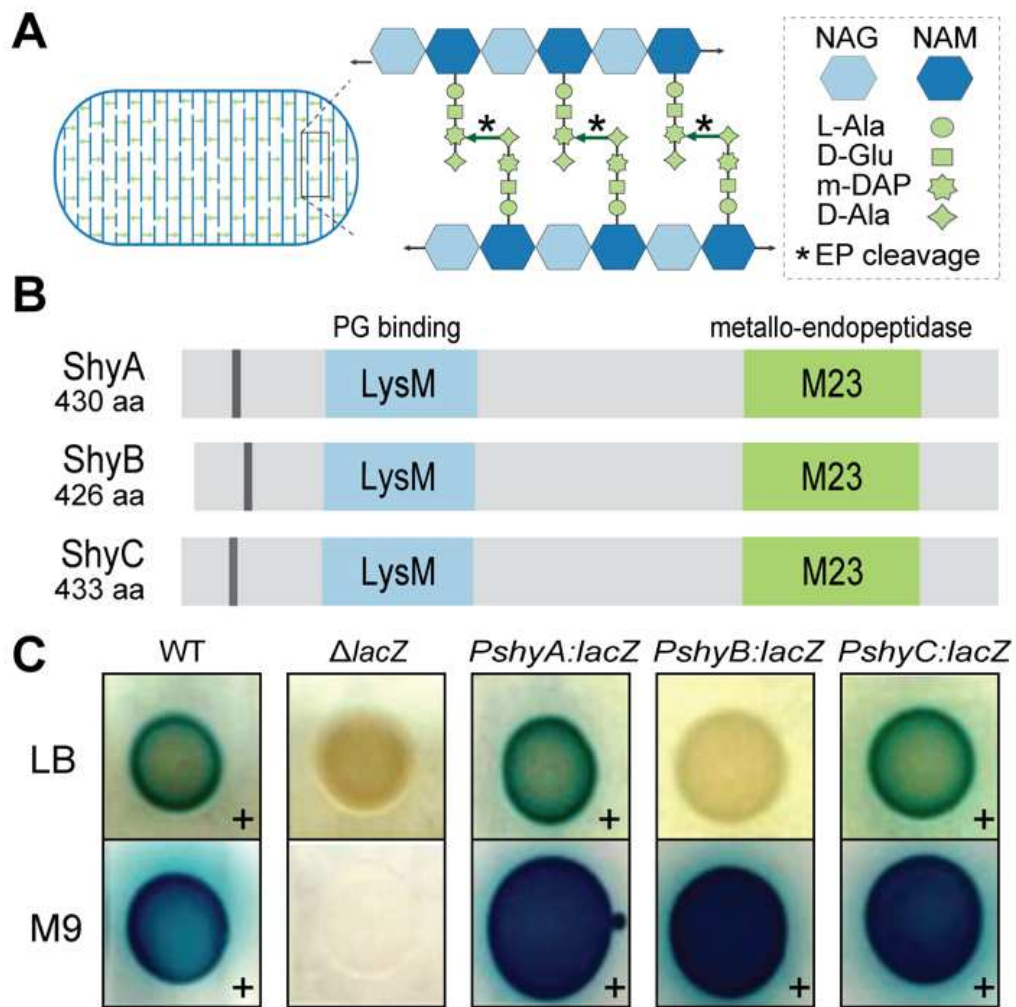


Figure 1. *shyB* encodes a LysM/M23 endopeptidase and is transcribed in minimal medium. (A) A model of the peptidoglycan sacculus, a polymer of β -(1,4) linked N-acetylglucosamine (NAG) and N-acetylmuramic acid (NAM) glycan strands (blue). Cross-linked peptides (green arrows) and endopeptidase cleavage sites (*) are shown. (B) The *V. cholerae* genome encodes three endopeptidases (ShyA, ShyB, ShyC) possessing a hydrophobic region (gray), a PG binding domain (LysM, blue), and metallo-endopeptidase domain (M23, green). Protein domains were annotated using UniProt (64). (C) Promoter:*lacZ* transcriptional reporters for each endopeptidase were spotted onto LB (top row) and M9 (bottom row) agar containing X-gal. A blue colony color (+) indicates that the promoter is actively transcribed. Wild-type (WT) and $\Delta lacZ$ strains are included as positive and negative controls, respectively.

***shyB* is induced by zinc starvation.**

To elucidate the specific growth conditions that favor *shyB* expression, we sought to identify the genetic factors regulating *shyB* transcription. To this end, we subjected the *shyB* transcriptional reporter strain to Himar1 mariner transposon mutagenesis and screened for *lacZ* induction (blue colonies) on LB agar. After two independent rounds of mutagenesis (50,000 total colonies), the screen yielded 26 blue-colored insertion mutants. These were divided into two distinct classes according to colony color: 12 dark blue and 14 light blue colonies. Strikingly, arbitrary PCR (24) mapped all 26 transposon insertions to only two chromosomal loci; both contained genes whose products play roles in zinc homeostasis: *vc2081-2083/znuABC* (light blue colonies) and *vc0378/zur* (dark blue colonies) (**Fig. 2A**). *znuABC* encodes *V. cholerae*'s high affinity zinc uptake system (25), while Zur is a Fur-family transcriptional regulator and the central repressor in the zinc starvation response (26). In zinc-rich conditions, Zur and its Zn²⁺ corepressor bind to promoters containing a “Zur box” and block transcription (27). In low-zinc conditions, Zur dissociates from promoters to induce the zinc starvation response (28). This response includes genes encoding zinc uptake systems (i.e. *znuABC*, *zrgABCDE*) (25) and zinc-independent paralogs that replace proteins that ordinarily require zinc for function (i.e. ribosomal proteins) (29).

To validate these transposon hits, we constructed clean deletions of *zur* and *znuA* in the P_{*shyB*}:*lacZ* reporter strain. Deletion of either gene resulted in activation of the *shyB* promoter, as indicated by blue colony color on LB agar (**Fig. S2 A**) or β-Galactosidase activity measured in LB broth (**Fig. 2B**). P_{*shyB*} repression was restored by expressing the deleted genes *in trans* (**Fig. S2 A; Fig. 2B**). Thus, *shyB* is induced under conditions that

are expected to either mimic (*zur* inactivation) or impose (*znuA(BC)* inactivation) zinc starvation.

If zinc starvation is the factor inducing *shyB* expression in M9, we would expect the $P_{shyB}:lacZ$ reporter to be repressed by external zinc addition. Indeed, supplementing M9 agar plates with 10 μ M of $ZnSO_4$ was sufficient to turn off the *shyB* promoter in a wild-type (WT) background (**Fig. 2C**), whereas repression could not be achieved by addition of other transition metals (iron and manganese) (**Fig. S2 B**). Zinc supplementation repressed the reporter in a $\Delta znuABC$ mutant, but not in a Δzur mutant (**Fig. 2C**). This suggests that the P_{shyB} activation in $\Delta znuABC$ is caused by zinc deficiency, while activation in Δzur is due to loss of zinc-sensing repression mechanism. To quantify the effect of zinc on *shyB* promoter activity, we grew the WT, Δzur , and $\Delta znuABC$ reporter strains in M9 supplemented with increasing concentrations of zinc and measured β -Galactosidase activity. As expected, $P_{shyB}:lacZ$ expression in WT and in $\Delta znuABC$ tapered off at higher zinc concentrations, whereas expression in Δzur was zinc-independent (**Fig. 2D**). These data demonstrate that *shyB* transcription is repressed by high zinc availability and that the repression mechanism requires Zur.

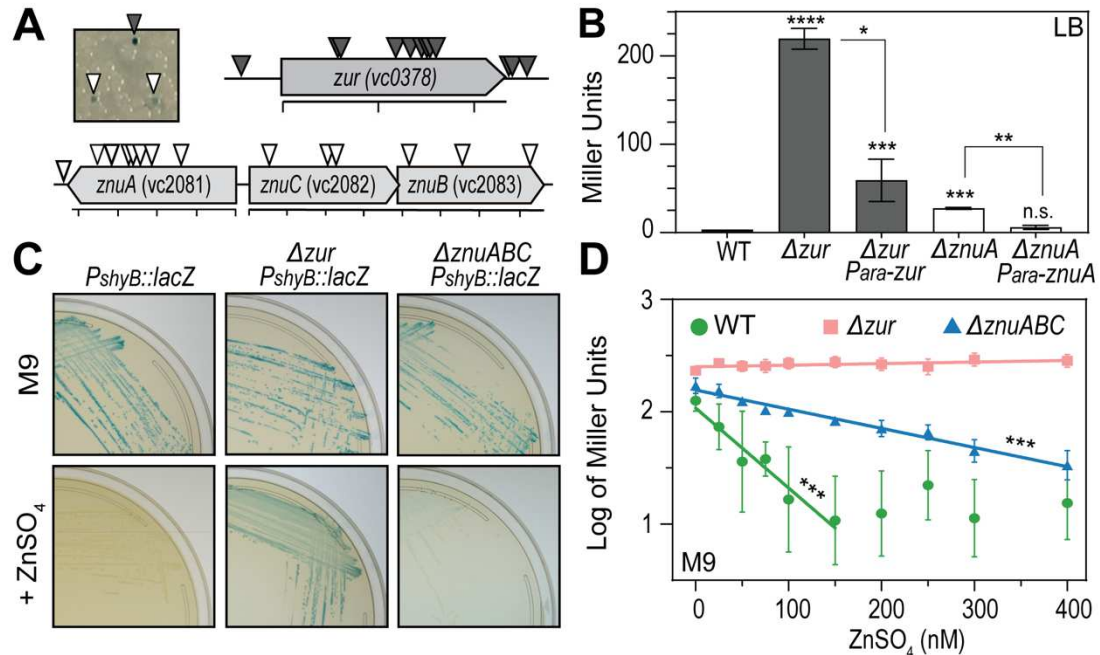


Figure 2. *shyB* transcription is regulated by zinc availability.

(A) The *shyB* transcriptional reporter (*lacZ::P_{shyB}::lacZ*) was mutagenized with a HimarI mariner transposon and screened for *P_{shyB}* induction (blue colonies) on LB agar containing X-gal and selective antibiotics (see Methods). Representative Tn mutants are shown. Insertion sites producing dark blue colonies (gray triangles) and light blue colonies (white triangles) were mapped using arbitrary PCR (scale bar = 200 bp increments). (B) *shyB* promoter activity was quantified using β -galactosidase assays (see Methods) in a WT, Δzur , and $\Delta znuA$ background. Each strain carries an arabinose-inducible plasmid (pBAD) that is either empty or complements the deleted gene *in trans*. Assays were conducted in LB containing chloramphenicol and arabinose (0.2%). Error bars represent the standard error of the mean (SEM) of three biological replicates. Statistical significance was measured using one-way analysis of variance (ANOVA) on natural log transformed data followed by Dunnett's multiple comparison test (****, $p < 0.0001$; ***, $p < 0.001$; **, $p < 0.01$; *, $p < 0.05$; n.s., $p > 0.05$). (C). The *shyB* transcriptional reporter in a WT, Δzur , or $\Delta znuABC$ background was grown on M9 X-gal agar without (top row) or with 10 μ M ZnSO₄ (bottom row). (D) β -galactosidase activity of the *P_{shyB}::lacZ* reporter in a WT, Δzur , or $\Delta znuABC$ background was measured in M9 minimal medium supplemented with increasing concentrations of ZnSO₄ (0 – 400 nM). Miller units were log transformed and plotted against exogenous zinc concentration (nM). The linear portions of the graph were fit with a regression line (WT, $R^2 = 0.95$; Δzur , $R^2 = 0.35$; $\Delta znuABC$ $R^2 = 0.98$) and asterisks indicate that slope of the regression is significantly non-zero. Error bars represent the standard error of the mean (SEM) of three biological replicates.

Zur directly binds the shyB promoter.

Given Zur's well-defined role as a zinc-sensing transcriptional regulator (27) and its requirement for P_{shyB} repression in zinc-rich media, we hypothesized that Zur directly binds the *shyB* promoter. To test this, we retrieved a Zur box sequence logo built from 62 known regulatory targets in the Vibrionaceae family (30, 31) and aligned it with the *shyB* promoter region. This alignment identified a highly conserved Zur box, which is characterized by an inverted, AT-rich repeat (**Fig. 3A**). We used 5'-RACE to locate the *shyB* transcriptional start site (+1, tss) and found that the putative Zur box overlaps both the -10 region and the tss. A bound Zur/Zn²⁺ complex at this position likely prevents RNA polymerase binding and thereby prevents transcription (32).

To determine if Zur binds the *shyB* promoter *in vitro*, we then incubated purified Zur with a labeled DNA probe encoding the P_{shyB} Zur box. Binding was assessed in the presence of ZnCl₂ using an electrophoretic mobility shift assay (EMSA). As evident by a band shift, Zur forms a complex with the P_{shyB} DNA *in vitro* (**Fig. 3B, Lanes 1-2**). To examine DNA binding specificity, a 100-fold molar excess of unlabeled specific (S) or non-specific (NS) competitor DNA was included in the binding reaction. The S competitor, which carries an identical sequence as the labeled probe, effectively sequestered Zur and increased the amount of unbound, labeled probe (**Lane 3**). Meanwhile, the NS competitor was ineffective at binding Zur (**Lane 4**). These data indicate that the *shyB* promoter contains an authentic Zur box and we conclude that *shyB* is a novel member of the Zur regulon.

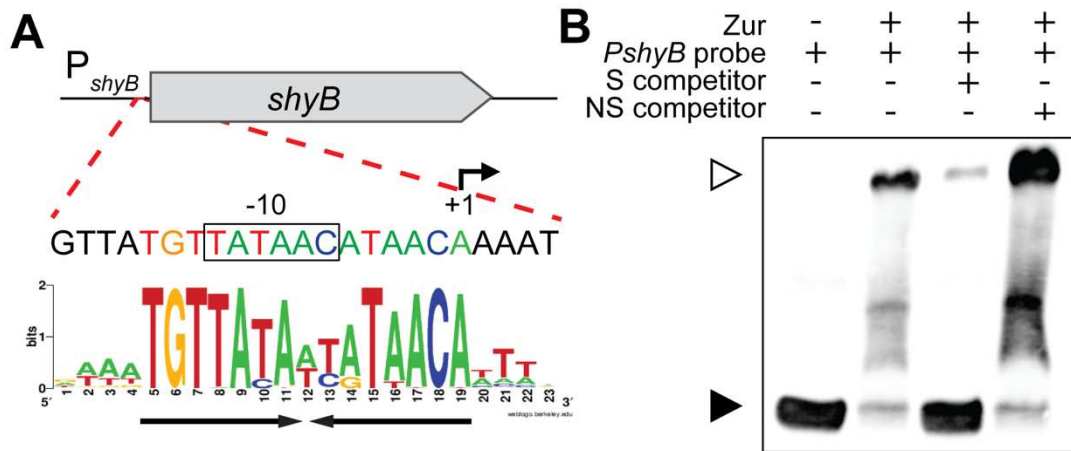


Figure 3. Zur directly binds the *shyB* promoter.

(A) The *shyB* promoter, annotated with a 5'-RACE transcription start site (+1) and putative -10 region (box), was aligned with a *Vibrio* Zur sequence logo (30, 31). The inverted AT-rich repeat in the putative Zur-box is underlined with black arrows. (B) A chemiluminescent probe containing the putative *shyB* Zur box was incubated with purified Zur in the presence of $ZnCl_2$ (5 μ M). Zur binding specificity was tested by adding 100-fold molar excess of unlabeled specific (S, Lane 3) or non-specific (NS, Lane 4) competitor DNA. Samples were electrophoresed on a 6% DNA retardation gel to separate unbound (black arrow) and bound probe (white arrow).

ShyB supports growth in chelator-treated medium.

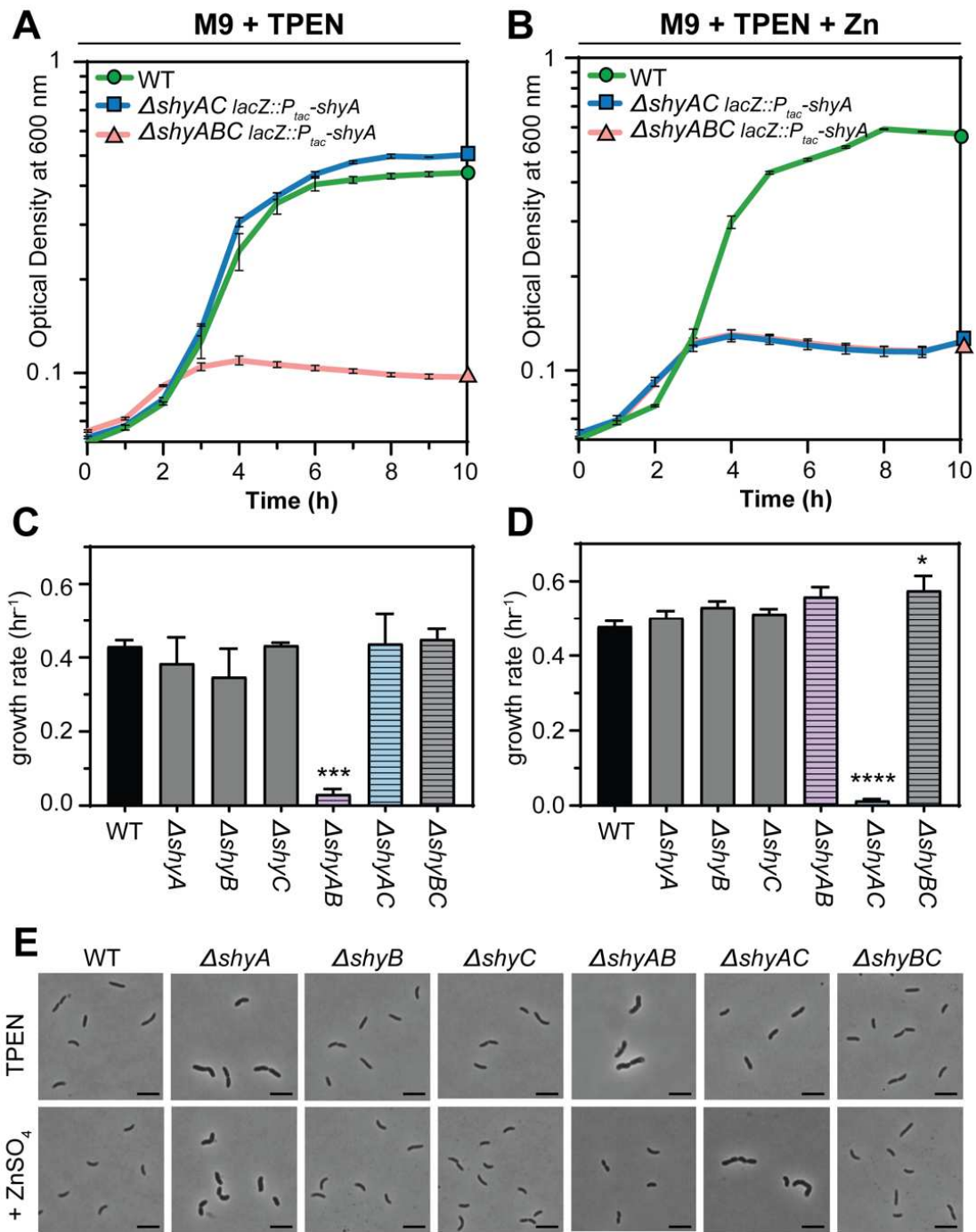
As *shyB* is part of the Zur-mediated zinc starvation response, we hypothesized that *V. cholerae* relies on ShyB endopeptidase activity when zinc availability is low. To induce zinc starvation and robustly derepress the Zur regulon, *V. cholerae* strains were grown in M9 minimal medium supplemented with TPEN (N,N,N',N'-Tetrakis(2-pyridylmethyl)ethylenediamine), a cell permeable metal chelator with high affinity for zinc (33). As expected from our genetic analysis, TPEN addition resulted in the production of ShyB protein (as measured by Western Blot), which could be reversed by adding zinc (**Fig. S3 A**).

We first tested whether native *shyB* could restore growth to Δ *shyAC* under zinc-starvation conditions. *shyA* and *shyC* deletions were generated in a parent strain expressing an IPTG-inducible copy of *shyA* (*lacZ::P_{tac}:shyA*), as these genes are conditionally essential in rich media (12). In the absence of IPTG, we found that chelation with either TPEN or EDTA (a more general divalent metal ion chelator) induced growth of Δ *shyAC*, but not in the mutant that additionally lacked *shyB* (**Fig. 4A; Fig. S4 A**). As expected, chelation-dependent growth of Δ *shyAC* could be suppressed by adding zinc (**Fig. 4B; Fig. S4 A**). These data suggest that induction of *shyB* alone is sufficient to sustain *V. cholerae* growth, and synthetic lethality of *shyA* and *shyC* is due to the lack of *shyB* expression under laboratory growth conditions. Consistent with this interpretation, exogenous *shyB* expression restored growth to Δ *shyABC P_{tac}-shyA* (**Fig. S4 B**) and we were able to generate a Δ *shyAC* knockout in a Δ *zur* background that grows robustly in LB medium (**Fig. S4 C**).

A *shyB* deletion alone did not result in a significant defect in growth rate or

morphology in TPEN-treated M9 (**Fig. 4C,E**); however, autolysins often need to be deleted in combination to result in a substantial phenotype (11). We therefore generated all possible combinations of LysM/M23 endopeptidase deletions to broadly dissect the relevance of zinc concentrations for EP activity. $\Delta shyA$ cells were somewhat enlarged in either growth condition but did not exhibit a strong growth rate defect (**Fig. 4C-E**). The $\Delta shyAB$ double mutant failed to grow in TPEN-treated M9 (**Fig. 4C**) and cells exposed to this condition were aberrantly thick and long (**Fig 4E**). This indicates that ShyC, the only essential LysM/M23 EP in the $\Delta shyAB$ mutant, cannot support growth in zinc-starved media. In zinc-replete medium, $\Delta shyAC lacZ::P_{tac}:shyA$ failed to grow in the absence of IPTG and displayed a similar aberrant cell morphology (**Fig. 4D,E**), consistent with a lack of *shyB* expression under these conditions. This tradeoff in synthetic lethality partners in low ($\Delta shyAB$) and high zinc ($\Delta shyAC$) growth media tentatively suggests that ShyB may function as a replacement for ShyC during zinc starvation. ShyC protein levels, as measured by Western Blot, were not reduced in the presence of TPEN (**Fig. S3 A**), ruling out the possibility that $\Delta shyAB$ lethality reflects downregulation or degradation of ShyC. Rather, these observations suggest that ShyC activity is more sensitive to zinc-chelation than the other EPs. Alternatively, TPEN might induce changes in PG architecture that make it resistant to cleavage by ShyC.

Figure 4. ShyB supports cell growth and is conditionally essential in a $\Delta shyA$ mutant in TPEN-treated medium. Mid-exponential cultures of the indicated *V. cholerae* mutants were washed to remove IPTG before being diluted 1:100 into M9 glucose / streptomycin plus TPEN (250 nM) in the absence (A,C) or presence (B,D) of ZnSO₄ (1 μ M). Growth of each strain was monitored by optical density at 600 nm in a Bioscreen C 100-well plate. Error bars report standard error of the mean (SEM) for three independent biological replicates. (A-B) Growth curves on a log-scale are shown for WT (green circle), $\Delta shyAC lacZ::P_{tac}:shyA$ (blue square), and $\Delta shyABC lacZ::P_{tac}:shyA$ (red triangle). (C-D) Growth rate (hr⁻¹) of WT (solid black), single EP mutants (solid gray) and double EP mutants (striped) were calculated from changes in optical density during exponential phase. Error bars report standard error of the mean (SEM) for three independent biological replicates. Statistical difference relative to WT was assessed using a one-way ANOVA followed by Dunnett's multiple comparison test (****, p-value <0.0001; ***, p-value < 0.001; *, p-value <0.05). (E) Phase contrast images of *V. cholerae* (C-D) sampled from mid-log phase (scale bar = 5 μ M).



ShyB is an EDTA-resistant D,D-endopeptidase in vitro.

ShyB is predicted to be a zinc-dependent D,D-endopeptidase but biochemical evidence is lacking. Thus, we measured the *in vitro* hydrolytic activity of each EP against *V. cholerae* sacculi. Recombinant Shy proteins were purified without the N-terminal hydrophobic sequence (ShyA $_{\Delta 1-35}$, ShyB $_{\Delta 1-34}$, and ShyC $_{\Delta 1-33}$) to increase solubility *in vitro* (**Fig. S5**) and, as a negative control, we purified ShyB $_{\Delta 1-34}$ with a mutation (H370A) in the active site that is expected to abolish activity. Each EP was incubated with purified *V. cholerae* sacculi; the soluble PG fragments released by digestion, as well as the remaining insoluble pellet, were treated with muramidase to process long glycan strands into their subunits (**Fig 5A**). The resulting muropeptides were then separated using ultra-high performance liquid chromatography (UPLC) and quantified by spectrophotometry (see Methods for details).

The muramidase-digested insoluble fraction shows PG that was not released by EP digestion (**Fig. 5B**). The no enzyme control shows a large peak corresponding to D44 dimers, indicating that these peptide crosslinks are abundant in the *V. cholerae* sacculi substrate (**Fig 5B**). This D44 peak is noticeably absent from the ShyA, ShyB, and ShyC digested sacculi. Instead, each of the Shy endopeptidases (but not the H370A mutant) hydrolyzed sacculi and generated a profile of soluble fragments (**Fig. 5C**). ShyA and ShyC produced similar muropeptide profiles, indicating similar hydrolytic activity *in vitro*, while the ShyB chromatogram contained more peaks with shorter retention times (**Fig S6**). MS/MS analysis determined that these ShyB-generated peaks correspond to uncrosslinked oligo-NAG-NAM-tetrapeptide chains [M4] $_{2-4}$, as well as small amounts of M4, M4N, and M0-M4 monomers. Consistent with a differential

cleavage activity, ShyB was able to further process PG pre-digested with ShyA or ShyC, while these EPs only slightly modified ShyB-digested PG (**Fig. S7**).

The soluble EP-digestion products were further treated with muramidase (**Fig. 5D**). Each of the EP-treated samples contained a large peak near 4 min, corresponding to a M4 monomer, in addition to lesser amounts of M4N monomer and chains of monomers (M0-M4, M4-M4N). These peaks were absent from the negative controls (no enzyme and ShyB H370A). There was virtually no D44 peak detected in the Shy-treated samples, indicating that all three LysM/M23 EPs function as a D,D-endopeptidase *in vitro* (**Fig. 5B**). We speculate that the apparent unique activity of ShyB on whole sacculi may reflect its ability to process substrate with a more diverse set of conformations than ShyA and ShyC.

M23 domains typically require a coordinated zinc ion to carry out PG hydrolysis (23). We have previously demonstrated that ShyA requires zinc for activity *in vitro* (12) and others have modeled zinc in the active site of a ShyB crystal structure (34). Based on its regulation by Zur, we hypothesized that ShyB evolved to function in zinc-limited environments. To test this, we repeated the *in vitro* PG hydrolysis assays under metal-limited conditions by using the divalent cation chelator EDTA. Strikingly, ShyB EP activity was largely unaffected by EDTA at the wide range of concentrations tested (0.1 mM – 20 mM) (**Fig. 6, Fig. S8**). ShyA and ShyC had reduced activity in 0.5 mM EDTA and suffered total loss of activity at higher concentrations, consistent with results previously obtained for ShyA (12). ShyC activity appeared to be more sensitive to EDTA than ShyA (at 1 and 5 mM), but this difference was not statistically significant. These *in vitro* assays suggest that ShyB has a high affinity for, or can function without,

divalent cations like zinc.

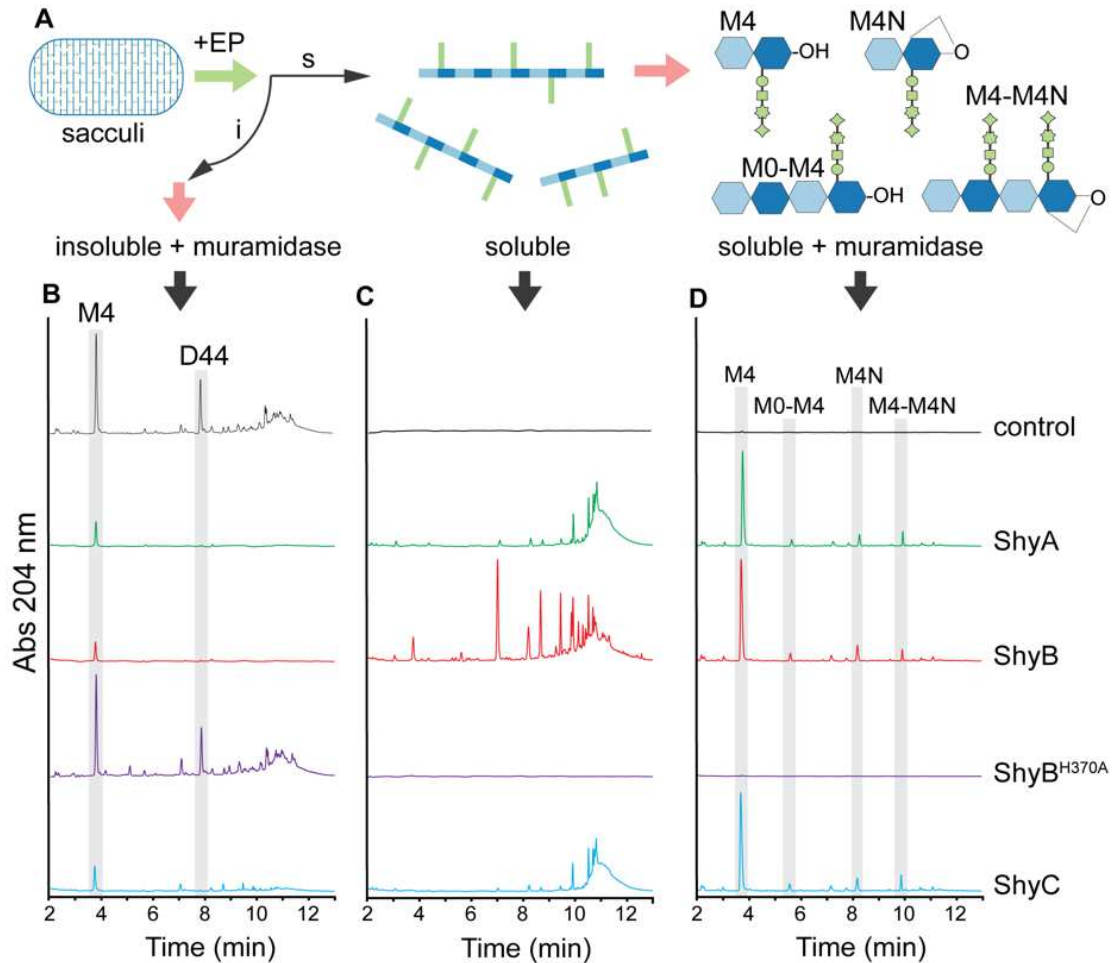


Figure 5. ShyB is a D,D-endopeptidase *in vitro*.

(A) *V. cholerae* sacculi was digested with 10 μg of endopeptidase (ShyA, ShyB, ShyB^{H370A}, ShyC) or a no enzyme control for 16 h at 37 $^{\circ}\text{C}$. The sample was separated into insoluble (i) and soluble (s) fractions and each component was further digested with muramidase (pink arrows). The digestion products were separated by ultra-high performance liquid chromatography (UPLC) and quantified by absorbance (204 nm). The chromatograms show (B) the insoluble fraction digested with muramidase, (C) the soluble fraction, and (D) the soluble fraction digested with muramidase. Highlighted peaks indicate D44 (disaccharide tetrapeptide), M4 (monomer disaccharide tetrapeptide), M4N (anhydrous monomer disaccharide tetrapeptide) muropeptides and oligo-monomeric chains.

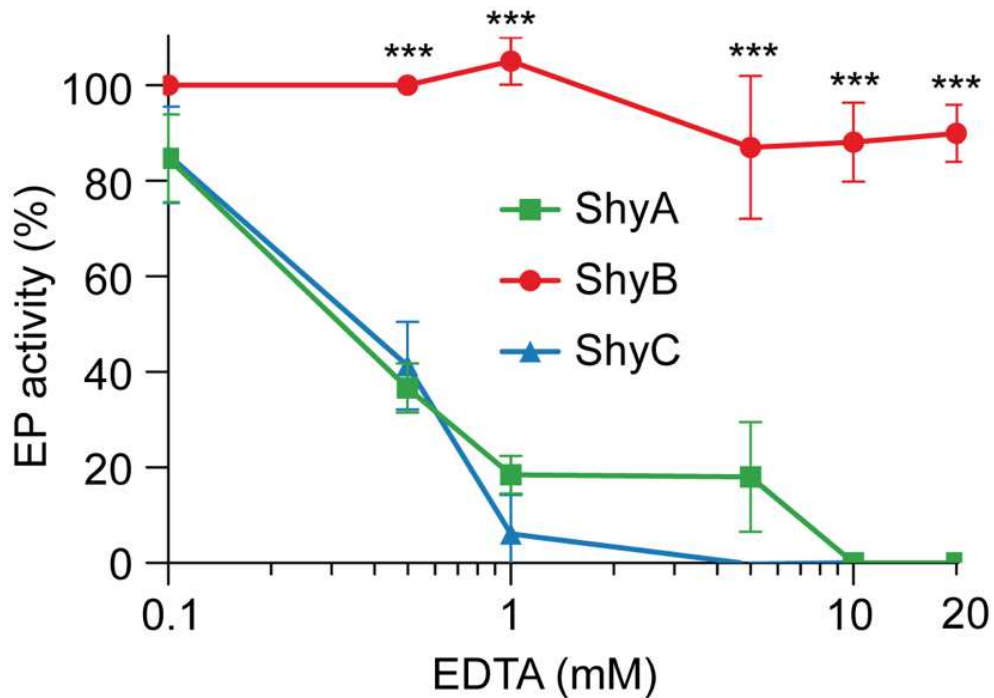


Figure 6. ShyB retains endopeptidase activity in the presence of EDTA *in vitro*.

V. cholerae sacculi was digested with 10 μ g of purified ShyA, ShyB, or ShyC for 16 h at 37 $^{\circ}$ C in the absence or presence of EDTA, with concentrations ranging from 0.1 mM to 20 mM. The soluble products released by digested sacculi were separated by UPLC and quantified by absorbance (204 nm). EP activity was measured by integrating the chromatogram profile of muramidase-digested insoluble fraction (as shown in **Fig. 5B**) and normalizing to the no EDTA treatment (100% activity) and no enzyme control (0% activity). Error bars represent the SEM of at least two biological replicates and statistical significance was assessed using a two-way ANOVA followed by Dunnett's multiple comparison test (***, $p < 0.0001$)

Zur-regulated endopeptidases are widespread in divergent bacteria.

Zur-regulated EPs appear to be widespread in the *Vibrio* genus. Using BLAST homology searches, we have identified isolates from 30 different non-cholera *Vibrio* species that contain a ShyB homolog with a Zur box directly upstream of the open reading frame (**Table S1**) (35). To assess the significance of zinc homeostasis for EP regulation more broadly, we surveyed published microarray and RNAseq datasets from diverse bacteria for differential EP expression (36-45). *Yersinia pestis* CO92, the causative agent of plague, encodes a ShyB homolog (YebA, YPO2062) whose gene is significantly upregulated in a Δ zur mutant (36). The *yebA* gene does not contain its own Zur box, but is positioned adjacent to *znuA* and may thus be co-transcribed as part of the same operon (**Fig. 7**). Similarly, *mepM* (b1856) is located adjacent to the *znu* locus in laboratory (K12 MG1655) and pathogenic *E. coli* (Enterohemorrhagic O157:H7 and Enteropathogenic O127:H6) strains. Two microarray studies in *E. coli*, one of which was validated by qPCR, showed that *mepM* is transcriptionally upregulated in response to zinc starvation (44, 45). Notably, this *znu*/EP arrangement is conserved in many other Gram-negative pathogens, including *Salmonella enterica* (STM1890, STY2098), *Enterobacter cloacae* (ECL_01442), *Klebsiella pneumoniae* (KPK_1913), *Shigella dysenteriae* (Sdy_1143), *Citrobacter freundii* (CFNIH1_20440), *Serratia marcescens* (SM39_2246), and *Proteus mirabilis* (PMI1153) (**Fig. 7**). Collectively, these data suggest that zinc homeostasis and cell wall turnover may be linked in many Gram-negative bacteria.

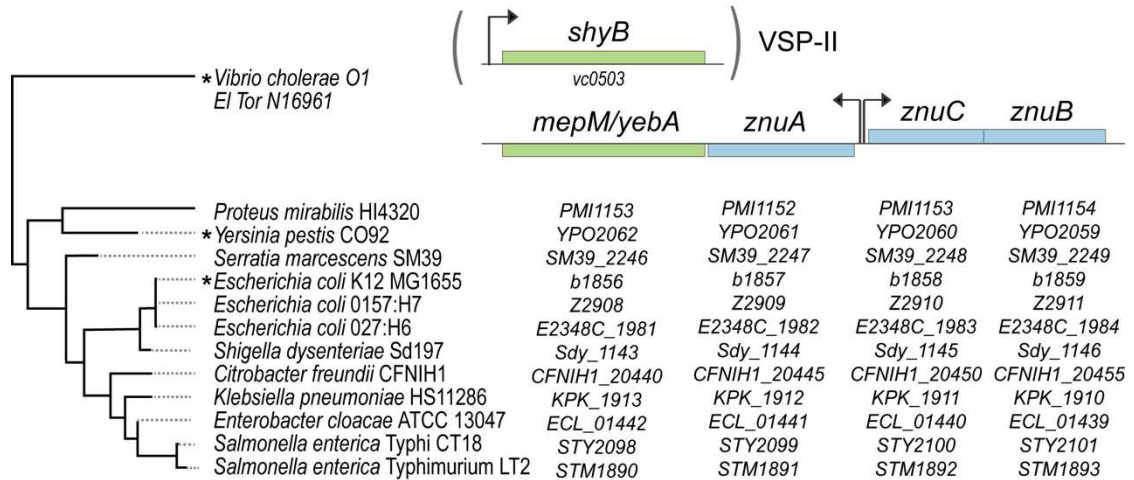


Figure 7. *shyB* exists as a single gene in *V. cholerae* N16961, while other pathogenic Gram-negative bacteria encode a ShyB homolog adjacent to the Zur-controlled *znu* operon. Gene neighborhood alignments, generated using the Prokaryotic Sequence Homology Analysis Tool (PSAT) (65), show the arrangement of a LysM/M23 endopeptidase gene (*mepM/yebA*, green) and adjacent zinc importer genes (*znuABC*, blue) in twelve Gram-negative organisms. *shyB*, in *V. cholerae* O1 El Tor N16961, exists as a single gene on a *Vibrio* Seventh Pandemic Island (VSP-II), separate from the *znuABC* locus. Arrows indicate the approximate location of the unidirectional or bidirectional promoter and site of Zur-binding. Asterisks signify published datasets that support Zur- and/or zinc-dependent regulation of the endopeptidase. Evolutionary history of the species shown was inferred using alignments of 16S rRNA genes (66) and the Neighbor Joining Method for tree construction (67) in MEGA7 (68). Evolutionary distances were computed using the Maximum Composite Likelihood Method (69) and are in units of number of base substitutions per site.

DISCUSSION

Functionally redundant endopeptidases support cell growth.

The importance of EPs has been established in both Gram-negative and Gram-positive bacteria (10-12), supporting the long-standing hypothesis that autolysins create space in the PG meshwork for the insertion of new cell wall material (8). As with other autolysins, EPs are often functionally redundant under laboratory growth conditions but exhibit slight differences in cellular localization (12, 20, 46), substrate specificity (10, 47) and relative abundance during each growth phase (11, 46). Our previous work in *V. cholerae* identified three LysM/M23 zinc metallo-endopeptidases: two (ShyA and ShyC) are housekeeping enzymes that are conditionally essential for growth, while the role of the third (ShyB) has remained unknown (12). In this study, we define *shyB* as a new member of the Zur regulon and demonstrate that ShyB can replace the other EPs *in vivo* when derepressed by zinc limitation. This is a novel mechanism for regulating autolysins and establishes a link between two essential processes: cell wall turnover and metal ion homeostasis.

Zinc availability affects the expression and activity of cell wall hydrolases.

We initially observed that the *shyB* promoter is active on M9 and repressed on LB agar. LB contains ~12.2 μM of zinc (48), while presumably the concentrations are much lower for the defined M9 medium (which does not contain any added zinc). Consistent with a role for the *zur* regulon in *shyB* regulation, we found that supplementing M9 with nanomolar concentrations of zinc was sufficient to repress the *shyB* promoter in liquid culture (**Fig 2D**). As a cautionary note, this suggests that *V.*

cholerae is starved for zinc in M9 (and possibly other minimal media as well), a complication not usually considered when interpreting results obtained in this medium.

Based on its membership in the Zur regulon, it is likely that ShyB evolved to function in low-zinc environments. Indeed, ShyB endopeptidase activity *in vitro* is unaffected by EDTA ($k_d_{(Zn^{2+})} = 10^{-16}$ M) (49), even at chelator concentrations (e.g. 20 mM) that induce levels of metal starvation that far exceed those encountered in nature (**Fig. 6**). We found that a mutation in a metal-coordinating residue (H370A) abolished ShyB activity (**Fig. 5**), but further biochemical characterization of the active site is required to explain how ShyB retains EP activity in low-zinc environments. It is possible that the ShyB active site (i) binds zinc with very high affinity, (ii) utilizes an alternative metal co-factor, or (iii) functions independently of a bound metal co-factor.

ShyA appears to have an intermediate ability to function in low zinc environments. The ability to sustain growth in the presence of TPEN or EDTA indicates that ShyA function is less affected by metal starvation than ShyC; however, ShyA's activity can still be inhibited by higher concentrations of EDTA *in vitro*. Collectively, our data suggest a model where ShyA is the predominant housekeeping endopeptidase. ShyC appears to partially overlap in function with ShyA when zinc availability is high. During zinc-starvation, we speculate that *shyB* is derepressed specifically to compensate for loss of ShyC activity.

ShyB can function as the sole EP in both high and low zinc conditions (**Fig. 4A**, **Fig. S5**), so why is it repressed under normal growth conditions rather than just replacing ShyA and ShyC altogether? One possible explanation is that ShyB activity might be more destructive than the other EPs, requiring more careful control. Indeed,

our activity assays demonstrated that ShyB has a slightly altered activity profile, processing the sacculus into smaller fragments with shorter retention times (**Fig. 5C**) and doing so at a faster rate (**Fig. S7 D-F**). Additionally, native ShyB protein-levels (constitutively transcribed in a Δzur mutant) are substantially lower than either ShyA or ShyC (**Fig. S3 B**), suggesting that less enzyme is required to support growth.

Zur-regulated endopeptidases are present in divergent Gram-negative bacteria.

Zur-regulated EPs are a novel adaptation to zinc-limitation; however, ShyB activity is not essential to wild-type *V. cholerae* growth under the laboratory conditions tested. This might be due to functional overlap with the other Shy EPs, but it should also be noted that pandemic *V. cholerae* horizontally acquired *shyB* on a pathogenicity island (VSP-II) recently in its evolutionary history (1960s) (50). It is thus possible that ShyB activity is of advantage under conditions that also positively selected for acquisition of VSP-II, such as pathogenesis.

Importantly, Zur-regulated EPs are not confined to *Vibrios*: divergent Gram-negative bacteria encode conserved ShyB/MepM/YebA homologs adjacent to the Zur-controlled *znu* operon (**Fig. 7**). Transcriptomic data from both *Y. pestis* and *E. coli* support the prediction that this EP is upregulated along with the zinc importer, though it is unclear whether these EPs can also be transcribed from a Zur-independent promoter internal to *znuA*. Parts of the zinc starvation response (e.g. zinc importers) have been shown to be required for host colonization by divergent human pathogens (51-54), since vertebrates and other hosts sequester metals as a form of nutritional immunity (55). It has also been shown that ShyB homolog YebA in *Y. pestis* is important for virulence in

the plague pathogen (56). It is therefore tempting to speculate that regulation of endopeptidase activity in low zinc environments may play a general role in pathogenesis.

EXPERIMENTAL PROCEDURES

Bacterial growth conditions.

Cells were grown by shaking (200 rpm) at 37 °C in 5 mL of LB medium unless otherwise indicated. M9 minimal medium with glucose (0.4%) was prepared with ultrapure Milli-Q water to minimize zinc contamination. When appropriate, antibiotics were used at the following concentrations: streptomycin (200 µg mL⁻¹), ampicillin (100 µg mL⁻¹), kanamycin (50 µg mL⁻¹), and chloramphenicol (5 µg mL⁻¹). IPTG (200 µM) was added to all liquid and solid media if required to sustain *V. cholerae* growth. X-gal (40 µg mL⁻¹) was added to plates for blue-white screening.

Plasmid and strain construction.

All genes were PCR amplified from *V. cholerae* El Tor N16961 genomic DNA. Plasmids were built using isothermal assembly (57) with the oligonucleotides summarized in **Table S2**. The suicide vector pCVD442 was used to make gene deletions via homologous recombination (58); 700 bp regions flanking the gene of interest were amplified for Δzur (SM89/90 + SM91/92), $\Delta znuA$ (SM107/108 + SM109/110), and $\Delta znuABC$ (SM93/94, SM95/96) and assembled into XbaI digested pCVD442. Endopeptidase deletion constructs were built as described previously (12). Chromosomal delivery vectors (pJL-1 and pTD101) were used to insert genes via

double cross-over into native *lacZ*. To construct the *shyB* transcriptional reporter, 500 bp upstream of *shyB* were amplified (SM1/2) and assembled into NheI-digested pAM325 to yield a *P_{shyB}:lacZ* fusion. This fusion was amplified (SM3/4) and cloned into StuI-digested pJL-1 (59).

To complement gene deletions, *zur* (SM99/100) and *znuA* (SM113/114) were cloned into SmaI-digested pBAD: a chloramphenicol resistant, arabinose-inducible plasmid. For chromosomal delivery of an IPTG-inducible system into *lacZ*, pTD101(*shyB*) was constructed with SM181/182 and pTD100(*shyA*) was built as previously described (12). An additional chromosomal delivery vector (pSGM100) was built for crossover into VC1807. *shyB* (SM141/SM55) was placed under arabinose-inducible control by cloning into SmaI-digested pSGM100. All assemblies were initially transformed into *E. coli* DH5α λpir and then into SM10 λpir for conjugation into *V. cholerae*.

All strains are derivatives of *V. cholerae* El Tor N16961 (WT), unless otherwise indicated. To conjugate plasmids into *V. cholerae*, SM10 λpir donor strains carrying pCVD442, pTD101, pJL-1, or pSGM100 plasmids were grown in LB/ampicillin and strains carrying pBAD were grown in LB/chloramphenicol. Recipient *V. cholerae* strains were grown overnight in LB/streptomycin. Stationary phase cells were pelleted by centrifugation (6,500 rpm for 3 min) and washed with fresh LB to remove antibiotics. Equal ratios of donor and recipient (100μL:100 μL) were mixed and spotted onto LB agar plates. After a 4-hour incubation at 37 °C, cells were streaked onto LB containing streptomycin and an antibiotic (ampicillin or chloramphenicol) to select for transconjugants. Colonies carrying integration vectors were cured through two rounds

of purification on salt free sucrose (10%) agar with streptomycin. Insertions into native *lacZ* (via pJL-1, pTD101) were identified by blue-white colony screening on X-gal plates. Insertions into VC1807 were checked via PCR screening (SM/SM). Gene deletions (via pCVD442) were checked via PCR screening with the following primers: $\Delta shyA$ (TD503/504), $\Delta shyB$ (SM30/31), $\Delta shyC$ (TD701/702), Δzur (SM122/123), $\Delta znuA$ (SM119/120), and $\Delta znuABC$ (SM119/121).

Transposon mutagenesis and arbitrary PCR.

The *shyB* transcriptional reporter was mutagenized with Himar1 mariner transposons, which were delivered via conjugation by an SM10 λ pir donor strain carrying pSC189 (60). The recipient and donor were grown overnight in LB/streptomycin and LB/ampicillin, respectively. Stationary phase cells were pelleted by centrifugation (6,500 rpm for 3 min) and washed with fresh LB to remove antibiotics. For each reaction, equal ratios of donor and recipient (500 μ L:500 μ L) were mixed and spotted onto 0.45 μ m filter disks adhered to pre-warmed LB plates. After a 4-hour incubation at 37 °C, cells were harvested by aseptically transferring the filter disks into conical tubes and vortexing in fresh LB. The cells were spread onto LB agar containing streptomycin to kill the donor strain, kanamycin to select for transposon mutants, and X-gal to allow for blue-white colony screening. Plates were incubated at 30°C overnight followed by two days at room temperature. To identify the transposon insertion site, purified colonies were lysed via boiling and used directly as a DNA template for arbitrary PCR. As described elsewhere, this technique amplifies the DNA sequence adjacent to the transposon insertion site through successive rounds of PCR (24).

Amplicons were Sanger sequenced and high quality sequencing regions were aligned to the *N16961* genome using BLAST (35).

β-Galactosidase activity measurements.

Strains containing promoter-*lacZ* fusions were grown from single colony in 5 mL of culture media (LB, M9, or M9 plus 500 uM ZnSO₄) at 30 °C shaking. Cells from 0.5 mL of exponential-phase culture were harvested and β-Galactosidase assays were performed as described previously (61, 62).

5' rapid amplification of cDNA ends.

The *shyB* transcription start site was identified with 5' rapid amplification of cDNA ends (5' RACE). To obtain a *shyB* transcript, *Azur* was grown in LB at 37 °C until cells reached mid-log phase (OD₆₀₀ = 0.5) and RNA was extracted using Trizol and acid:phenol chloroform (Ambion). DNA contamination was removed through two RQ1 DNase (Promega) treatments and additional acid:phenol chloroform extractions. cDNA synthesis was performed with MultiScribe reverse transcriptase (ThermoFisher) and a *shyB* specific primer (SM270). cDNA was column purified and treated with terminal transferase (New England BioLabs) to add a homopolymeric cytosine tail to the 3' end. The cDNA was amplified through two rounds of touchdown PCR with a second gene-specific primer (SM271) and the Anchored Abridged Primer (ThermoFisher). The PCR product was Sanger sequenced using primer SM271.

Electrophoretic mobility shift assay.

The LightShift Chemiluminescent EMSA kit (ThermoFisher) was used to detect Zur-promoter binding. 41 bp complimentary oligos (SM264/265) containing the putative *shyB* Zur box, with and without a 5' biotin label, were annealed according to commercial instructions (Integrated DNA Technologies). 20 μL binding reactions contained buffer, Poly dI-dC (50 ng μL^{-1}), ZnCl_2 (5 μM), labeled probe (1 pmol), and purified Zur (600 nM). Unlabeled specific or non-specific competitor oligos were added in 100-fold molar excess. Reactions were incubated on ice for 1 hour, electrophoresed on a 6% DNA retardation gel (100 V, 40 min), and wet transferred to a Biotodyne B membrane (100 V, 30 min) (ThermoFisher) in a cold room. The membrane was developed using chemiluminescence according to the manufacturer's instructions and imaged using a Bio-Rad ChemiDoc MP imaging system.

Protein expression and purification.

DNA encoding N-terminally truncated LysM/M23 endopeptidases (ShyA Δ_{1-35} , ShyB Δ_{1-34} , and ShyC Δ_{1-33}) and full length Zur was PCR amplified from genomic DNA, while template for the ShyB H370A mutation was commercially synthesized (Integrated DNA Technologies). Shy constructs were cloned into pCAV4, and Zur into pCAV6, both modified T7 expression vectors that introduce an N-terminal 6xHis-NusA tag (pCAV4) or 6xHis-MBP tag (pCAV6) followed by a Hrv3C protease site upstream of the inserted sequence. Constructs were transformed into BL21(DE3) cells, grown at 37 °C in Terrific Broth supplemented with carbenicillin (100 mg mL^{-1}) to an OD₆₀₀ of 0.8-1.0, and then induced with IPTG (0.3 mM) overnight at 19 °C. ZnCl_2 (50 μM) was added

during Zur induction. Cells were harvested via centrifugation, washed with nickel loading buffer (NLB) (20 mM HEPES pH 7.5, 500 mM NaCl, 30 mM imidazole, 5% glycerol (v:v), 5 mM β -Mercaptoethanol), pelleted in 500mL aliquots, and stored at -80 °C.

Pellets were thawed at 37 °C and resuspended in NLB supplemented with PMSF (10 mM), DNase (5 mg), $MgCl_2$ (5 mM), lysozyme (10 mg mL⁻¹), and one tenth of a complete protease inhibitor cocktail tablet (Roche). All buffers used in Zur purification were supplemented with $ZnCl_2$ (1 μ M). Cell suspensions were rotated at 4 °C, lysed via sonication, centrifuged, and the supernatant was syringe filtered using a 0.45 μ M filter. Clarified samples were loaded onto a $NiSO_4$ charged 5 mL HiTrap chelating column (GE Life Sciences), and eluted using an imidazole gradient from 30 mM to 1M. Hrv3C protease was added to the pooled fractions and dialyzed overnight into cation exchange loading buffer (20 mM HEPES pH 7.5, 50 mM NaCl, 1 mM EDTA, 5% glycerol (v:v), 1 mM DTT). Cleaved Shy proteins were loaded onto a 5 mL HiTrap SP HP column and cleaved Zur was loaded onto a 5mL HiTrap Heparin HP column (GE Life Sciences). All constructs were eluted along a NaCl gradient from 50mM to 1M. Fractions were concentrated and injected onto a Superdex 75 16/600 equilibrated in Size Exclusion Chromotography buffer (20 mM HEPES pH7.5, 150 mM KCl, 1 mM DTT). Zur dimers coeluted with MBP on the sizing column and were subsequently incubated with amylose resin (New England BioLabs) at 4 °C and Zur was collected from a gravity column. Final purified protein concentrations were determined by SDS-PAGE (**Fig. S5**) and densitometry compared against BSA standards: ShyA, 5.72 mg mL⁻¹; ShyB, 5.72 mg mL⁻¹; ShyB H320A, 2.35 mg mL⁻¹; ShyC, 17.93 mg mL⁻¹; Zur, 0.31 mg mL⁻¹.

Sacculi digestion assay and separation by UPLC.

Peptidoglycan from stationary phase *V. cholerae* cells was extracted and purified via SDS boiling and digested with muramidase (63). 10 μ L of sacculi and 10 μ g of enzyme were mixed in 50 μ L buffered solution (50 mM Tris-HCl pH 7.5, 100 mM NaCl) in the absence or presence of EDTA (0 – 20 mM). Digestions were incubated for 16 h at 37 °C and enzymes were inactivated by boiling during 10 min and centrifugation for 15 min at 22,000 g. The soluble fraction and the insoluble pellet were separated and each sample was further digested with muramidase. All soluble products were reduced with sodium borohydride, their pH adjusted, and injected into a Waters UPLC system (Waters, Massachusetts, USA) equipped with an ACQUITY UPLC BEH C18 Column, 130 Å, 1.7 μ m, 2.1 mm \times 150 mm (Waters) and a dual wavelength absorbance detector. Eluted fragments were separated at 45 °C using a linear gradient from buffer A [formic acid 0.1% (v/v)] to buffer B [formic acid 0.1% (v/v), acetonitrile 40% (v/v)] in a 12 min run with a 0.175 ml min⁻¹ flow, and detected at 204 nm. Muropeptide identity was confirmed by MS/MS analysis, using a Xevo G2-XS QToF system (Waters Corporation, USA) and the same separation conditions.

Growth curve analysis.

Strains were grown overnight in LB/streptomycin with IPTG. Cells were washed in 1X phosphate buffered solution (PBS) and subcultured 1:10 into M9 glucose plus IPTG. After 2 hours shaking at 37°C, cells were washed and subcultured 1:100 into M9 glucose containing combinations of TPEN (250 nM), ZNSO₄ (1 μ M), and IPTG (200 μ M). The

growth of each 200 μ L culture in a 100-well plate was monitored by optical density (OD₆₀₀) on a Bioscreen C plate reader (Growth Curves America).

Microscopy.

Cells were imaged under phase contrast on an agarose patch (0.8% agarose in M9 minimal medium) using a Leica DMI8 inverted microscope.

ACKNOWLEDGEMENTS

We thank all the members of the Doerr and Chappie Labs for helpful discussions and assistance with this work. We thank members of the John Helmann Lab for lending their expertise and reagents. We thank the faculty, staff, and students at the Weill Institute for Cell and Molecular Biology (WICMB) for their support. Research in the Doerr Lab is supported by start-up funds from Cornell University. Research in the Cava lab is supported by MIMS, the Knut and Alice Wallenberg Foundation (KAW), the Swedish Research Council and the Kempe Foundation.

REFERENCES

1. **Schneider T, Sahl H-G.** 2010. An oldie but a goodie – cell wall biosynthesis as antibiotic target pathway. *Int J Med Microbiol* **300**:161–169.
2. **Typas A, Banzhaf M, Gross CA, Vollmer W.** 2012. From the regulation of peptidoglycan synthesis to bacterial growth and morphology. *Nat Rev Microbiol* **10**:123–136.
3. **Höltje JV.** 1998. Growth of the stress-bearing and shape-maintaining murein sacculus of *Escherichia coli*. *Microbiol Mol Biol Rev* **62**:181–203.
4. **Silhavy TJ, Kahne D, Walker S.** 2010. The Bacterial Cell Envelope. *Cold Spring Harb Perspect Biol* **2**:a000414–a000414.
5. **Cabeen MT, Jacobs-Wagner C.** 2005. Bacterial cell shape. *Nat Rev Microbiol* **3**:601–610.
6. **Vollmer W, Joris B, Charlier P, Foster S.** 2008. Bacterial peptidoglycan (murein) hydrolases. *FEMS Microbiol Rev* **32**:259–286.
7. **Tomasz A.** 1979. The mechanism of the irreversible antimicrobial effects of penicillins: how the beta-lactam antibiotics kill and lyse bacteria. *Annu Rev Microbiol* **33**:113–137.
8. **Vollmer W.** 2012. Bacterial growth does require peptidoglycan hydrolases. *Molecular Microbiology* **86**:1031–1035.
9. **Cho H, Wivagg CN, Kapoor M, Barry Z, Rohs PDA, Suh H, Marto JA, Garner EC, Bernhardt TG.** 2016. Bacterial cell wall biogenesis is mediated by SEDS and PBP polymerase families functioning semi-autonomously. *Nat Microbiol* **1**:123.
10. **Singh SK, SaiSree L, Amrutha RN, Reddy M.** 2012. Three redundant murein endopeptidases catalyse an essential cleavage step in peptidoglycan synthesis of *Escherichia coli* K12. *Molecular Microbiology* **86**:1036–1051.
11. **Hashimoto M, Ooiwa S, Sekiguchi J.** 2011. The synthetic lethality of *lytE* *cw10* in *Bacillus subtilis* is caused by lack of d,l-endopeptidase activity at the lateral cell wall. *Journal of Bacteriology* **194**:796–803.
12. **Dörr T, Cava F, Lam H, Davis BM, Waldor MK.** 2013. Substrate specificity of an elongation-specific peptidoglycan endopeptidase and its implications for cell wall architecture and growth of *Vibrio cholerae*. *Molecular Microbiology* **89**:949–962.
13. **Lai GC, Cho H, Bernhardt TG.** 2017. The mecillinam resistome reveals a role

for peptidoglycan endopeptidases in stimulating cell wall synthesis in *Escherichia coli*. *PLoS Genet* **13**:e1006934.

14. **Dörr T, Davis BM, Waldor MK.** 2015. Endopeptidase-Mediated Beta Lactam Tolerance. *PLoS Pathog* **11**:e1004850.
15. **Kitano K, Tuomanen E, Tomasz A.** 1986. Transglycosylase and endopeptidase participate in the degradation of murein during autolysis of *Escherichia coli*. *Journal of Bacteriology* **167**:759–765.
16. **Singh SK, Parveen S, SaiSree L, Reddy M.** 2015. Regulated proteolysis of a cross-link-specific peptidoglycan hydrolase contributes to bacterial morphogenesis. *Proc Natl Acad Sci USA* **112**:10956–10961.
17. **Srivastava D, Seo J, Rimal B, Kim SJ, Zhen S, Darwin AJ.** 2018. A Proteolytic Complex Targets Multiple Cell Wall Hydrolases in *Pseudomonas aeruginosa*. *mBio* **9**:e00972–18.
18. **Britton RA, Eichenberger P, Gonzalez-Pastor JE, Fawcett P, Monson R, Losick R, Grossman AD.** 2002. Genome-Wide Analysis of the Stationary-Phase Sigma Factor (Sigma-H) Regulon of *Bacillus subtilis*. *Journal of Bacteriology* **184**:4881–4890.
19. **Ishikawa S, Hara Y, Ohnishi R, Sekiguchi J.** 1998. Regulation of a New Cell Wall Hydrolase Gene, *cwIF*, Which Affects Cell Separation in *Bacillus subtilis*. *Journal of Bacteriology* **180**:2549–2555.
20. **Ohnishi R, Ishikawa S, Sekiguchi J.** 1999. Peptidoglycan Hydrolase *LytF* Plays a Role in Cell Separation with *CwIF* during Vegetative Growth of *Bacillus subtilis*. *Journal of Bacteriology* **181**:3178–3184.
21. **Yamaguchi H, Furuhashi K, Fukushima T, Yamamoto H, Sekiguchi J.** 2004. Characterization of a new *Bacillus subtilis* peptidoglycan hydrolase gene, *yvcE* (named *cwIO*), and the enzymatic properties of its encoded protein. *J Biosci Bioeng* **98**:174–181.
22. **Buist G, Steen A, Kok J, Kuipers OP.** 2008. *LysM*, a widely distributed protein motif for binding to (peptido)glycans. *Molecular Microbiology* **68**:838–847.
23. **Rawlings ND, Barrett AJ, Thomas PD, Huang X, Bateman A, Finn RD.** 2018. The MEROPS database of proteolytic enzymes, their substrates and inhibitors in 2017 and a comparison with peptidases in the PANTHER database. *Nucleic Acids Res* **46**:D624–D632.
24. **O'Toole GA, Pratt LA, Watnick PI, Newman DK, Weaver VB, Kolter R.** 1999. Genetic approaches to study of biofilms. *Methods Enzymol* **310**:91–109.

25. **Sheng Y, Fan F, Jensen O, Zhong Z, Kan B, Wang H, Zhu J.** 2015. Dual Zinc Transporter Systems in *Vibrio cholerae* Promote Competitive Advantages over Gut Microbiome. *Infection and Immunity* **83**:3902–3908.
26. **Patzer SI, Hantke K.** 1998. The ZnuABC high-affinity zinc uptake system and its regulator Zur in *Escherichia coli*. *Molecular Microbiology* **28**:1199–1210.
27. **Gilston BA, Wang S, Marcus MD, Canalizo-Hernández MA, Swindell EP, Xue Y, Mondragón A, O'Halloran TV.** 2014. Structural and Mechanistic Basis of Zinc Regulation Across the *E. coli* Zur Regulon. *PLoS Biol* **12**:e1001987.
28. **Shin J-H, Helmann JD.** 2016. Molecular logic of the Zur-regulated zinc deprivation response in *Bacillus subtilis*. *Nat Commun* **7**:1–9.
29. **Panina EM, Mironov AA, Gelfand MS.** 2011. Comparative genomics of bacterial zinc regulons: Enhanced ion transport, pathogenesis, and rearrangement of ribosomal proteins. *Proc Natl Acad Sci USA* **100**:9912–9917.
30. **Novichkov PS, Kazakov AE, Ravcheev DA, Leyn SA, Kovaleva GY, Sutormin RA, Kazanov MD, Riehl W, Arkin AP, Dubchak I, Rodionov DA.** 2013. RegPrecise 3.0 – A resource for genome-scale exploration of transcriptional regulation in bacteria. *BMC Genomics* **14**:745.
31. **Crooks GE, Hon G, Chandonia J-M, Brenner SE.** 2004. WebLogo: a sequence logo generator. *Genome Res* **14**:1188–1190.
32. **Napolitano M, Rubio MÁ, Camargo S, Luque I.** 2013. Regulation of internal promoters in a zinc-responsive operon is influenced by transcription from upstream promoters. *Journal of Bacteriology* **195**:JB.01488–12–1293.
33. **Arslan P, Di Virgilio F, Beltrame M, Tsien RY, Pozzan T.** 1985. Cytosolic Ca²⁺ homeostasis in Ehrlich and Yoshida carcinomas. A new, membrane-permeant chelator of heavy metals reveals that these ascites tumor cell lines have normal cytosolic free Ca²⁺. *J Biol Chem* **260**:2719–2727.
34. **Ragumani S, Kumaran D, Burley SK, Swaminathan S.** 2008. Crystal structure of a putative lysostaphin peptidase from *Vibrio cholerae*. *Proteins: Struct, Funct, Bioinf* **72**:1096–1103.
35. **Altschul SF, Gish W, Miller W, Myers EW, Lipman DJ.** 1990. Basic local alignment search tool. *J Mol Biol* **215**:403–410.
36. **Li Y, Qiu Y, Gao H, Guo Z, Han Y, Song Y, Du Z, Wang X, Zhou D, Yang R.** 2009. Characterization of Zur-dependent genes and direct Zur targets in *Yersinia pestis*. *BMC Microbiol* **9**:128.
37. **Mortensen BL, Rathi S, Chazin WJ, Skaar EP.** 2014. *Acinetobacter*

- baumannii response to host-mediated zinc limitation requires the transcriptional regulator Zur. *Journal of Bacteriology* **196**:JB.01650–14–2626.
38. **Maciąg A, Dainese E, Rodriguez GM, Milano A, Provvedi R, Pasca MR, Smith I, Palù G, Riccardi G, Manganelli R.** 2007. Global analysis of the *Mycobacterium tuberculosis* Zur (FurB) regulon. *Journal of Bacteriology* **189**:730–740.
 39. **Pawlik M-C, Hubert K, Joseph B, Claus H, Schoen C, Vogel U.** 2012. The zinc-responsive regulon of *Neisseria meningitidis* comprises seventeen genes under control of a Zur element. *Journal of Bacteriology* **194**:JB.01091–12–6603.
 40. **Mazzon RR, Braz VS, da Silva Neto JF, do Valle Marques M.** 2014. Analysis of the *Caulobacter crescentus* Zur regulon reveals novel insights in zinc acquisition by TonB-dependent outer membrane proteins. *BMC Genomics* **15**:734.
 41. **Gaballa A, Wang T, Ye RW, Helmann JD.** 2002. Functional analysis of the *Bacillus subtilis* Zur regulon. *Journal of Bacteriology* **184**:6508–6514.
 42. **Schröder J, Jochmann N, Rodionov DA, Tauch A.** 2010. The Zur regulon of *Corynebacterium glutamicum* ATCC 13032. *BMC Genomics* **11**:12.
 43. **Kallifidas D, Pascoe B, Owen GA, Strain-Damerell CM, Hong H-J, Paget MSB.** 2010. The zinc-responsive regulator Zur controls expression of the coelibactin gene cluster in *Streptomyces coelicolor*. *Journal of Bacteriology* **192**:608–611.
 44. **Sigdel TK, Easton JA, Crowder MW.** 2006. Transcriptional response of *Escherichia coli* to TPEN. *Journal of Bacteriology* **188**:6709–6713.
 45. **Hensley MP, Gunasekera TS, Easton JA, Sigdel TK, Sugarbaker SA, Klingbeil L, Breece RM, Tierney DL, Crowder MW.** 2012. Characterization of Zn(II)-responsive ribosomal proteins YkgM and L31 in *E. coli*. *J Inorg Biochem* **111**:164–172.
 46. **Fukushima T, Afkham A, Kurosawa S-I, Tanabe T, Yamamoto H, Sekiguchi J.** 2006. A New d,l-Endopeptidase Gene Product, YojL (Renamed CwlS), Plays a Role in Cell Separation with LytE and LytF in *Bacillus subtilis*. *Journal of Bacteriology* **188**:5541–5550.
 47. **Smith TJ, Blackman SA, Foster SJ.** 2000. Autolysins of *Bacillus subtilis*: multiple enzymes with multiple functions. *Microbiology* **146**:249–262.
 48. **Takahashi H, Oshima T, Hobman JL, Doherty N, Clayton SR, Iqbal M, Hill PJ, Tobe T, Ogasawara N, Kanaya S, Stekel DJ.** 2015. The dynamic balance of import and export of zinc in *Escherichia coli* suggests a heterogeneous

population response to stress. *J R Soc Interface* **12**:20150069–20150069.

49. **Yatsunyk LA, Easton JA, Kim LR, Sugarbaker SA, Bennett B, Breece RM, Vorontsov II, Tierney DL, Crowder MW, Rosenzweig AC.** 2007. Structure and metal binding properties of ZnuA, a periplasmic zinc transporter from *Escherichia coli*. *J Biol Inorg Chem* **13**:271–288.
50. **Dziejman M, Balon E, Boyd D, Fraser CM, Heidelberg JF, Mekalanos JJ.** 2002. Comparative genomic analysis of *Vibrio cholerae*: Genes that correlate with cholera endemic and pandemic disease. *Proc Natl Acad Sci USA* **99**:1556–1561.
51. **Ammendola S, Pasquali P, Pistoia C, Petrucci P, Petrarca P, Rotilio G, Battistoni A.** 2007. High-Affinity Zn²⁺ Uptake System ZnuABC Is Required for Bacterial Zinc Homeostasis in Intracellular Environments and Contributes to the Virulence of *Salmonella enterica*. *Infection and Immunity* **75**:5867–5876.
52. **Cerasi M, Ammendola S, Battistoni A.** 2013. Competition for zinc binding in the host-pathogen interaction. *Front Cell Infect Microbiol* **3**.
53. **Hood MI, Mortensen BL, Moore JL, Zhang Y, Kehl-Fie TE, Sugitani N, Chazin WJ, Caprioli RM, Skaar EP.** 2012. Identification of an *Acinetobacter baumannii* Zinc Acquisition System that Facilitates Resistance to Calprotectin-mediated Zinc Sequestration. *PLoS Pathog* **8**:e1003068.
54. **Ma L, Terwilliger A, Maresso AW.** 2015. Iron and zinc exploitation during bacterial pathogenesis. *Metallomics* **7**:1541–1554.
55. **Kehl-Fie TE, Skaar EP.** 2010. Nutritional immunity beyond iron: a role for manganese and zinc. *Current Opinion in Chemical Biology* **14**:218–224.
56. **Pradel E, Lemaître N, Merchez M, Ricard I, Reboul A, Dewitte A, Sebbane F.** 2014. New Insights into How *Yersinia pestis* Adapts to Its Mammalian Host during Bubonic Plague. *PLoS Pathog* **10**:e1004029.
57. **Gibson DG, Young L, Chuang R-Y, Venter JC, Hutchison CA III, Smith HO.** 2009. Enzymatic assembly of DNA molecules up to several hundred kilobases. *Nat Methods* **6**:343–345.
58. **Donnenberg MS, Kaper JB.** 1991. Construction of an *eae* deletion mutant of enteropathogenic *Escherichia coli* by using a positive-selection suicide vector. *Infection and Immunity* **59**:4310–4317.
59. **Butterton JR, Beattie DT, Gardel CL, Carroll PA, Hyman T, Killeen KP, Mekalanos JJ, Calderwood SB.** 1995. Heterologous antigen expression in *Vibrio cholerae* vector strains. *Infection and Immunity* **63**:2689–2696.

60. **Chiang SL, Rubin EJ.** 2002. Construction of a mariner-based transposon for epitope-tagging and genomic targeting. *Gene* **296**:179–185.
61. **Miller J.** 1972. *Experiments in molecular genetics.* Cold Spring Harbor Laboratory, Cold Spring Harbor, NY.
62. **Zhang X, Bremer H.** 1995. Control of the Escherichia coli rrnB P1 promoter strength by ppGpp. *J Biol Chem* **270**:11181–11189.
63. **Alvarez L, Hernandez SB, de Pedro MA, Cava F.** 2016. Ultra-Sensitive, High-Resolution Liquid Chromatography Methods for the High-Throughput Quantitative Analysis of Bacterial Cell Wall Chemistry and Structure, pp. 11–27. *In* *Bacterial Cell Wall Homeostasis.* Humana Press, New York, NY, New York, NY.
64. **Apweiler R, Bairoch A, Wu CH, Barker WC, Boeckmann B, Ferro S, Gasteiger E, Huang H, Lopez R, Magrane M, Martin MJ, Natale DA, O'Donovan C, Redaschi N, Yeh LSL.** 2004. UniProt: the universal protein knowledgebase. *Nucleic Acids Res* **32**:D115–D119.
65. **Fong C, Rohmer L, Radey M, Wasnick M, Brittnacher MJ.** 2008. PSAT: A web tool to compare genomic neighborhoods of multiple prokaryotic genomes. *BMC Bioinformatics* **9**:170.
66. **Kanehisa M, Goto S, Kawashima S, Okuno Y, Hattori M.** 2004. The KEGG resource for deciphering the genome. *Nucleic Acids Res* **32**:D277–D280.
67. **Saitou N, Nei M.** 1987. The neighbor-joining method: a new method for reconstructing phylogenetic trees. *Mol Biol Evol* **4**:406–425.
68. **Kumar S, Stecher G, Tamura K.** 2016. MEGA7: Molecular Evolutionary Genetics Analysis Version 7.0 for Bigger Datasets. *Mol Biol Evol* **33**:1870–1874.
69. **Tamura K, Nei M, Kumar S.** 2004. Prospects for inferring very large phylogenies by using the neighbor-joining method. *Proc Natl Acad Sci USA* **101**:11030–11035.

Supplementary information for:

Endopeptidase regulation as a novel function of the Zur-dependent zinc starvation response

Shannon G. Murphy^{1,2}, Laura Alvarez³, Myfanwy C. Adams⁴, Shuning Liu^{1,2}, Joshua S. Chappie⁴, Felipe Cava³, Tobias Dörr^{1,2}#

¹ Department of Microbiology, Cornell University, Ithaca, New York, USA.

² Weill Institute for Cell and Molecular Biology, Cornell University, Ithaca, New York, USA.

³ Laboratory for Molecular Infection Medicine, Department of Molecular Biology, Umeå University, Umeå, Sweden.

⁴ Department of Molecular Medicine, College of Veterinary Medicine, Cornell University, Ithaca, NY, USA.

To whom correspondence should be addressed: Tobias Dörr, tdoerr@cornell.edu.

Supplementary Tables (available online)

Table S1. Summary of ShyB homologs that contain an upstream, canonical Zur box.

Table S2. Summary of oligonucleotides used in this study.

Supplementary Figures

Figure S1. *shyA* and *shyC* transcriptional reporters are active in both LB and M9 minimal medium. Related to Figure 1.

Figure S2. The *shyB* promoter is induced by Δ *zur* and Δ *znuABC* deletions on LB agar and repressed by exogenous zinc addition on M9 agar. Related to Figure 2.

Figure S3. Western Blots comparing ShyB and ShyC protein levels in M9 minimal or LB medium. Related to Figure 4.

Figure S4. *shyB* expression driven by chelation, induction, or *zur* deletion restores growth to Δ *shyAC*. Related to Figure 4.

Figure S5. SDS-page gel of purified Shy proteins. Related to Figure 5 & 6.

Figure S6. Identification of mucopeptides released by ShyB digestion of whole *V. cholerae* sacculi. Related to Figure 5.

Figure S7. Sequential and time-dependent digestion of *V. cholerae* sacculi by Shy endopeptidases. Related to Figure 5.

Figure S8. ShyB retains endopeptidase activity in the presence of EDTA *in vitro*. Related to Figure 6.

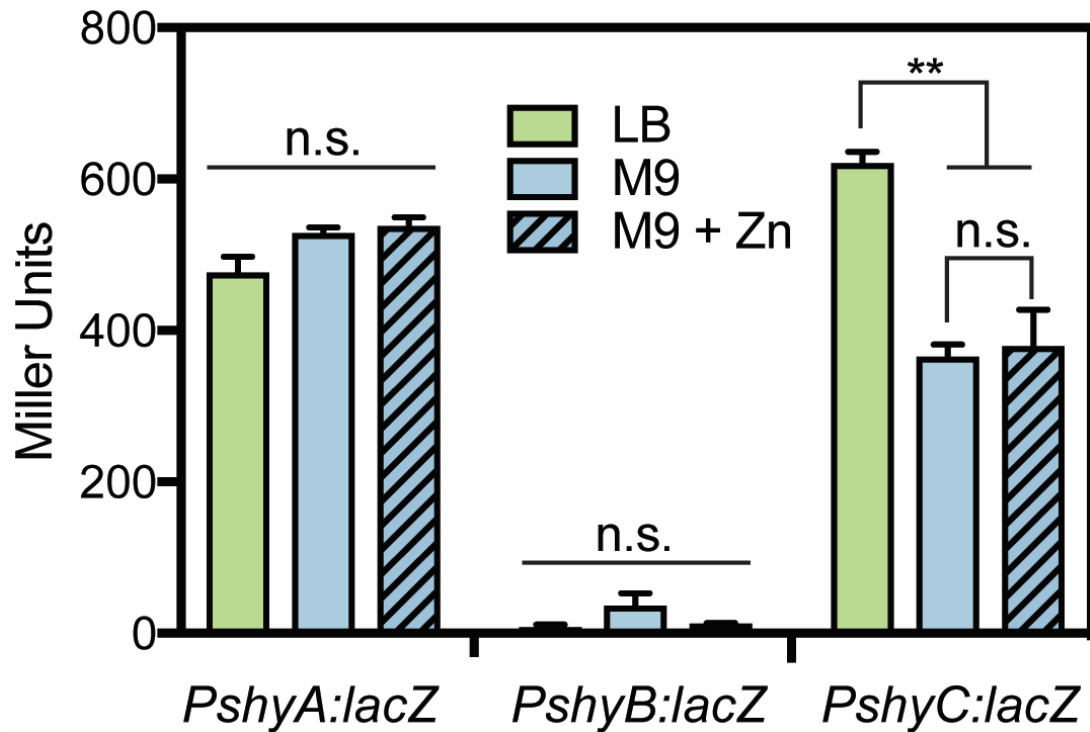


Figure S1. *shyA* and *shyC* transcriptional reporters are active in both LB and M9 minimal medium.

V. cholerae C6706 carrying *PshyA*, *PshyB*, or *PshyC:lacZ* transcriptional fusions were grown from single colony in 5 mL of LB, M9 minimal medium, or M9 plus ZnSO₄ (500 nM) in a 30 °C shaker. β-galactosidase assays were performed (see details in Methods) with 0.5 mL of exponential-phase culture. Error bars represent the standard error of the mean (SEM) of three biological replicates. Statistical significance was measured using a one-way analysis of variance (ANOVA) followed by Dunnett's multiple comparison test (**, p-value < 0.01; n.s., p > 0.05).

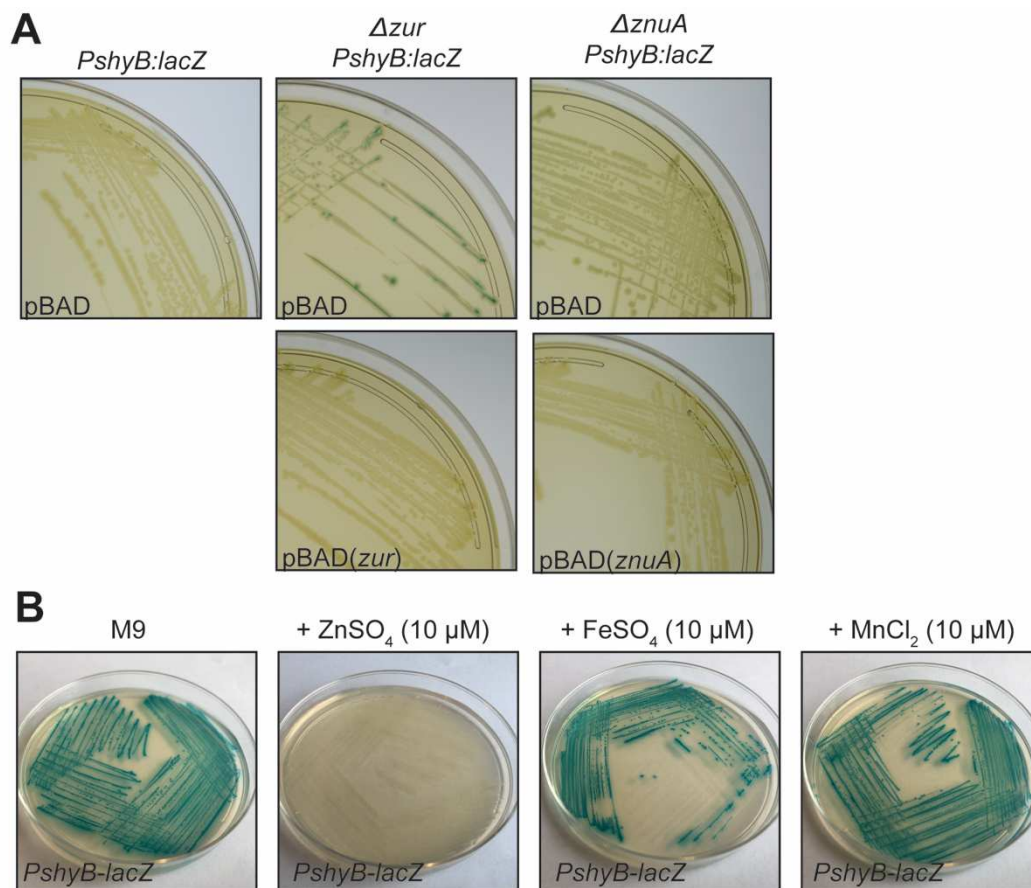


Figure S2. The shyB promoter is induced by Δzur and $\Delta znuABC$ deletions on LB agar and repressed by exogenous zinc addition on M9 agar.

(A) Clean deletions of Δzur and $\Delta znuA$ in *V. cholerae* N16961 carrying the $\Delta lacZ::P_{shyB}:lacZ$ transcriptional reporter were complemented with an arabinose-inducible (pBAD) plasmid that is either empty or carries the respective gene *in trans*. Strains were plated onto LB agar containing X-gal (40 $\mu\text{g mL}^{-1}$), chloramphenicol (10 $\mu\text{g mL}^{-1}$), and arabinose (0.2%). (B) *V. cholerae* N16961 carrying the $\Delta lacZ::P_{shyB}:lacZ$ transcriptional reporter was plated on M9 X-gal (40 $\mu\text{g mL}^{-1}$) agar containing 10 μM of ZnSO₄, FeSO₄, or MnCl₂. (A,B) All plates were incubated overnight at 30 °C and then at room temperature for 2 days.

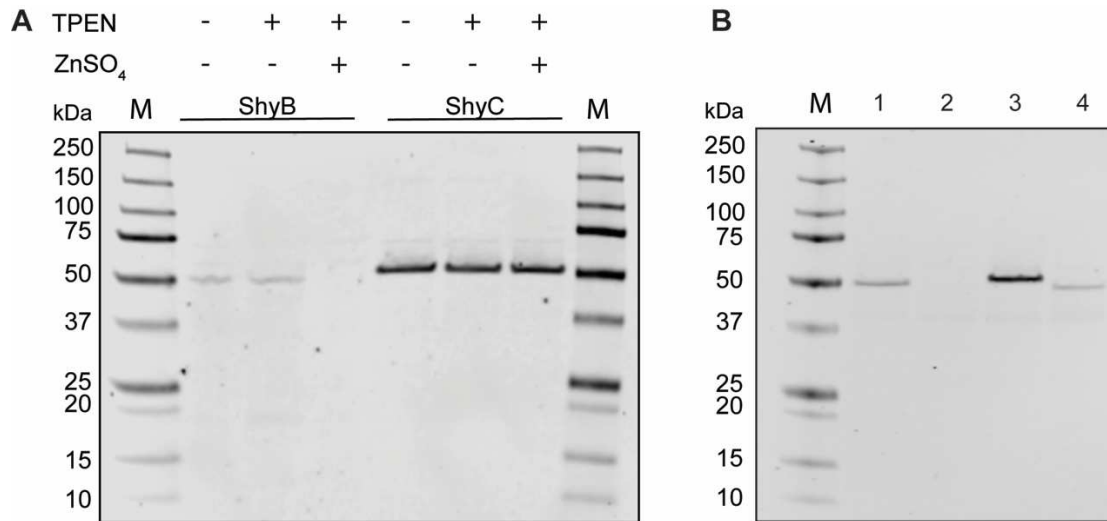
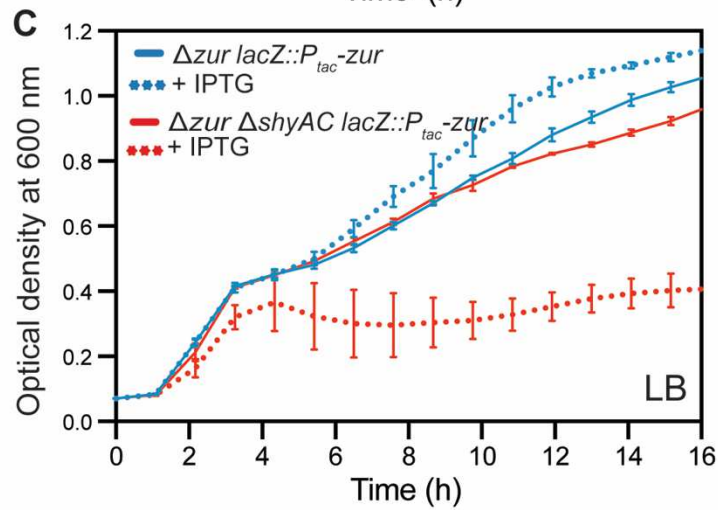
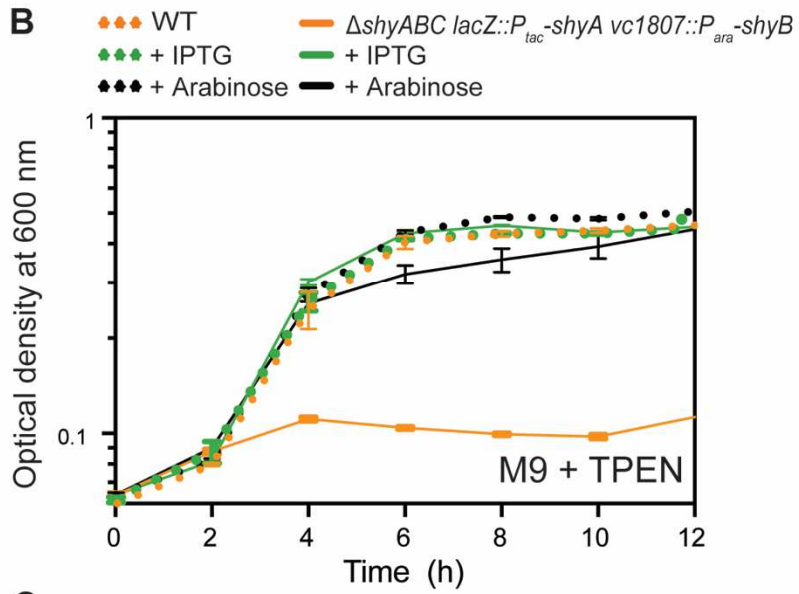
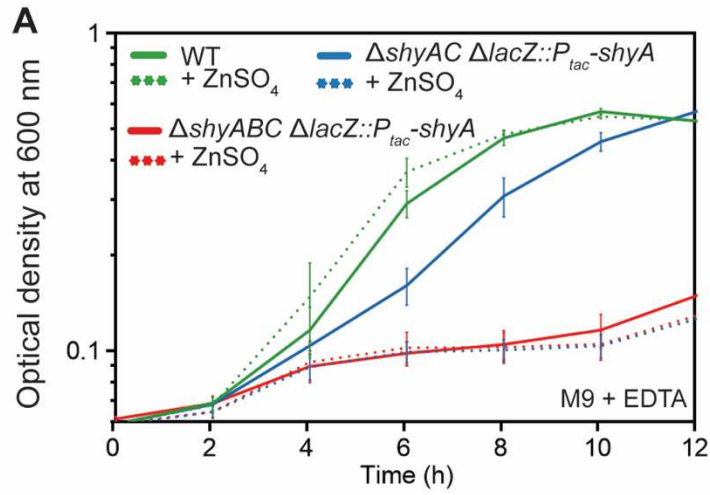


Figure S3. Western Blots comparing ShyB and ShyC protein levels in M9 minimal or LB medium.

(A) N16961 strains encoding tagged chromosomal versions of ShyB Δ LysM::His₆-FLAG (sandwich fusion) or ShyC-His₆-FLAG (C-terminal fusion) were grown in M9 glucose (0.4%) with added TPEN (250 nM) or TPEN plus ZnSO₄ (1 μ M). Cells were harvested at mid-log (OD₆₀₀ = 0.4) and lysed via SDS boiling and sonication. Western blot was performed using standard techniques. Blots were developed using a mouse anti-FLAG F1804 primary antibody (Sigma Aldrich) and Goat anti-Mouse IR CW800 secondary antibody (LI-COR Biosciences). Blots were imaged using a Lycor Odyssey CLx imager. Standard protein marker (M) is shown. (B) N16961 strains with tagged chromosomal versions of ShyA Δ LysM::His/FLAG (Lane 1), ShyB Δ LysM::His/FLAG (Lane 2), and ShyC-His/FLAG (Lane 3) were grown in LB and harvested at mid-log phase (OD₆₀₀ = 0.5). Lane 4 shows ShyB Δ LysM::His/FLAG in a Δ zur background. Western blots were performed as described in above.

Figure S4. *shyB* expression driven by chelation, induction, or *zur* deletion restores growth to $\Delta shyAC$.

(A-B) Strains were grown overnight in LB/streptomycin plus IPTG (200 μ M) at 37 °C. Cells were washed, subcultured 1:10 into M9 glucose (0.4%), and grown at 37 °C for 2 hours. (A) EDTA-chelation restores growth to a $\Delta shyAC$ mutant. Wt (green), $\Delta shyAC lacZ::P_{tac-shyA}$ (blue), and $\Delta shyABC lacZ::P_{tac-shyA}$ (red) strains were diluted 1:100 into M9 glucose (0.4%) containing (A) EDTA (30 μ M) (solid lines) or EDTA plus ZnSO₄ (60 μ M) (dashed lines). (B) Exogenous *shyB* expression supports growth in a $\Delta shyABC lacZ::P_{tac-shyA}$ mutant. Wt (dotted lines) and $\Delta shyABC lacZ::P_{tac-shyA} vc1807::P_{ara-shyB}$ (solid lines) strains were diluted 1:100 in M9 glucose (0.4%) (orange), with 200 μ M IPTG (green) or with 0.2% arabinose (black). (C) *zur* deletion restores growth to a $\Delta shyAC$ mutant in LB medium. Overnight cultures (grown in LB/streptomycin at 37 °C) were subcultured 1:100 into fresh media and grown at 37 °C for 2 hours. $\Delta zur lacZ::P_{tac-zur}$ (blue) and $\Delta zur \Delta shyAC lacZ::P_{tac-zur}$ (red) were diluted 1:100 into LB (solid lines) or in LB plus IPTG (200 μ M) (dashed lines). (A-C) Growth of each 200 μ L culture was measured by optical density (600 nm) in a Bioscreen C 100-well plate. Error bars report standard error of the mean (SEM) for three biologically independent replicates.



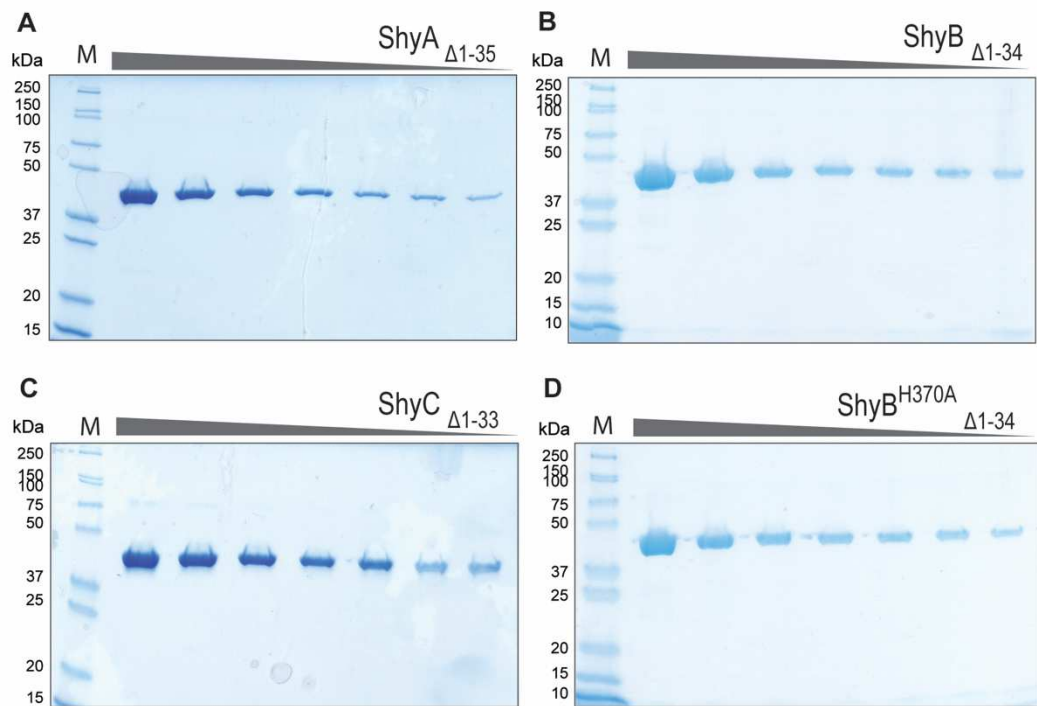
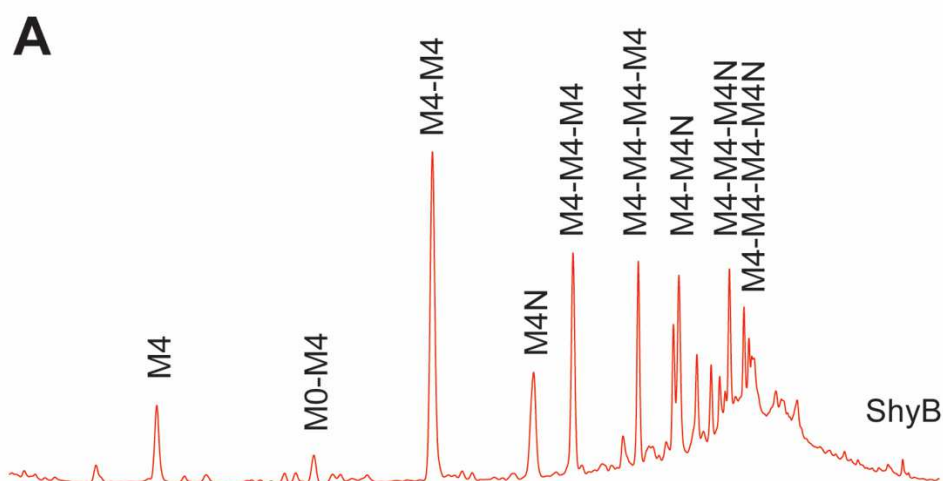


Figure S5. SDS-page gel of purified Shy proteins. Purified recombinant proteins (A) ShyA $\Delta 1-35$, (B) ShyB $\Delta 1-34$, (C) ShyC $\Delta 1-33$, and (D) ShyB^{H370A} $\Delta 1-34$ were run on a SDS-page gel and stained with Coomassie blue. Each lane represents a greater fold dilution of the purified protein. A standard protein marker (M) is shown.



B

Peak	Muropeptide	Monoisotopic mass (g/mol)		Diff.
		Theoretical	Observed	
1	M4	941.408	941.405	0.003
2	M0-M4	1419.588	1419.581	0.006
3	M4-M4	1860.774	1860.753	0.021
4	M4N	921.382	921.377	0.005
5	M4-M4-M4	2782.155	2782.111	0.044
6	M4-M4-M4-M4	3703.537	3703.601	-0.07
7	M4-M4N	1842.763	1842.742	0.021
8	M4-M4-M4N	2764.144	2764.074	0.071
9	M4-M4-M4-M4N	3685.526	3685.478	0.048

Figure S6. Identification of muropeptides released by ShyB digestion of whole *V. cholerae* sacculi. (A) Chromatogram showing the soluble products released by ShyB digestion (same as Fig. 5C). (B) Table of identified muropeptide peaks. Muropeptide identity was confirmed by MS/MS analysis, using a Xevo G2-DX QT of system (Waters Corporation, USA). The difference in theoretical and observed monoisotopic mass (g/mol) was computed for each peak.

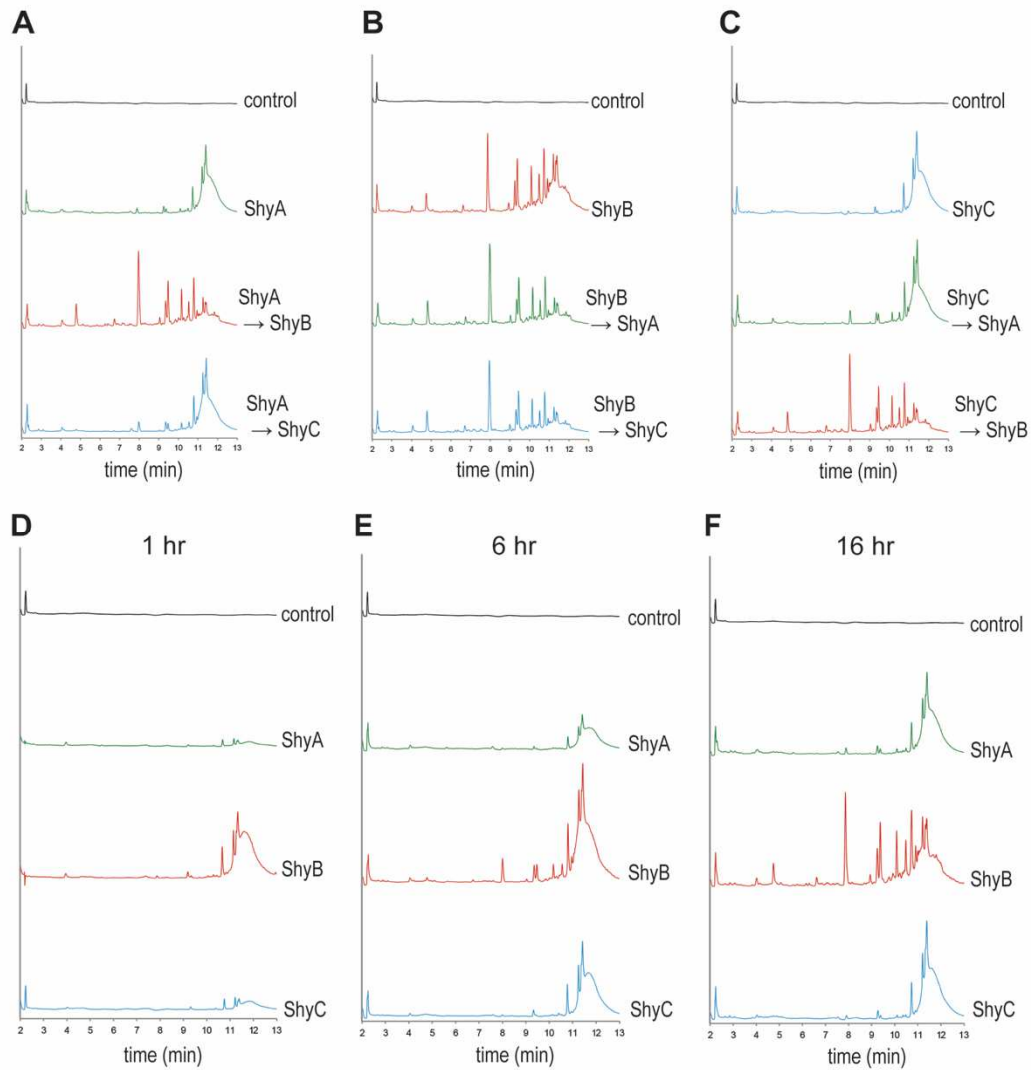


Figure S7. Sequential and time-dependent digestion of *V. cholerae* sacculi by Shy endopeptidases. 10 μ g of purified (A) ShyA, (B) ShyB, and (C) ShyC were incubated with *V. cholerae* sacculi for 16 h at 37 °C, followed by secondary digestion with a different endopeptidase. The soluble products released by digested sacculi were separated by UPLC and quantified by absorbance (204 nm). In a similar experiment, analysis of the soluble muropeptides generated by EP activity was conducted at (D) 1 hr, (E) 6 hr, and (F) 16 hr time points.

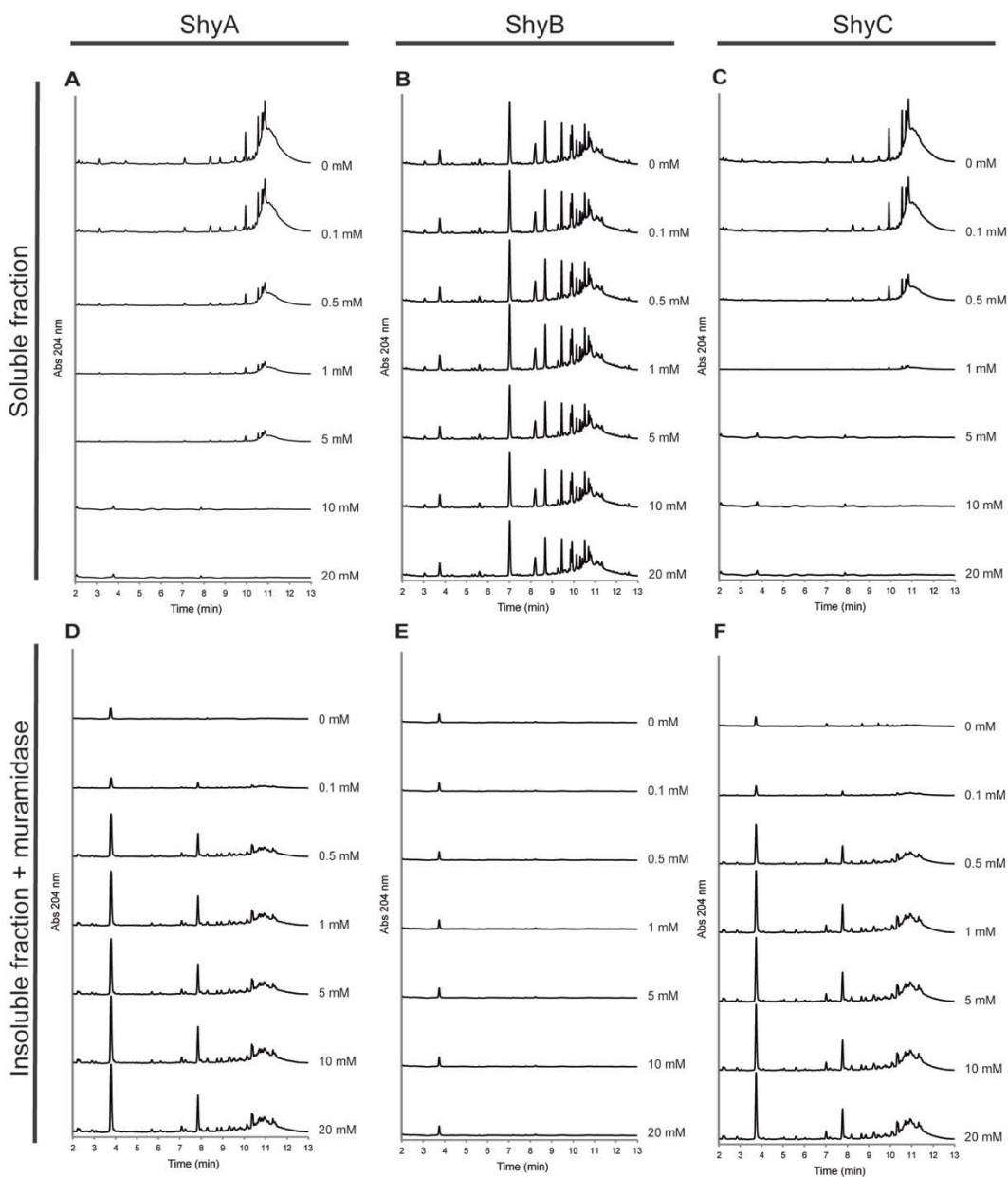


Figure S8. ShyB retains endopeptidase activity in the presence of EDTA *in vitro*. 10 μ g of purified ShyA, ShyB, and ShyC were incubated with *V. cholerae* sacculi for 16 h at 37 °C across a range of EDTA concentrations (0 mM – 20 mM). Muropeptides were separated by UPLC and quantified by absorbance (204 nm) (see Methods for details). The chromatograms for the (A-C) soluble fraction and the (D-F) muramidase-digested insoluble pellet for ShyA (A/D), ShyB (B/E) or ShyC (C/F) treated sacculi are shown.

Chapter 3. *Vibrio cholerae*'s mysterious Seventh Pandemic island (VSP-II) encodes novel Zur-regulated zinc starvation genes involved in chemotaxis and cell congregation

Vibrio cholerae's mysterious Seventh Pandemic island (VSP-II) encodes novel Zur-regulated zinc starvation genes involved in chemotaxis and cell congregation

Shannon G. Murphy^{1,2}, Brianna A. Johnson^{1,3}, Camille M. Ledoux^{1,3}, Tobias Dörr^{1,2,3#}

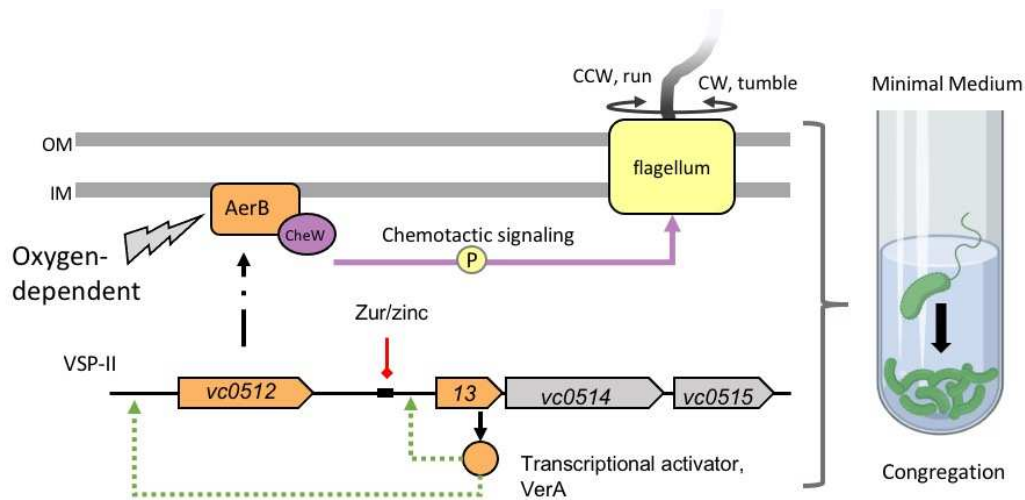
¹ Weill Institute for Cell and Molecular Biology, Cornell University, Ithaca, NY 14853, USA

² Department of Microbiology, Cornell University, Ithaca NY 14853, USA

³ Cornell Institute of Host-Microbe Interactions and Disease, Cornell University, Ithaca NY 14853, USA

To whom correspondence should be addressed: Tobias Dörr, tdoerr@cornell.edu.

GRAPHICAL SUMMARY



ABSTRACT

Vibrio cholerae is the causative agent of cholera, a notorious diarrheal disease that is typically transmitted via contaminated drinking water. The current pandemic agent, the El Tor biotype, has undergone several genetic changes that include horizontal acquisition of two genomic islands (VSP-I and VSP-II). VSP-I and -II presence strongly correlates with pandemicity; however, the contribution of these islands to *V. cholerae*'s life cycle, particularly the 26-kb VSP-II, remains poorly understood. VSP-II-encoded genes are not expressed under standard laboratory conditions, suggesting that their

induction requires an unknown signal from the host or environment. One signal that bacteria encounter under both host and environmental conditions is metal limitation. While studying *V. cholerae*'s zinc-starvation response *in vitro*, we noticed that a mutant constitutively expressing zinc-starvation genes (Δzur) congregates at the bottom of a culture tube when grown in nutrient-poor medium. Using transposon mutagenesis, we found that flagellar motility, chemotaxis, and VSP-II encoded genes were required for congregation. The VSP-II genes encode an AraC-like transcriptional activator (VerA) and a methyl-accepting chemotaxis protein (AerB). Using RNA-seq and *lacZ* transcriptional reporters, we show that VerA is a novel Zur target and activator of the nearby AerB chemoreceptor. AerB interfaces with the chemotaxis system to drive oxygen-dependent congregation and energy taxis. Importantly, this work suggests a functional link between VSP-II, zinc-starved environments, and energy taxis, yielding insights into the role of VSP-II in a metal-limited host or aquatic reservoir.

AUTHOR SUMMARY

The Vibrio Seventh Pandemic island was horizontally acquired by El Tor pandemic strain, but its role in pathogenicity or environmental persistence is unknown. A major barrier to VSP-II study was the lack of stimuli favoring its expression. We show that zinc starvation induces expression of this island and describe a transcriptional network that activates a VSP-II encoded energy taxis receptor. Importantly, aerotaxis may enable *V. cholerae* to locate more favorable microenvironments, possibly to colonize anoxic portions of the gut or environmental sediments.

INTRODUCTION

The Gram-negative bacterium *Vibrio cholerae*, the causative agent of cholera (1), is well-adapted to two distinct lifestyles: as a colonizer of macroinvertebrates in the aquatic environment and as a potentially lethal pathogen inside the human intestine (2). *V. cholerae* persists in aquatic reservoirs by colonizing a variety of (mostly chitinous) biotic surfaces, such as copepods (3-6), shellfish (7, 8), and arthropods (9, 10). *V. cholerae* is ingested via contaminated drinking water or, less commonly, via undercooked seafood (11, 12). Once inside the human host, pathogenic varieties of *V. cholerae* (typically O1 and O139 serovars (13)) rely on virulence factors to establish infection; the toxin co-regulated pilus (TCP) facilitates attachment to the intestinal wall (14, 15) and cholera toxin (CTX) secretion ultimately drives efflux of water and salts from the intestinal epithelium (16). CTX additionally promotes nutrient competition via depletion of free (i.e., not heme-bound) iron in the intestine (17).

The current (seventh) cholera pandemic agent, the O1 serovar El Tor biotype, arose from a non-pathogenic precursor via acquisition of TCP and CTX virulence factors (18). Unlike its pandemic predecessor (the classical biotype), El Tor underwent several changes that include, among others (19), the development of resistance against the antimicrobial peptide polymyxin B (20, 21) and horizontal acquisition of two genomic islands (VSP-I and VSP-II) (22, 23). Presence of islands VSP-I and -II strongly correlates with pandemicity; however, only genes encoded on VSP-I have been directly linked to increased fitness in a host (24). VSP-II is a poorly understood 26-kb island that contains 30 annotated ORFs spanning *vc0490-vc0516* {Taviani:vp}, only two of which have validated functions: an integrase (*vc0516*, (25)) and a peptidoglycan

endopeptidase (*vc0503*, (26)). The remaining uncharacterized genes are predicted to encode transcriptional regulators (VC0497, VC0513), ribonuclease H (VC0498), a type IV pilin (VC0502), a DNA repair protein (VC0510), methyl-accepting chemotaxis proteins (VC0512, VC0514), a cyclic di-GMP phosphodiesterase (VC0515), and 14 hypothetical proteins (23). It is unclear if or how VSP-II enhances the pathogenicity or environmental fitness of El Tor. Intriguingly, VSP-II genes are not expressed under standard laboratory conditions (27), suggesting that their induction requires an unknown signal from the host or environment.

One signal that bacteria encounter under both host and environmental conditions is metal limitation. Bacteria must acquire divalent zinc cofactors from their surroundings to perform essential cellular processes; however, vertebrate hosts actively sequester zinc and other essential transition metals to limit bacterial growth (i.e. nutritional immunity) (28-31). In the environment, *V. cholerae* frequently colonize the chitinous exoskeletons of aquatic and marine invertebrates and exposure to chitin oligomers has been suggested to induce zinc and iron starvation in *V. cholerae* (32). In order to cope with zinc starvation stress, *V. cholerae* encodes a set of genes under the control of the well-conserved Zur repressor. When zinc availability is low, Zur dissociates from a conserved promoter sequence, allowing for expression of downstream genes. *V. cholerae* genes containing a Zur binding region include those encoding zinc import systems (ZnuABC and ZrgABCDE) (33), ribosomal proteins (RpmE2, RpmJ) (34, 35), a GTP cyclohydrolase (RibA) (34), and the VSP-II-encoded peptidoglycan endopeptidase (ShyB) (26).

Here, we show that many genes of the VSP-II island are expressed during zinc starvation. These findings stemmed from an initial observation that a *V. cholerae* Δzur mutant accumulated at the bottom of nutrient-poor liquid cultures. We hypothesized that this behavior was mediated by unidentified members of the Zur regulon. Using a transposon mutagenesis screen and RNA-seq, we identified Zur-regulated congregation factors encoded on VSP-II. These included the transcriptional activator VerA encoded within the *vc0513-vc0515* operon. VerA (Vibrio energy taxis regulator A) activates expression of the AerB (aerotaxis B) chemotaxis receptor encoded by *vc0512*. We show that AerB mediates oxygen-dependent congregation and energy taxis. Importantly, these results implicate a role for VSP-II encoded genes in chemotactic movement in zinc-starved environments.

RESULTS

V. cholerae Δ zur mutant congregates in minimal medium

We noticed serendipitously that a *V. cholerae* N16961 Δ zur mutant (but not the wild type) accumulated at the bottom of a culture tube when grown shaking overnight in M9 minimal medium (**Fig. 1A**). A similar result was observed in static overnight cultures (**Fig. S1A**). Microscopic inspection of Δ zur cells transferred to an agar pad revealed mostly individual cells with no obvious changes in morphology (**Fig. 1B**); the lack of strong cell-to-cell interactions holding these “congregates” together is consistent with the ease at which the pellet was dispersed by agitation (**Movie S1**). *V. cholerae* aggregations in liquid culture are reportedly mediated by numerous mechanisms (e.g. quorum sensing, attachment pili, and O-antigen synthesis (36-43)) and stimuli (e.g. autoinducers, calcium ions (36), cationic polymers (42)), but none thus far have been tied to zinc homeostasis. We therefore sought to identify factors that were required for Δ zur to congregate. Congregation (quantified as the ratio of optical densities (OD_{600nm}) in the supernatant before and after vortexing) was alleviated by complementing *zur* *in trans*, excluding polar effects resulting from *zur* deletion (**Fig. 1C**). We next examined the role of zinc availability on congregation. Since metals can adsorb to the surface of borosilicate glass culture tubes (44), we instead grew *V. cholerae* in plastic tubes and noted that Δ zur still congregated at the bottom (**Fig. S1B**), indicating that this phenotype is not linked to the properties of the culture vessel. Imposing zinc starvation via deletion of genes encoding *V. cholerae*'s primary zinc importer ZnuABC caused cells to congregate similarly to the Δ zur mutant. Congregation of Δ znuABC (which still elaborates the low-affinity zinc transporter ZrgABC (33)) was reversed by zinc

supplementation (**Fig. 1D**). In contrast, the Δzur mutant, which constitutively expresses zinc starvation genes, congregated in both the presence and absence of exogenous zinc. These data indicate that congregation occurs in minimal medium when the Zur regulon is induced (i.e., during zinc deficiency or in a zur deletion strain) and is not a direct consequence of zinc availability *per se*. Surprisingly, none of the annotated members of the Zur regulon were required for congregation (**Fig. 1E, Fig. S1C**), suggesting that there may be other Zur-regulated congregation genes yet to be identified.

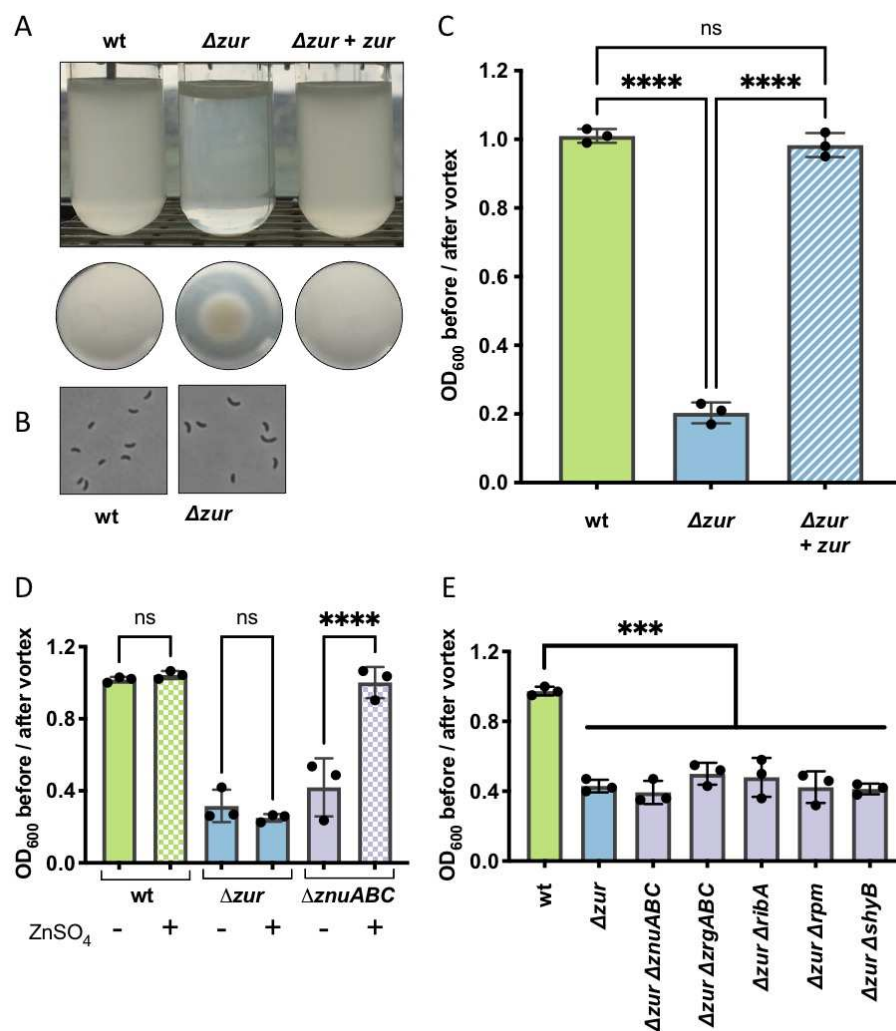


Figure 1. *V. cholerae* Δ zur mutant congregates in M9 minimal medium.

(A-C) Wild-type, Δ zur, and Δ zur carrying an integrated, IPTG-inducible copy of *zur* (denoted + *zur*) were grown overnight at 30°C in M9 minimal medium supplemented with glucose (0.2%) and inducer (IPTG, 500 μ M). (A) Representative side and bottom-view photos of overnight cultures are shown. (B) Cells collected from the bottom of the tube were imaged on an 0.8% agarose pad. (C) Congregation was quantified by measuring the optical density (at 600 nm) of the culture supernatant before and after a brief vortex. A ratio close to 1 represents a homogenous culture, a ratio closer to 0 indicates congregation. (D) Congregation was measured in wild type, Δ zur, and a zinc importer mutant (Δ znuABC) grown in M9 glucose (0.2%) in the absence (solid bars) or presence (checkered bars) of exogenous zinc (ZnSO₄, 1 μ M). (E) Congregation in M9 glucose (0.2%) was measured in wild type, Δ zur, and Δ zur lacking components of the zinc starvation response (*znuABC*, *zrgABC*, *ribA*, *rpmE2/rpmJ2*, or *shyB*). For all plots, the shown raw data points are biological replicates, error bars represent standard deviation, and asterisks denote statistical difference via Ordinary one-way ANOVA test (****, $p < 0.0001$; ***, $p < 0.001$; n.s., not significant).

***Δ zur* congregation requires motility, chemotaxis, and VSP-II encoded proteins**

We reasoned that we could leverage the Δ zur congregation phenotype to identify novel components of *V. cholerae*'s zinc starvation response. To find such Zur-regulated “congregation factors”, we subjected the Δ zur mutant to transposon mutagenesis and screened for insertions that prevent congregation (see Methods for details) (**Fig. 2A**). Δ zur transposon libraries were inoculated into M9 minimal medium and repeatedly sub-cultured until no pellet formed. Transposon insertions sites were identified using arbitrary PCR on isolated colonies (45). The insertions that prevented congregation overwhelmingly mapped to loci encoding motility and chemotaxis genes (**Fig. 2B**). Twenty-four out of 48 recovered transposon mutants were disrupted in flagellar components or motility regulators. We reconstituted these types of mutations in Δ zur by inactivating flagellum assembly (major flagellin subunit, *fliC*) or rotation (motor protein, *motB*). Both Δ zur Δ fliC and Δ zur Δ motB failed to form a pellet and congregation could be restored by complementing each of these genes *in trans* (**Fig. 2C**). These data

suggest that *Δzur* congregation is a motility-dependent process. Additionally, seven transposons inserted within genes encoding parts of *V. cholerae*'s chemotaxis machinery (*che-2*) (**Fig. 2B**); this system modulates bacterial movement in response to a chemical gradient. Mutating a component of this chemotactic phosphorelay (*cheA::STOP*) was sufficient to prevent congregation in *Δzur*, while *trans* expression of *cheA* restored pellet formation to the *Δzur cheA::STOP* mutant (**Fig. 2C**). Deletion of other *che-2* open reading frames also prevented *Δzur* from congregating (**Fig. S1D**). Collectively, these data suggest that motility and chemotaxis are required for *Δzur* congregation in minimal medium.

We noted that the *Δzur* phenotype resembles aggregation in *E. coli* rough mutants, which have reduced expression of lipopolysaccharides (46). We observed similar aggregation in *V. cholerae* rough mutants (*vc2205::kan*), but this aggregation did not require motility to form and is therefore mediated by a distinct mechanism (**Fig. S1E**). We anticipated initially that *Δzur* pellet formation was a group behavior that may require processes associated with surface attachment (e.g., biofilm formation, attachment pili) or cellular communication (e.g., quorum sensing); however, such mutants were not identified by the transposon screen. We thus separately assessed this in a targeted fashion by testing whether *Δzur* congregates when deficient in biofilm formation (*ΔvspL*) or type IV pili attachment ($\Delta 4$: *ΔtcpA ΔmshA ΔpilA*, and orphan pilin *Δvc0502*). Consistent with these processes not answering our screen, biofilm and type IV pili encoding genes were not required for *Δzur* to congregate (**Fig. S1F**). Notably, N16961 contains an authentic frameshift mutation in the quorum sensing gene *hapR* (47, 48); however, a repair to *hapR* (49) did not alter congregation dynamics in *Δzur*

(**Fig. S1G**). We additionally demonstrated that other quorum sensing genes (*ΔcsqA*, *ΔcsqS*, *Δtdh*, *ΔluxQ*, or *ΔluxS*) were dispensable for this phenotype (**Fig. S1F**). Taken together, these data indicate that *Δzur* pellet formation is not a clumping phenomenon driven by typical colonization and congregation factors, but rather a chemotaxis/motility-mediated assembly in the lower strata of a growth medium column.

Since congregation appeared to require induction of the Zur regulon, we were surprised that the transposon screen was not strongly answered by genes with an obvious Zur binding site in their promoters. We reasoned, however, that our screen did not reach saturation due to the large number of motility genes encoded in the *V. cholerae* genome. We therefore refined the screen by pre-selecting for mutants that retained motility on soft agar, followed by a subsequent screen for loss of pellet formation in the motile subset of the mutant pool, as described above. Interestingly, 19 of the 34 transposon insertions answering this screen mapped to the Vibrio Seventh Pandemic island (VSP-II) (**Fig. 2B**, **Fig. S2A-B**), a horizontally acquired genomic region that is strongly associated with the El Tor biotype and the current (seventh) cholera pandemic. Transposons concentrated in a section of VSP-II that encodes a putative AraC-like transcriptional activator (VC0513, henceforth “VerA”), two ligand-sensing chemotaxis proteins (VC0512, formerly Aer-1 is henceforth referred to as “AerB”, and VC0514), and a cyclic di-GMP phosphodiesterase (VC0515). Notably, the *verA/vc0513-vc0515* operon is preceded by a canonical Zur binding site and is thus a novel candidate for Zur-dependent regulation.

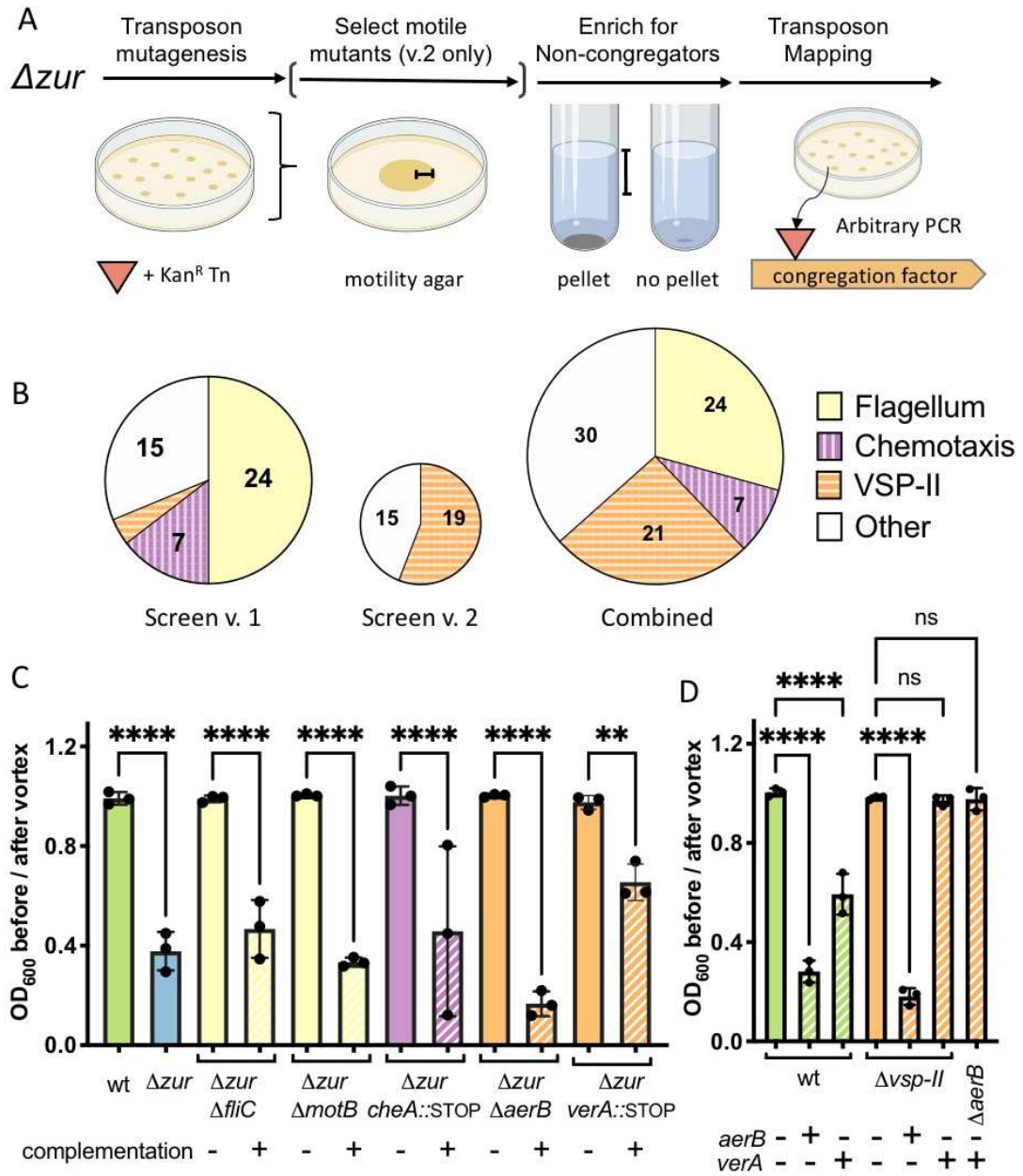
To validate the VSP-II genes’ involvement in *Δzur* congregation, we inactivated each gene in a *Δzur* background through either clean deletion or through insertion of a

premature stop codon. $\Delta aerB$ and $verA::STOP$ mutations prevented Δzur from congregating, whereas respective complementation with $aerB$ and $verA$ restored the pellet (**Fig. 2C**). We noted that although $verA$ and $aerB$ were both required for congregation, transposon hits were concentrated in $verA$. Since a $\Delta zur verA::STOP$ mutant (but not $\Delta zur \Delta aerB$) yields a significantly increased swarm diameter on soft agar (**Fig. S2C**), we speculate that $verA$ insertions were overrepresented in the motile subset of our transposon library. We additionally tested a deletion of the entire VSP-I island and mutations in all other open-reading frames on VSP-II (including $vc0514$ and $vc0515$), none of which were required for Δzur congregation under the conditions tested (**Fig. S1H**).

To determine if either $verA$ or $aerB$ are sufficient to generate congregates, we overexpressed each gene in a wild-type and a $\Delta vsp-II$ background. Both $aerB$ and $verA$ overexpression caused the wild-type to congregate, but only the $aerB$ chemoreceptor triggered congregation in a strain lacking other VSP-II genes (**Fig. 2D**). These data indicated that AerB drives the observed pellet formation and raised the possibility that VerA functions as a transcriptional activator of $aerB$. Altogether, these two screens indicate that pellet formation in Δzur is driven by chemotactic flagellar movement, with assistance from a VSP-II encoded transcriptional activator (VerA) and chemoreceptor (AerB). These results were intriguing given that very little is known about the regulation or function of VSP-II encoded genes.

Figure 2. *zur* pellet formation requires motility and components of VSP-II.

(A) Δzur was mutagenized with mariner transposons to generate a library of insertion mutants (see Methods for details). Non-congregating mutants within the library were enriched via repeated subculturing of the supernatant until no pellet formed. Single brackets indicate harvested zones. Transposon insertions were mapped using arbitrary PCR. In a modified version of this screen (v.2), the transposon library was pre-filtered to select for motile mutants on soft agar (0.3%). Schema created with BioRender.com. (B) Transposon insertions mapped to VSP-II genes (21 hits, orange/horizontal lines), genes encoding flagellar components and regulators (24 hits, yellow) and chemotaxis proteins (7 hits, purple/vertical lines). (C) Select motility (*fliC*, *motB*), chemotaxis (*cheA*), and VSP-II genes (*vc0512/aerB*, *vc0513/verA*) were mutated in a Δzur background (solid bars) and complemented back *in trans* (+) under an IPTG inducible promoter integrated within chromosomal *lacZ*. (Note: P_{iptg} -*verA* on a multicopy plasmid was used for complementing the Δzur *verA*::*STOP* mutant. These cultures were grown with kanamycin to ensure retention of either the empty or *verA*-expressing plasmid). Congregation in M9 glucose (0.2%) supplemented with inducer (IPTG, 100 μ M) was quantified by measuring the optical density (at 600 nm) of the culture supernatant before and after a brief vortex. (D) Integrated, chromosomal copies of *aerB* or *verA* were overexpressed in wild-type and $\Delta vsp-II$ (or a $\Delta aerB$) backgrounds in M9. Ten and 200 μ M of IPTG were used for *aerB* and *verA* induction, respectively. For all plots, the shown raw data points are biological replicates, error bars represent standard deviation, and asterisks denote statistical difference via Ordinary one-way ANOVA test (****, $p < 0.0001$; **, $p < 0.01$; n.s., not significant).



Several VSP-II genes are significantly upregulated in a Δzur mutant

Prior inquiry into VSP-II function was made difficult by a lack of native gene expression under laboratory conditions; thus, we prioritized mapping the transcriptional networks embedded in this island. Our data implies that the VSP-II genes of interest are expressed in Δzur . Indeed, the *verA* promoter region contains a highly conserved Zur-binding sequence approximately 200 bp upstream of the mapped transcription start site (determined by 5'-RACE in a Δzur mutant, **Fig. 3A, S3**). Although the distance between the Zur box and transcriptional start site is greater than that observed for most *V. cholerae* Zur targets, equivalent or greater distances are noted for the Zur-regulated *ribA* (140-210 bp upstream of the ORF) and *zbp* (~380 bp upstream of ORF) in closely related *Vibrio spp.*, respectively (34). To verify regulation by Zur, we measured *verA* promoter activity via a *lacZ* transcriptional fusion ($P_{verA-lacZ}$), which encodes β -galactosidase (LacZ) and gives a colorimetric readout in the presence of a cleavable substrate (e.g., ONPG). As expected, transcription from the *verA* promoter in zinc-rich LB medium was robust in Δzur relative to wild-type or a *zur* complemented strain (**Fig. 3B**). This data indicates that Zur negatively regulates *verA* transcription in a rich medium. We also tested $P_{verA-lacZ}$ expression in M9 minimal medium in a wild-type, Δzur , and $\Delta znuABC$ background and noted that promoter activity corresponded to the conditions in **Fig. 1D** that triggered congregation (**Fig. 3C**). P_{verA} activity was low in the wild-type background, indicating that *V. cholerae* is not zinc-deficient in our M9 liquid culture. In contrast, P_{verA} activity was robust in both Δzur and a mutant deficient in zinc uptake ($\Delta znuABC$). Consistent with Zur's zinc sensing function, $\Delta zur P_{verA-lacZ}$ strain retained high levels of β -galactosidase activity regardless of zinc availability, whereas $P_{verA-lacZ}$

in *ΔznuABC* was repressible with exogenous zinc. These data, in conjunction with the highly conserved Zur binding site, suggest that the VerA-encoding *vc0513-vc0515* operon is a novel component of the Zur-regulated zinc starvation response in N16961.

Global transcriptomic studies of the Zur regulon have been conducted in a number of bacteria, but none thus far have been reported in the *Vibrio* genera (50-67). We thus performed an RNA-seq experiment comparing transcript abundance in wild-type N16961 and *Δzur* to assess *V. cholerae*'s Zur regulon more comprehensively (including indirect effects). To ensure sufficient repression of Zur targets in the wild-type, cells were grown to mid-log phase in LB medium. Analyses identified 58 differentially expressed genes in *Δzur* (log 2-fold change >1, adjusted p-value <0.05) (**Fig. 3D, Fig. S4, Table S2**). Seven promoters (situated in proximity to 23 of the 42 upregulated genes) contained an upstream canonical Zur-binding site. Among them were known or inferred (based on *E. coli*) Zur regulon components, including genes that encode zinc uptake systems (ZnuABC, ZrgACD), an alternative ribosomal protein (RpmE2), and a GTP cyclohydrolase (RibA). This transcriptomic analysis also uncovered what appears to be a bidirectional promoter with a Zur box: this locus encodes a strongly upregulated ABC-type transporter (*vca1098-vca1101*) in one direction and upregulated portions of the chemotaxis-3 (*che-3*) cluster (*vca1091-vca1095*, *vca1097*) in the other. Using a *lacZ* transcriptional reporter, we verified that the ABC-type transporter is indeed Zur-regulated (**Fig. S5**). Neither the transporter nor the *che-3* cluster (*vca1090-vca1097*), however, were required for *Δzur* congregation (**Fig. S1C**). We observed a striking cluster of nine up-regulated genes on VSP-II (comprising 35% of the open reading frames on VSP-II), including the previously

characterized peptidoglycan hydrolase ShyB (encoded by *vc0503*) and the *verA/vc0513-vc0515* operon, consistent with our transcriptional fusion data and the transposon screen (**Fig. 3D-E**).

The RNA-seq analysis also identified 36 differentially expressed genes that lacked canonical Zur binding sites (**Fig. 3D-E, Fig. S4, Table S2**). Nineteen of these genes were significantly up-regulated in Δzur , including several genes on VSP-II (*vc0504-vc0508* and *vc0512*) and VSP-I (*vspR/vc0177*, *capV/vc0178*). Other upregulated transcripts in Δzur encode for cholera toxin (*ctxA/B*), the toxin co-regulated pilus biosynthesis proteins (*tcpT/H*), and a chitin binding protein (*gbpA*). Seventeen genes were significantly down-regulated in Δzur , many of which were related to vibrio polysaccharide (VPS) synthesis and biofilm formation (68). Thus, a *zur* deletion affects numerous genes indirectly, possibly through Zur-dependent secondary regulators (e.g. VC0515, cyclic di-GMP phosphodiesterase; VerA, AraC-like transcriptional regulator), via secondary responses to the influx of zinc that the Δzur mutant is expected to experience, or via Zur-dependent small RNA interference. We did conduct a perfunctory analysis of small RNAs and encourage interested research communities to utilize our data deposited in NCBI GEO to pursue additional lines of inquiry.

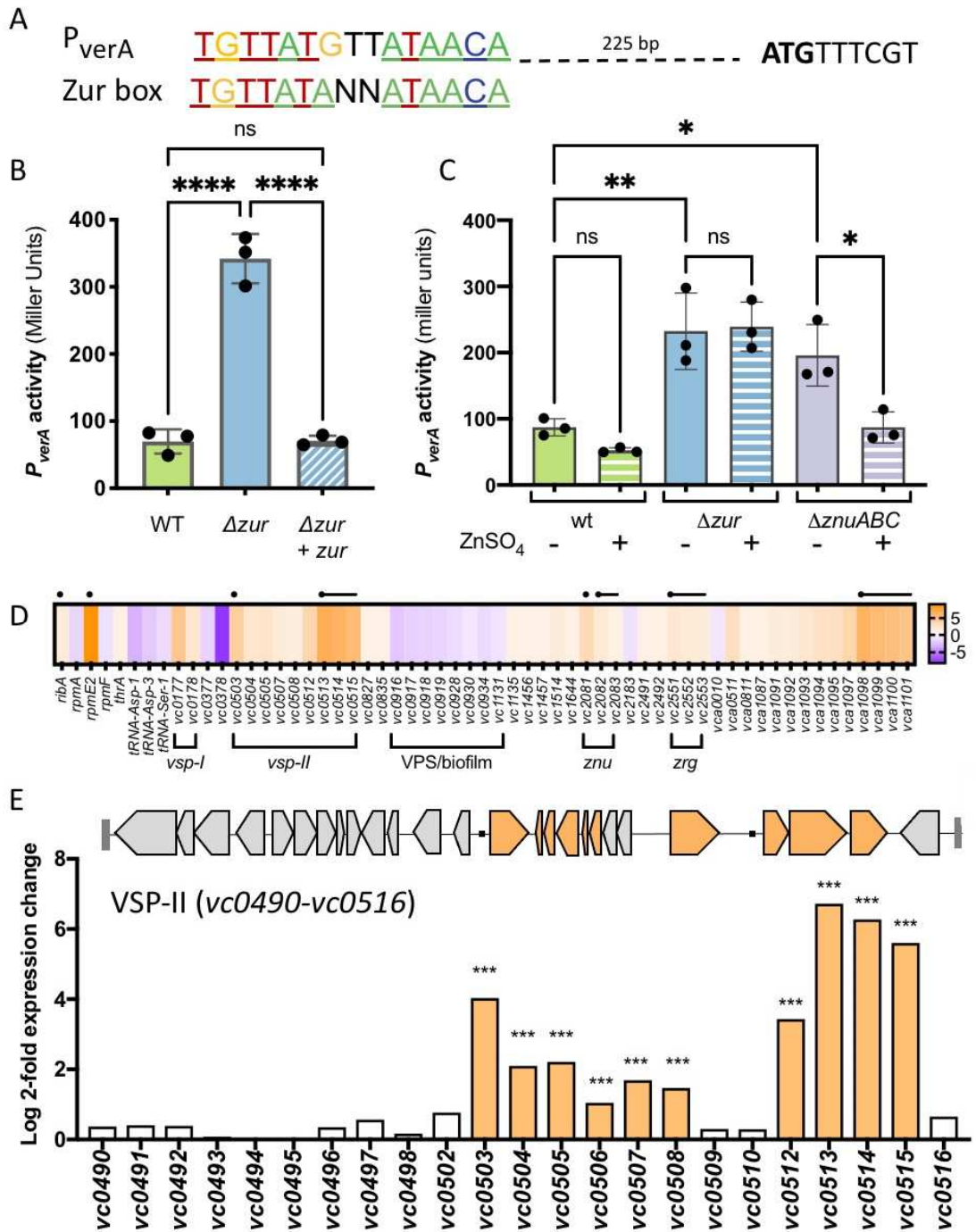
Figure 3. Several VPS-II genes are upregulated in a Δzur mutant.

(A) A predicted Zur-binding site (TGTTATGTTATAACA) located approximately 200 bp upstream of the *verA* open reading frame was aligned with the *Vibrionaceae* Zur binding consensus sequence (34). A predicted start codon (ATG) is indicated in bold.

(B) *P_{verA}-lacZ* transcriptional reporters were introduced into a wild-type and Δzur background, paired with either an empty vector or IPTG-inducible copy of *zur* (+ *zur*). Strains were grown overnight and diluted 1:100 into LB with kanamycin and inducer (IPTG, 200 μ M). After 3 hours of growth at 37°C (to mid/late exponential phase), promoter activity was quantified in Miller Units by measuring β -galactosidase (LacZ) activity against an ONPG chromogenic substrate (see Methods for more details).

(C) Wild-type, Δzur , and $\Delta znuABC$ mutants carrying the *P_{verA}-lacZ* reporter were grown in M9 minimal medium in the presence (+) and absence (-) of exogenous zinc ($ZnSO_4$, 1 μ M). After overnight growth (~16 h), promoter activity was measured in Miller units. For bar graphs, raw data points represent biological replicates, error bars represent standard deviation, and asterisks denote statistical difference via Ordinary one-way ANOVA (****, $p < 0.0001$; **, $p < 0.01$; *, $p < 0.05$; and n.s., not significant).

(D-E) RNA was isolated from cells at mid-log phase and prepared for RNA-seq (see Methods and Materials). Genes with significant differential expression in Δzur (log 2-fold change > 1 , adjusted p-value < 0.05) relative to wild-type N16961 are shown. (D) The heat map indicates increased (orange) or decreased (purple) expression relative to the wild-type strain. Black circles represent putative Zur binding sites and lines represent corresponding operons. (E) Log 2-fold expression changes for all VSP-II genes (*vc0490-vc0516*) are shown alongside a schematic of VSP-II open reading frames. Black circles indicate present of canonical Zur binding sites on VSP-II.



VerA is a Zur-regulated transcriptional activator of aerB

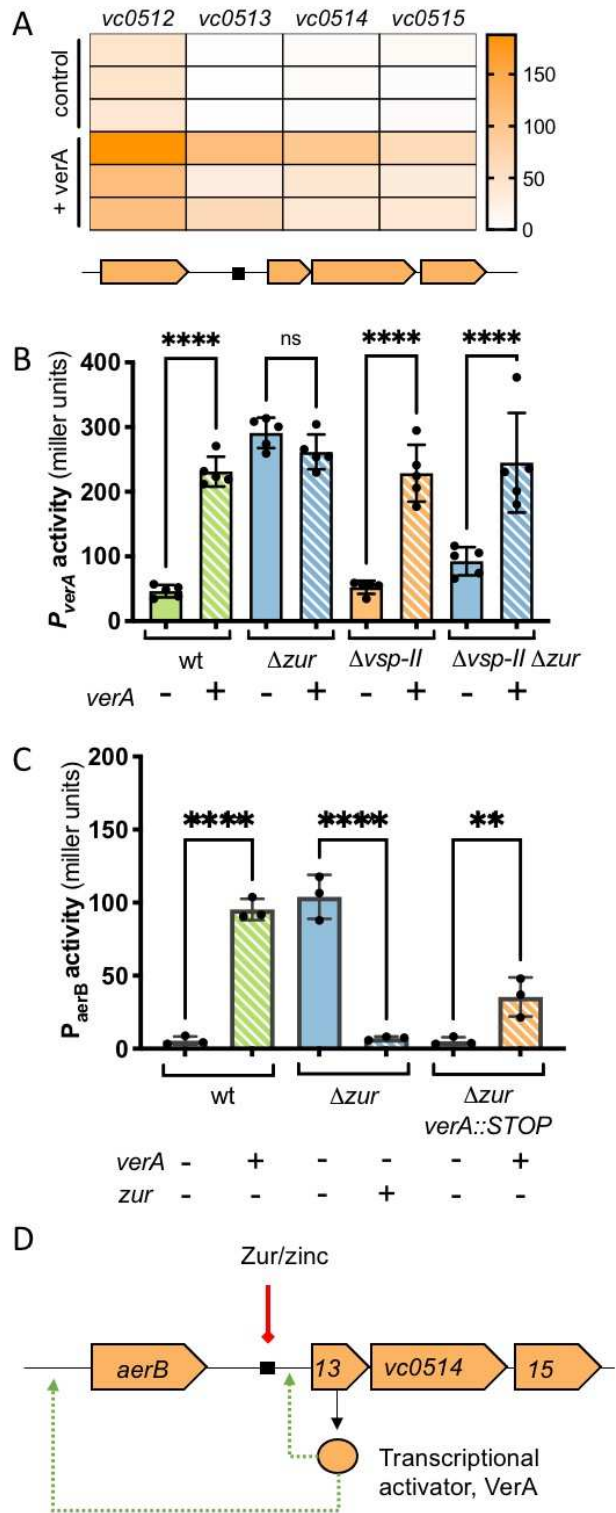
Our mutational analyses above raised the possibility that the putative methyl accepting chemotaxis protein (MCP) AerB is controlled by the transcriptional activator VerA. Given the importance of AraC-family regulators in governing *V. cholerae*'s host-associated behaviors (e.g., ToxT, intestinal colonization and virulence (69-72); Tfos, chitin-induced natural competence (73-75)) we sought to characterize the full VerA regulon. We performed an RNA-seq experiment comparing transcript abundance in N16961 overexpressing *verA*, relative to an empty vector control. Surprisingly, only three other genes were significantly upregulated (log 2-fold change >1, adjusted p-value <0.05): *vc0512/aerB*, *vc0514*, and *vc0515* (**Fig. 4A, Table S3**). We validated these findings using *lacZ* transcriptional reporters. Plasmid-mediated *verA* overexpression was sufficient to induce P_{verA} -*lacZ* in rich LB medium, suggesting that this operon is autoregulated by VerA (**Fig. 4B**). To remove the autoregulatory effect of native VerA from our analysis, we performed additional measurements in a parent strain lacking VSP-II (and thus native *verA*). These data suggest that loss of Zur binding may lead to only a small increase in *verA* transcription, which is further amplified by a VerA-dependent positive feedback loop.

Interestingly, the *aerB* promoter lacks a conserved Zur binding site; however, our transcriptomic data suggests that Zur-regulated VerA promotes *aerB* transcription. To verify this, we constructed a P_{aerB} -*lacZ* transcriptional reporter. Our initial attempt using a small (400 bp) promoter fragment did not yield detectable signal under inducing conditions (**Fig. S6**). 5'-RACE mapping of the transcription start indicated that *aerB* is part of a much longer transcript (extending >1 kb upstream of the start codon). Thus,

we designed a new reporter construct to include this entire region. P_{aerB} activity in standard LB medium fell below our threshold for detection, but we found that VerA overexpression was sufficient to activate the *aerB* promoter (**Fig. 4C**). P_{aerB} was strongly induced in a Δzur strain background – consistent with our initial RNA-seq – but only if the strain also carried a native or *trans* copy of *verA*. These data indicate that *aerB* expression is dependent upon VerA-mediated activation. In summary, we found that VerA is a Zur-regulated, transcriptional activator that upregulates four genes (*aerB*, *verA/vc0513-vc0515*) (**Fig. 4D**).

Figure 4. VerA is an AraC-like transcriptional activator that positively regulates *aerB* and the *vc0513-vc0515* operon.

(A) Overnight cultures of wild-type N16961 carrying either an IPTG-inducible copy of *verA* (+ *verA*) or empty vector (control) were diluted 1:100 in fresh LB containing kanamycin and IPTG (1 mM). RNA was isolated from cells at mid-log phase and prepared for RNA-seq (see Methods and Materials). Heat map shows normalized expression values for differentially expressed genes across three biological replicates. (B-C) Overnight cultures strains carrying *lacZ* transcriptional reporters were diluted 1:100 in LB and grown for 3 h at 37°C. Kanamycin and inducer IPTG (500 μ M) were included in the growth medium for *trans* expression (+) of *verA* or *zur* from an IPTG-inducible promoter. Promoter activity (in Miller Units) was measured via β -galactosidase assays (See Methods and Materials). (B) $P_{verA-lacZ}$ activity was measured in wild-type, Δzur , $\Delta vsp-II$, and $\Delta zur \Delta vsp-II$ strains carrying a plasmid-borne, IPTG-inducible copy of *verA* (+, striped bars) or an empty vector control (-, solid bars). (C) Activity from a $P_{aerB-lacZ}$ reporter was measured in wild-type, Δzur , and $\Delta zur verA::STOP$ backgrounds harboring a plasmid-borne, IPTG-inducible copy of *verA* or *zur* (+, striped bars) or empty vector control (-, solid bars). (D) Proposed model for Zur repression of the *verA* promoter (solid line, red) via a conserved Zur binding site and subsequent VerA-dependent activation (green dashed arrow) of the *aerB* and *verA* promoters.



AerB mediates energy taxis away from air-liquid interface

VerA-mediated induction of AerB drives *V. cholerae* to congregate in minimal medium. AerB is predicted to encode an MCP that senses concentration gradients of a particular ligand (either an attractant or repellent) and relays that signal via Che proteins that alter flagellar rotation (76). To determine if AerB indeed functions as a chemotaxis receptor, we first tested whether AerB interacts with the chemotaxis coupling protein, CheW. In a bacterial two hybrid assay, AerB and CheW were each fused with one domain of the adenylate cyclase (AC) protein (T18 or T25) and co-transformed into an *E. coli* strain. If the proteins of interest interact, the proximal AC domains will synthesize cAMP and induce *lacZ* expression via a cAMP-CAP promoter; thus, a positive protein interaction will yield blue colonies in the presence of X-gal. *E. coli* co-transformed with T18-AerB and CheW-T25 (or the reciprocal tags) yielded bright blue spots (**Fig. 5A**). We additionally detected strong protein-protein interaction between T18-AerB and T25-AerB, indicating that our chemoreceptor can dimerize (or oligomerize) like other MCPs (77). To confirm that AerB's MCP signaling domain is required for congregation, we next mutated a glycine residue within the highly conserved C-terminal hairpin loop (R-A-G-E/D-X-G) (78) of AerB (**Fig. S7**), which is required for *in vitro* signal generation in other MCPs (79). A $\Delta vsp-II$ strain expressing AerB[G385C] was unable to congregate (**Fig. 5B**), consistent with MCP function. Together, these data strongly suggest that AerB indeed functions as a chemotaxis receptor.

Intriguingly, the chemical ligands for AerB and the vast majority of *V. cholerae*'s 46 encoded MCPs are yet to be determined (80). The AerB N-terminus harbors a PAS domain (81), a protein family that typically senses light, oxygen, redox

stress, or electron acceptors (82). We hypothesized that the PAS-containing chemoreceptor mediates energy taxis along the oxygen gradient in our vertical culture tubes. We first tested whether oxygen was required for Δzur to congregate. Wild-type and Δzur were cultured in both aerobic and anoxic tubes in M9 minimal medium with the terminal electron acceptor fumarate to enable anaerobic glucose respiration. Unlike the aerobic cultures, Δzur did not congregate under anoxic conditions (**Fig. 5C-D**). A similar result was observed under glucose-fermenting conditions (i.e., when fumarate was omitted from the medium) (**Fig. S8**). These data indicate that Δzur congregation is oxygen-dependent and implicate AerB in energy taxis.

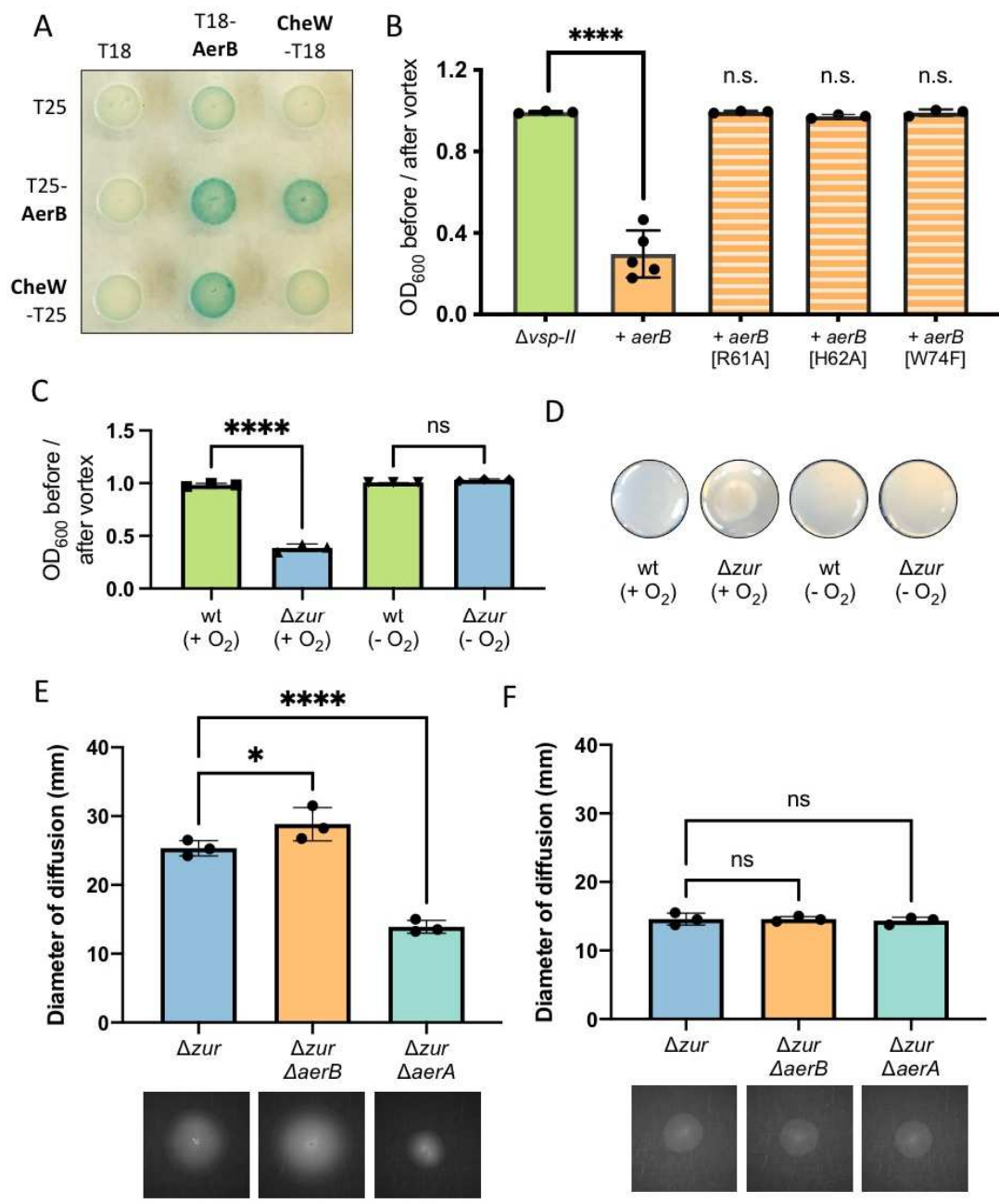
AerB shares 31% amino acid identity with *V. cholerae*'s aerotaxis receptor Aer-2 (renamed here to AerA, as numbers in bacterial gene names can be confused with mutant alleles) (**Fig. S7A**), which exhibits a positive response to oxygen (83). Other homologs include *E. coli*'s Aer^{EC} (B0372, 31% identity), which positively responds to oxygen via sensing the electron acceptor FAD (82, 84, 85). Alignment of AerB with homologs from *Azospirillum brasilense* (86) and *Shewanella oneidensis* (87) revealed conservation of a critical FAD-binding tryptophan residue, among others (**Fig. S7B**). The corresponding amino acids were mutated in *aerB* and each mutant was expressed in a $\Delta vsp-II$ background to determine whether they still promoted congregation. Strains expressing W74F failed to congregate, suggesting the FAD-binding residue is essential for function (**Fig. 5B**). Two additional mutants (R61A and H62A), corresponding to *E. coli* FAD-binding residues, were also unable to congregate. The requirement for oxygen and these highly conserved FAD-binding residues suggests that AerB may bind FAD or a similar ligand to facilitate energy taxis.

Based on our congregation phenotype, we hypothesized that, in contrast to AerA and Aer^{EC}, AerB appears to mediate a negative response to oxygen and cause cells to accumulate at the bottom of the culture tube. To further interrogate energy taxis, we examined the swarming dynamics of *V. cholerae* in an established aerotaxis assay, which uses soft agar with carbon sources that vary in their ability to accentuate aerotaxis behavior (83, 84). Succinate, for example, can only be catabolized via respiration, which consumes oxygen, thereby generating an O₂ gradient that increases with distance from the inoculation site. Since no other classical attractants/repellents are present, motility on succinate plates reveals aerotaxis as the primary taxis behavior (84). In contrast, maltose agar provides other cues for chemotaxis (including chemotaxis towards maltose itself), obscuring an aerotactic response. The diameter of diffusion in succinate and maltose (at 30°C) was measured two days post-inoculation. All assays were performed in a Δzur background to ensure robust expression of *aerB* from the native promoter and *aerA* mutants were included as a control. Compared to Δzur , the diameter of $\Delta zur \Delta aerB$ migration on succinate was significantly increased (**Fig. 5E**, **Fig. S9A-B**). This is consistent with AerB promoting a negative response to oxygen. Conversely, $\Delta zur \Delta aerA$ showed a significant decrease in swarming ability, consistent with AerA promoting a positive response to oxygen, as previously reported (83). In contrast to swarming behavior on succinate, there were no significant differences between the swarm diameter of Δzur and the *aer* mutants on maltose plates (**Fig. 5F**, **Fig. S9C-D**). These assays were additionally performed in a wild-type background and *aerB* showed no effect on swarming behavior (**Fig. S9**), consistent with lack of *aerB* transcriptional expression in wild-type background. These results corroborate AerB's function as an

energy taxis receptor and suggest that it mediates an inverse response relative to AerA.

Figure 5. AerB encodes a methyl-accepting chemotaxis protein involved in energy taxis.

(A) In a bacterial two-hybrid assay, *E. coli* BTH101 was co-transformed with vectors carrying one domain of adenylate cyclase (T18 or T25) or an adenylate cyclase fusion with a protein of interest: CheW-T(18/25) or T(18/25)-AerB. Co-transformants were spotted onto an LB agar containing kanamycin and ampicillin (for selection), X-gal (for blue-white detection), and inducer (IPTG, 500 μ M). Plates were incubated overnight at 30°C and for an additional day at room temperature. Blue color signifies positive protein-protein interactions. (B) Δ *vsp-II* strains carrying an integrated, IPTG-inducible copy of either *aerB* or *aerB* point mutants (G385C, R61A, H62A, or W74F) were grown shaking overnight in M9 minimal medium supplemented with glucose (0.2%) and inducer (IPTG, 10 μ M) at 30°C. Congregation was quantified by measuring the optical density (at 600 nm) of the culture supernatant before and after a brief vortex. (C) Wild-type and Δ *zur* were grown overnight in 5 mL M9 minimal medium plus glucose (0.5%) and a terminal electron acceptor (fumarate, 50 mM). Cultures were grown aerobically (+ O₂) or anoxically (- O₂) (see Methods for details). Tubes were grown shaking overnight at 30°C and congregation was quantified as described above. (D) Representative images of the bottom of each culture tube are shown. (E-F) Strains were grown overnight in LB medium and washed thrice in M9 minimal medium lacking a carbon source. A sterile toothpick was used to inoculate cells into M9 soft agar (0.3%) containing either (E) succinate (30 mM) or (F) maltose (0.1 mM) as a carbon source. The diameter of diffusion (mm) was measured following a 48-hr incubation at 30°C and representative diffusion patterns are shown for each strain. For all bar graphs, raw data points represent biological replicates, error bars represent standard deviation, and asterisks denote statistical difference via Ordinary one-way ANOVA test (****, $p < 0.0001$; *, $p < 0.05$; n.s., not significant).



Ectopic AerB induces congregation in El Tor strains with atypical VSP-II islands

Although the VSP-II island is strongly correlated with the 7th pandemic strain, variants of this island have been detected in other El Tor isolates (**Fig. 6A**). The Zur-regulated VSP-II genes characterized in this study appear to be in a hotspot for island variation: C6706 (Peru, 1991) lacks *vc0511-vc0515* while the Haiti strain (2010) lacks *vc0495-vc0512*. We predicted that only El Tor Δzur strains with prototypical islands (harboring *aerB/vc0512* and *verA/vc0513*) will congregate in minimal medium. As expected, the prototypical VSP-II strains (N16961 and E7946) lacking *zur* congregated in overnight culture (**Fig. 6B**). This suggests that Δzur congregation phenomenon is likely not due to strain-specific variations outside of VSP-II. In contrast, neither the C6706 nor the Haiti mutant congregated in minimal medium, presumably due to the absence of *aerB*. To test whether we could promote congregation in these VSP-II variants, we expressed a chromosomally integrated, inducible copy of *aerB* in C6706 and Haiti. Similar to the N16961 $\Delta vsp-II$ control, C6706 and Haiti expressing *aerB* congregated in minimal medium (**Fig. 6C**). These data suggest that AerB's interaction partners are conserved in other *V. cholerae* El Tor isolates.

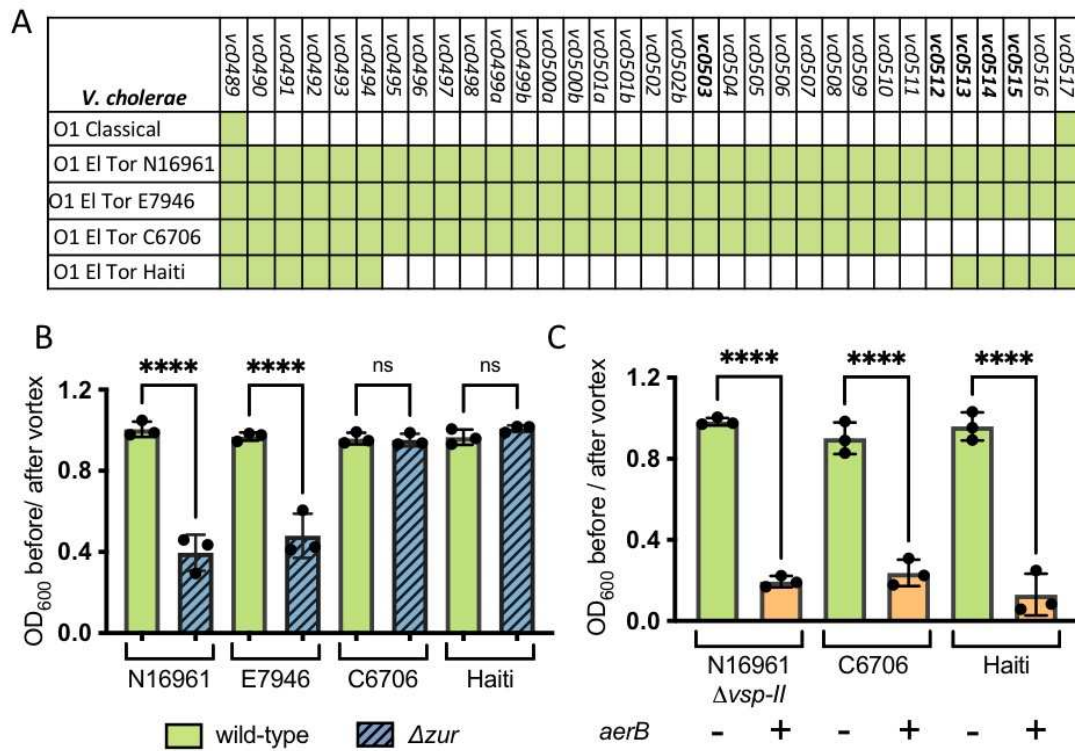


Figure 6. Ectopic AerB expression causes atypical El Tor strains to congregate.

(A) Presence (green) or absence (white) of VSP-II open reading frames in *V. cholerae* strains with prototypical (N16961, E7946) and variant (Haiti, C6706) VSP-II islands are shown. (B) Wild-type or Δzur varieties of *V. cholerae* (N16961, E7946, C6706, Haiti) were grown overnight (~15 hr) shaking at 30°C in M9 minimal medium with glucose (0.2%). Congregation was quantified by measuring the optical density (at 600 nm) of the culture supernatant before and after a brief vortex. (C) *V. cholerae* strains with (+) or without (-) IPTG-inducible, chromosomal copy of *aerB* were grown as described in B but with the addition of IPTG (10 μ M). For all bar graphs, raw data points represent biological replicates, error bars represent standard deviation, and asterisks denote statistical difference via Ordinary one-way ANOVA (****, $p < 0.0001$; n.s., not significant).

A model for oxygen-dependent V. cholerae congregation in zinc starved environments

In summary, we propose the following model for Δzur congregation in M9 minimal medium (Fig. 7). In zinc rich conditions, Zur acts as a repressor of the VerA-encoding *vc0513-vc0515* operon on VSP-II. In the absence of Zur or in zinc starvation, the VerA transcriptional activator induces expression of its own operon and the nearby *aerB*. AerB serves as a receptor for oxygen-dependent energy taxis and relays changes in signal concentration to the core chemotaxis machinery and the flagellum. This results in cells congregating at the bottom of the culture tube in an oxygen-dependent manner.

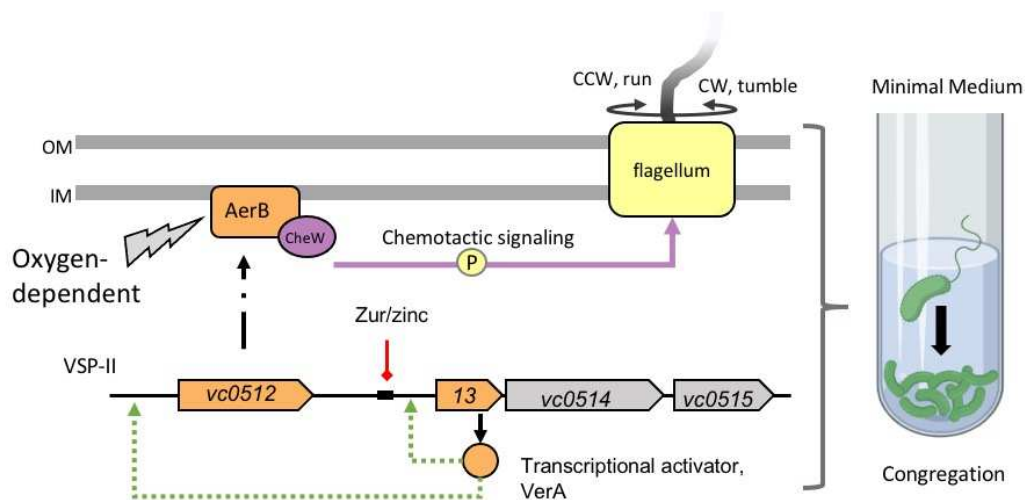


Figure 7. Proposed model of Zur-regulation of VSP-II encoded genes and its effect on chemotaxis. Zur (orange hexagon) forms a complex with divalent zinc ions (blue circle) and binds with high affinity to specific DNA sequences (black rectangle), repressing transcription of downstream genes (red line). In the absence of *zur* or during zinc starvation, VSP-II genes, including the *vc0513-vc0515* operon are derepressed. The *vc0513*-encoded transcriptional activator VerA induces transcription (green arrow) of *aerB*, which encodes a chemotaxis receptor. AerB interacts with the chemotaxis coupling protein CheW (purple) and mediates a signal relay that alters flagellar (yellow) rotation and tumbling. AerB induction in minimal medium causes *V. cholerae* to congregate in an oxygen-dependent manner away from the air-liquid interface. Model created with BioRender.com.

DISCUSSION

The mysterious Vibrio Seventh Pandemic Island (VSP-II) present in the El Tor biotype has largely evaded characterization due to lack of knowledge of stimuli that favor its induction. We report that Zur, the transcriptional repressor of the zinc starvation response, is a direct and indirect regulator of other VSP-II genes. Novel Zur targets reported here include the *vc0513-vc0515* operon, which encodes the VerA transcriptional activator that increases expression of VSP-II chemotaxis and motility-related genes. One of these secondary targets, AerB, encodes a chemoreceptor involved in energy taxis.

The role of zinc availability in VSP-II induction

It has long been suspected that the VSP islands function as either pathogenicity or environmental persistence islands. Recent work interestingly suggests that VSP-I may function as a phage defense system (88, 89). In contrast, we and others have not yet identified a set of growth conditions under which VSP-II confers a fitness benefit (23, 90-92) (**Fig. S10**). Given the robust expression of VSP-II loci in the absence of Zur, we propose two contexts where *V. cholerae* may encounter zinc starvation and express these island-encoded genes: within the human host, and/or on (chitinous) biotic surfaces in aquatic reservoirs.

The human host is a well-studied example of a metal-limited environment. Vertebrate hosts sequester desirable metal cofactors (e.g. zinc) in order to restrict the growth of potentially harmful bacteria (i.e. nutritional immunity, (28-31)). Pathogens lacking zinc acquisition systems often exhibit colonization defects *in vivo* (33, 93-100),

potentially because they are unable to compete against the microbiota for precious metal cofactors (101). Induction of zinc starvation genes in pathogenic *V. cholerae* appears to be dependent upon the *in vivo* model used; for example, the primary zinc importer and the *vc0513-vc0515* operon are upregulated in a mouse but not in a rabbit model (relative to LB) (27). *In vivo* fitness assays showed that loss of *V. cholerae*'s zinc importers led to modest colonization defects in both mouse (33) and rabbit infection models (102); however, the latter Tn-Seq analysis did not observe any significant fitness defects among VSP-II mutants in the rabbit model (102).

More generally, *V. cholerae* experiences metal starvation within thick bacterial communities and thus metal transporters and regulators contribute optimal *V. cholerae* biofilm formation (103). Zur-regulated genes (including *vc0503* and *vc0513-vc0515*) are reportedly induced by exposure to chitin oligomers (32), raising the possibility that *V. cholerae* is zinc-limited while colonizing copepods or crustaceans in the environment. It is thus plausible that the Zur-regulated VSP-II genes may be expressed in either of *V. cholerae*'s distinct lifestyles.

VSP-II-encoded genes facilitate chemotactic responses

Connections between zinc homeostasis and altered motility patterns have been reported in other bacteria, but these phenotypes appear to be indirect consequences of zinc availability rather than Zur repression of secondary transcriptional regulators (97, 104-106). The VerA-regulated chemoreceptor, AerB, generates congregation in liquid culture and appears to mediate energy taxis. This is in apparent contradiction with a report that did not find a role for AerB (referred to as *Aer-1*) in aerotaxis (83); however,

this may be explained by a lack of native *aerB* expression under their experimental conditions. *aerA* expression, on the other hand, does not appear to be regulated by Zur and native levels are sufficient to alter motility on soft agar. The balanced action of aerotactic responses conferred by AerA and AerB may function analogously to the Aer and Tsr receptors (107), which enable *E. coli* to navigate to an optimum oxygen concentration. However, we do not exclude the possibility that the AerB chemotactic response is more complex than the model proposed here.

Although the role of chemotaxis in autoaggregation has not been previously reported in *V. cholerae*, this phenomenon has been characterized in several distantly related bacteria (108). *A. brasilense*, for example, aggregates in response to oxygen/redox stress via a PAS-containing chemoreceptor homologous to AerB (33% amino acid identity, **Fig. S7A**) (86, 109, 110). As a second example, *Shewanella oneidensis* “congregates” around insoluble electron acceptors (111) via an MCP with a PAS domain (SO_1385, 39% amino acid identity to AerB), an MCP with a Ca²⁺-sensing Cache domain (SO_2240, 39% amino acid identity to VC0514), and a protein involved in extracellular electron transport (CymA, SO_4591) (87). This study, along with a correlogy analysis of VSP genes (89), suggests that the AerB/VC0512 and VC0514 MCPs may be functionally linked. Future work will investigate the relationship between these VerA-regulated MCPs.

The energy taxis system described here may enable *V. cholerae* to avoid redox stress in low-zinc environments, since deletion of zinc importer systems is associated with heightened redox susceptibility in *E. coli* (98). We speculate that AerB may allow *V. cholerae* to colonize other niches within the host (e.g., anaerobic parts of the gut),

similar to a redox-repellent chemotaxis system in *Helicobacter pylori* that enables gland colonization *in vivo* (112, 113). Alternatively, this chemotaxis system may allow *V. cholerae* to exploit different niches within the aquatic reservoir (e.g., anoxic sediments with chitin detritus); however, each of these biologically relevant conditions are difficult to recapitulate *in vitro*.

Chemotaxis enhances virulence in a number of enteric pathogens, but this does not seem to generally hold true for *V. cholerae* (114). In an infection model, non-chemotactic (counter-clockwise biased) mutants outcompeted wild-type *V. cholerae* and aberrantly colonized parts of the upper small intestine (115), suggesting that chemotaxis is dispensable and possibly deleterious for host pathogenesis. *V. cholerae* appears to broadly downregulate chemotaxis genes in a mouse infection model (27) and in stool shed from human patients (116). Intriguingly, this decrease may be mediated in part by VSP-I; the island-encoded DncV synthesizes a cyclic AMP-GMP signaling molecule that decreases expression of chemotaxis genes and enhances virulence (24). Specific chemoreceptors, however, are upregulated within a host and/or enhance virulence (see (117) for a review). Given the conflicting roles for chemotaxis within a host and the lack of evidence for VSP-II's role during infection, we alternatively suggest that VSP-II encoded chemotaxis genes may serve a purpose in an aquatic environment with oxygen and nutrient gradients.

Stress and starvation responses can be co-opted by acquired genetic elements

We report that targets of the Zur-regulated VerA appear to be restricted to VSP-II, at least under the conditions tested. This restriction is logical given that

transcriptional activators require specific DNA-binding sequences, and these may not be present in the native chromosome of a horizontal transfer recipient. Zur control of secondary regulators, including those that impact gene expression more broadly via signaling molecules (i.e., cyclic di-GMP phosphodiesterases like VC0515) may function to expand the complexity and tunability of the Zur-regulon in response to zinc availability and compounding environmental signals.

Horizontal acquisition of genomic islands can help bacteria (and pathogens) evolve in specific niches. VSP-II retains the ability to excise to a circular intermediate in N16961, indicating the potential for future horizontal transfer events (25). We observed that 35% of the ORFs on the prototypical VSP-II island are expressed in the absence of Zur. Intriguingly, genomic island “desilencing” in response to zinc starvation has been reported in diverse bacterium, including *Mycobacterium avium* ssp. Paratuberculosis (66) and *Cupriavidus metallidurans* (54). We note in this study that other El Tor isolates lack some Zur-regulated components of VSP-II. Given that the emergence of VSP-II containing 7th pandemic strains is recent on an evolutionary timescale, the contents of these islands may still be undergoing selection.

In summary, investigation of our Zur-associated congregation phenotype enabled identification of novel components of the zinc starvation response present on the El Tor Vibrio Seventh Pandemic Island -II. Further characterization of these island-encoded genes may aid in establishing VSP-II’s role as either a pathogenicity or environmental persistence island.

EXPERIMENTAL PROCEDURES

Bacterial growth conditions.

Bacterial strains were grown by shaking (200 rpm) in 5 mL of LB medium at 30°C (for *V. cholerae* and *E. coli* BTH101) or 37°C (for other *E. coli*) in borosilicate glass tubes, unless otherwise specified. M9 minimal medium with glucose (0.2%) was prepared with ultrapure Mili-Q water to minimize metal contamination. Antibiotics, where appropriate, were used at the following concentrations: streptomycin, 200 $\mu\text{g ml}^{-1}$; ampicillin, 100 $\mu\text{g ml}^{-1}$, and kanamycin, 50 $\mu\text{g ml}^{-1}$. IPTG was added to induce P_{iptg} promoters at indicated concentrations.

Plasmid and strain construction.

For all cloning procedures, N16961 gDNA was amplified via Q5 DNA polymerase (NEB) with the oligos summarized in **Table S1**. Fragments were Gibson assembled (118) into restriction-digested plasmids. For gene deletions, 700 bp flanking regions were assembled into XbaI-digested pCVD442 (Amp^R). For complementation experiments, genes of interest were amplified with a strong ribosome binding site and assembled into SmaI-digested pHLmob (kan^R) or pTD101 (Amp^R) downstream of an IPTG-inducible promoter. *lacZ* transcriptional reporters were built by amplifying the desired promoter region and assembling into NheI-digested pAM325 (Kan^R). The resulting promoter-*lacZ* fusions were amplified for assembly into StuI-digested pJL1 (Amp^R). Cloning for bacterial two-hybrid assays are described in a separate section below. All assemblies were initially transformed into DH5alpha λ pir and subsequently into an *E. coli* donor strain (MFD λ pir or SM10 λ pir). For conjugations into *V. cholerae*,

stationary phase recipients and MFD λ *pir* donor strains were washed of antibiotics, mixed in equal ratios, and spotted onto an LB DAP plate. After a 4-h incubation at 37°C, cells were streaked into a selective plate (LB plus ampicillin or kanamycin) to select for transconjugants. Conjugations using SM10 λ *pir* donors were performed in the absence of DAP and with the addition of streptomycin to selective plates. pHLmob transconjugants were purified on an additional kanamycin LB agar plate. Integration vectors (pCVD442, pTD101, and pJL1) were cured through two rounds of purification on salt-free sucrose (10%) agar. Gene deletions or STOP codon replacements introduced by pCVD442 were verified by PCR using the oligos indicated in **Table S1**. Successful integration of *lacZ* targeting vectors (pTD101, pJL1) were identified by blue-white screening on plates containing 5-Bromo-4-chloro-3-indolyl- β -D-galactopyranoside (X-Gal, 40 μ g ml⁻¹). pJL-1 vectors were additionally checked via PCR. All strains used in this study are summarized in **Table S1**. *V. cholerae* strains were derived from N16961, unless otherwise indicated as E7946 (119), C6706 (not strep^R) (14), or Haiti (19). The N16961 accession numbers for genes referenced in this study are as follows: *zur/vc0378*, *znuABC/vc2081-vc2083*, *zrgABC/vc2551-2553*, *ribA/vc1263*, *rpmE2/vc0878*, *rpmJ2/vc0879*, *shyB/vc0503*, *aerB/vc0512*, *verA/vc0513*, *fliC/vc2199*, *motB/vc0893*, *cheA-2/vc2063*, *cheW-1/vc2059*, *cheZ/vc2064*, *cheY/vc2065*, *vpsL/vc0934*, *csqS/vca0522*, *csqA/vc0523*, *tdh/vca0885*, *luxS/vc0557*, *luxQ/vca0736*, and *aerA/vca0658*.

Site-directed mutagenesis.

Site-directed mutagenesis was performed using NEB kit #E0554S according to manufacturer instructions. A pTD101 plasmid carrying *aerB* was used as the template for Q5 amplification with the following mutagenic primer pairs: R61A, SM-1294/1295; and H62A, SM-1296/1297 (**Table S1**). Products were purified and treated with kinase, ligase, and Dpn1 at 37°C for 30 minutes. This reaction mixture was transformed into DH5 α λ pir. Mutations were confirmed via Sanger Sequencing. *aerB* fragments containing W74F (SM-1306) and G395C (SM-1307) were chemically synthesized by Integrated DNA Technologies (IDT) and assembled into pTD101; sequences are listed in **Table S1**).

Congregation assays

Bacterial congregation was quantified by measuring absorbance (OD600) in a spectrophotometer of the culture supernatant before and after a brief vortex (5 seconds). Congregation score represents the ratio of before and after pellet disruption; a ratio closer to one indicates that the culture is homogenous, a ratio closer to zero indicates that the cells are concentrated at the bottom of the culture tube.

Transposon Mutagenesis Screen & Arbitrary PCR

V. cholerae N16961 Δ *zur* was mutagenized with Himar1 mariner transposons via an SM10 λ pir donor strain carrying pSC189 (120). Four independent Δ *zur* transposon libraries were generated, as previously described (26). Each library was separately harvested from the plate using sterile rubber scrapers, vortexed into LB, and preserved

in glycerol at -80°C. Individual culture tubes containing 5 mL of M9 minimal medium with glucose (0.2%) and kanamycin were inoculated with transposon libraries. Overnight cultures were back-diluted 1000-fold into fresh medium and incubated overnight; this process was repeated until no visible pellet had formed. Isolated colonies were tested to verify that they did not generate a pellet. The second screen was performed identically to the first, except that cultures were first inoculated into a M9 motility plate (0.3% agar) and allowed to migrate for 48 hours at 30°C degrees. Scrapings from the outer zone (collected with a 1 mL pipette tip) were inoculated a culture tube containing M9 minimal medium. For both screens, the transposon insertion site for each isogenic colony was identified by arbitrary PCR (45). As described elsewhere, this technique amplifies the chromosomal DNA adjacent to the mariner transposon. Amplicons were Sanger sequenced at the Cornell Institute of Biotechnology, and regions of high-quality were aligned to the N16961 reference genome using BLAST (121).

RNA-seq and analysis

Overnight cultures of wild-type N16961 and the *Azur* mutant were diluted 1:100 into LB and grown shaking at 37°C until cells reached mid-log phase (optical density at 600 nm [OD₆₀₀], 0.5). RNA was extracted using mirVana™ miRNA Isolation Kit (Invitrogen, AM1560). Genomic DNA contamination was removed through two DNAfree (Ambion) treatments each followed by glass fiber column purification. Library preparations, Illumina sequencing, and data analysis were performed by GENEWIZ (South Plainfield, NJ). Differentially expressed genes were those with log

2-fold change >1 and an adjusted p-value <0.05 .

For VC0513 overexpression, wild-type N16961 carrying either pHLmob or pHLmob(*P_{iptg}-vc0513*) was sub-cultured into LB kanamycin IPTG (500 μ M) and grown at 37°C for 3 hour (~ mid-log phase). Total RNA isolations and DNase treatments were performed as described above. Library preparations, Illumina sequencing, and data analysis (using DESeq2 (122)) were performed by the Cornell Transcriptional Expression Facility. Differentially expressed genes were those with log 2-fold change >1 and an adjusted p-value <0.05 .

5'-Rapid Amplification of cDNA Ends (5'-RACE).

Transcription start sites were identified with 5'-RACE. To obtain *vc0512*, *vc0513*, and *vca1098* transcripts, the *Azur* mutant was grown in LB at 37°C until cells reached mid-log phase (optical density at 600 nm [OD₆₀₀], 0.5) and RNA extractions and DNase treatments were performed as described for RNAseq. PCR was performed to check for genomic DNA contamination; no amplicons were detected within 34 cycles. Reverse transcription was performed with the Template Switching Reverse Transcriptase enzyme mix (NEB #M0466) according to manufacturer protocols using gene specific primers (*vc0512*, SM-1133; *vc0513*, SM-1131; *vca1098*, SM-1129) and the Template Switching Oligo (TSO). PCR Amplification of 5'-transcripts was performed with diluted cDNA, Q5 Hot Start High-Fidelity Master Mix (NEB #M0494), TSO-specific primer, and gene-specific primers (*vc0512*, SM-1134; *vc0513*, SM-1132, *vca1098*, SM-1130). Products were sanger sequenced using the following primers: SM-1134, SM-1156, and SM1157 for *vc0512*, SM-1132 for *vc0513*, and SM-1130 for *vca1098*. Primer

sequences are listed in **Table S1**.

β-galactosidase activity measurements.

V. cholerae strains carrying promoter-*lacZ* fusions were grown overnight in LB at 30°C, with kanamycin for plasmid maintenance. Strains were diluted 1:100 into LB containing kanamycin and IPTG (1 mM) and grown shaking at 37°C. Exponential phase cells were harvested (~ 3hr) and β-galactosidase activity against an ortho-Nitrophenyl-β-galactoside substrate (ONPG) substrate was quantified as described elsewhere (123, 124).

Motility Assays.

Motility plates (0.3% agar) were prepared with M9 minimal medium with variable carbon sources (succinate, 30 mM; and maltose, 0.1 mM; glucose, 0.2%). Strains were grown overnight in LB medium and washed three times in M9 without a carbon source. Plates were inoculated via toothpick stabs and incubated 30°C for 48-hr. The migration diameter (mm) was recorded.

Bacterial two hybrid assays.

Protein-protein interactions were detected using the BACTH bacterial two hybrid system (125). *cheW* and *aerB* (excluding transmembrane domains and native start/stop codons) were cloned into SmaI-digested pUT18(C) (Kan^R) or pK(N)T25 (Amp^R) expression vectors to yield N-terminal T(18/25)-Aer or C-terminal CheW-T(18/25) fusions. Electrocompetent *E. coli* BTH101 were co-transformed with a pUT18 and

pKT25 vector that carried either: an unfused adenylate cyclase domain (T18 or T25), the CheW-T(18/25) fusion or the T(18/25)-AerB fusion. Following 1 hour of outgrowth in SOC at 30°C, 10 µL of concentrated outgrowth was spotted onto LB agar containing kanamycin and ampicillin (for selection), X-gal (for blue-white detection), and inducer (IPTG, 500 µM). Plates were incubated overnight at 30°C and for an additional day at room temperature before being imaged.

Anaerobic Cultures.

5 mL of M9 minimal medium without MgSO₄, CaCl₂, or carbon source were added to glass culture tubes. Tubes were sealed with rubber stoppers, crimped, purged for 10 cycles (20 sec vacuum, 20 sec N₂ purge), and autoclaved (gravity, 20 min). Post-autoclaving, the medium was amended with sterile solutions of MgSO₄ (to 2 mM), CaCl₂ (to 0.1 mM), glucose (to 0.5%) and with or without fumarate (to 50mM) using sterile syringes and needles. Tubes were injected with a *V. cholerae* cell suspension and grown overnight shaking at 30°C. Aerobic tubes containing M9 glucose (0.5%) with or without fumarate were included as a control. Congregation was measured via spectrophotometry, as described above.

ACKNOWLEDGEMENTS

We thank Sean Murphy and Dr. Daniel Buckley for providing assistance with anoxic culturing, and Dr. John Mekalanos and Dr. Melanie Blokesch for generously sharing *V. cholerae* strains. We thank members of the Dörr lab for helpful discussions. This study was in part supported by NIH grant R01GM130971 to TD and by the Cornell Institute of Host-Microbe Interactions and Disease (CIHMID) (CML, BAJ). The funders had no role in study design, data collection and analysis, decision to publish, or preparation of the manuscript.

REFERENCES

1. **Clemens JD, Nair GB, Ahmed T, Qadri F, Holmgren J.** 2017. Cholera. *The Lancet* **390**:1539–1549.
2. **Reidl J, Kloese KE.** 2002. *Vibrio cholerae* and cholera: out of the water and into the host. *FEMS Microbiol Rev* **26**:125–139.
3. **Huq A, Small EB, West PA, Huq MI, Rahman R, Colwell RR.** 1983. Ecological relationships between *Vibrio cholerae* and planktonic crustacean copepods. *Appl Environ Microbiol* **45**:275–283.
4. **de Magny GC, Mozumder PK, Grim CJ, Hasan NA, Naser MN, Alam M, Sack RB, Huq A, Colwell RR.** 2011. Role of Zooplankton Diversity in *Vibrio cholerae* Population Dynamics and in the Incidence of Cholera in the Bangladesh Sundarbans. *Appl Environ Microbiol* **77**:6125–6132.
5. **Tamplin ML, Gauzens AL, Huq A, Sack DA, Colwell RR.** 1990. Attachment of *Vibrio cholerae* serogroup O1 to zooplankton and phytoplankton of Bangladesh waters. *Appl Environ Microbiol* **56**:1977–1980.
6. **Sochard MR, Wilson DF, Austin B, Colwell RR.** 1979. Bacteria associated with the surface and gut of marine copepods. *Appl Environ Microbiol* **37**:750–759.
7. **Twedt RM, Madden JM, Hunt JM, Francis DW, Peeler JT, Duran AP, Hebert WO, McCay SG, Roderick CN, Spite GT, Wazenski TJ.** 1981. Characterization of *Vibrio cholerae* isolated from oysters. *Appl Environ Microbiol* **41**:1475–1478.
8. **Hood MA, Ness GE, Rodrick GE.** 1981. Isolation of *Vibrio cholerae* serotype O1 from the eastern oyster, *Crassostrea virginica*. *Appl Environ Microbiol* **41**:559–560.
9. **Purdy AE, Watnick PI.** 2011. Spatially selective colonization of the arthropod intestine through activation of *Vibrio cholerae* biofilm formation. *Proc Natl Acad Sci USA* **108**:19737–19742.
10. **Broza M, Halpern M.** 2001. Chironomid egg masses and *Vibrio cholerae*. *Nature* **412**:40–40.
11. **DePAOLA A.** 1981. *Vibrio cholerae* in Marine Foods and Environmental Waters: A Literature Review. *Journal of Food Science* **46**:66–70.
12. **Kaysner CA, Hill WE.** 2014. *Toxigenic Vibrio cholerae O1 in Food and Water*. John Wiley & Sons, Ltd, Washington, DC, USA.

13. **Chatterjee SN, Chaudhuri K.** 2003. Lipopolysaccharides of *Vibrio cholerae*: I. Physical and chemical characterization. *Biochimica et Biophysica Acta (BBA) - Molecular Basis of Disease* **1639**:65–79.
14. **Thelin KH, Taylor RK.** 1996. Toxin-coregulated pilus, but not mannose-sensitive hemagglutinin, is required for colonization by *Vibrio cholerae* O1 El Tor biotype and O139 strains. *Infection and Immunity* **64**:2853–2856.
15. **Krebs SJ, Taylor RK.** 2011. Protection and Attachment of *Vibrio cholerae* Mediated by the Toxin-Coregulated Pilus in the Infant Mouse Model. *Journal of Bacteriology* **193**:5260–5270.
16. **Sanchez J, Holmgren J.** 2008. Cholera toxin structure, gene regulation and pathophysiological and immunological aspects. *Cell Mol Life Sci* **65**:1347–1360.
17. **Rivera-Chávez F, Mekalanos JJ.** 2019. Cholera toxin promotes pathogen acquisition of host-derived nutrients. *Nature* **572**:244–248.
18. **Hu D, Liu B, Feng L, Ding P, Guo X, Wang M, Cao B, Reeves PR, Wang L.** 2016. Origins of the current seventh cholera pandemic. *Proc Natl Acad Sci USA* **113**:E7730–E7739.
19. **Son MS, Megli CJ, Kovacicova G, Qadri F, Taylor RK.** 2011. Characterization of *Vibrio cholerae* O1 El Tor biotype variant clinical isolates from Bangladesh and Haiti, including a molecular genetic analysis of virulence genes. *J Clin Microbiol* **49**:3739–3749.
20. **Henderson JC, Herrera CM, Trent MS.** 2017. AlmG, responsible for polymyxin resistance in pandemic *Vibrio cholerae*, is a glycytransferase distantly related to lipid A late acyltransferases. *J Biol Chem* **292**:21205–21215.
21. **Hankins JV, Madsen JA, Giles DK, Brodbelt JS, Trent MS.** 2012. Amino acid addition to *Vibrio cholerae* LPS establishes a link between surface remodeling in Gram-positive and Gram-negative bacteria. *Proc Natl Acad Sci USA* **109**:8722–8727.
22. **Dziejman M, Balon E, Boyd D, Fraser CM, Heidelberg JF, Mekalanos JJ.** 2002. Comparative genomic analysis of *Vibrio cholerae*: Genes that correlate with cholera endemic and pandemic disease. *Proc Natl Acad Sci USA* **99**:1556–1561.
23. **O'Shea YA.** 2004. The *Vibrio* seventh pandemic island-II is a 26.9 kb genomic island present in *Vibrio cholerae* El Tor and O139 serogroup isolates that shows homology to a 43.4 kb genomic island in *V. vulnificus*. *Microbiology* **150**:4053–4063.

24. **Davies BW, Bogard RW, Young TS, Mekalanos JJ.** 2012. Coordinated Regulation of Accessory Genetic Elements Produces Cyclic Di-Nucleotides for *V. cholerae* Virulence. *Cell* **149**:358–370.
25. **Murphy RA, Boyd EF.** 2008. Three Pathogenicity Islands of *Vibrio cholerae* Can Excise from the Chromosome and Form Circular Intermediates. *Journal of Bacteriology* **190**:636–647.
26. **Murphy SG, Alvarez L, Adams MC, Liu S, Chappie JS, Cava F, Dörr T.** 2019. Endopeptidase Regulation as a Novel Function of the Zur-Dependent Zinc Starvation Response. *mBio* **10**:e02620–18.
27. **Mandlik A, Livny J, Robins WP, Ritchie JM, Mekalanos JJ, Waldor MK.** 2011. RNA-Seq-Based Monitoring of Infection-Linked Changes in *Vibrio cholerae* Gene Expression. *Cell Host & Microbe* **10**:165–174.
28. **Palmer LD, Skaar EP.** 2016. Transition Metals and Virulence in Bacteria. *Annu Rev Genet* **50**:67–91.
29. **Kehl-Fie TE, Skaar EP.** 2010. Nutritional immunity beyond iron: a role for manganese and zinc. *Current Opinion in Chemical Biology* **14**:218–224.
30. **Hood MI, Skaar EP.** 2012. Nutritional immunity: transition metals at the pathogen–host interface. *Nat Rev Microbiol* **10**:525–537.
31. **Hennigar SR, McClung JP.** 2016. Nutritional Immunity: Starving Pathogens of Trace Minerals. *American Journal of Lifestyle Medicine* **10**:170–173.
32. **Meibom KL, Li XB, Nielsen AT, Wu C-Y, Roseman S, Schoolnik GK.** 2004. The *Vibrio cholerae* chitin utilization program. *Proc Natl Acad Sci USA* **101**:2524–2529.
33. **Sheng Y, Fan F, Jensen O, Zhong Z, Kan B, Wang H, Zhu J.** 2015. Dual Zinc Transporter Systems in *Vibrio cholerae* Promote Competitive Advantages over Gut Microbiome. *Infection and Immunity* **83**:3902–3908.
34. **Novichkov PS, Kazakov AE, Ravcheev DA, Leyn SA, Kovaleva GY, Sutormin RA, Kazanov MD, Riehl W, Arkin AP, Dubchak I, Rodionov DA.** 2013. RegPrecise 3.0 – A resource for genome-scale exploration of transcriptional regulation in bacteria. *BMC Genomics* **14**:745.
35. **Panina EM, Mironov AA, Gelfand MS.** 2011. Comparative genomics of bacterial zinc regulons: Enhanced ion transport, pathogenesis, and rearrangement of ribosomal proteins. *Proc Natl Acad Sci USA* **100**:9912–9917.
36. **Jemielita M, Wingreen NS, Bassler BL.** 2018. Quorum sensing controls

Vibrio cholerae multicellular aggregate formation. eLife 7:e1002210.

37. **Taylor RK, Miller VL, Furlong DB, Mekalanos JJ.** 1987. Use of *phoA* gene fusions to identify a pilus colonization factor coordinately regulated with cholera toxin. Proc Natl Acad Sci USA **84**:2833–2837.
38. **Sun D, Lafferty MJ, Peek JA, Taylor RK.** 1997. Domains within the *Vibrio cholerae* toxin coregulated pilin subunit that mediate bacterial colonization. Gene **192**:79–85.
39. **Kirn TJ, Lafferty MJ, Sandoe CMP, Taylor RK.** 2000. Delineation of pilin domains required for bacterial association into microcolonies and intestinal colonization by *Vibrio cholerae*. Molecular Microbiology **35**:896–910.
40. **Adams DW, Stutzmann S, Stoudmann C, Blokesch M.** 2019. DNA-uptake pili of *Vibrio cholerae* are required for chitin colonization and capable of kin recognition via sequence-specific self-interaction **4**:1545–1557.
41. **Trunk T, Khalil HS, Leo JC.** 2018. Bacterial autoaggregation. AIMS Microbiology **4**:140–164.
42. **Perez-Soto N, Creese O, Fernandez-Trillo F, Krachler A-M.** 2018. Aggregation of *Vibrio cholerae* by Cationic Polymers Enhances Quorum Sensing but Overrides Biofilm Dissipation in Response to Autoinduction. ACS Chemical Biology **13**:3021–3029.
43. **Zamorano-Sánchez D, Xian W, Lee CK, Salinas M, Thongsomboon W, Cegelski L, Wong GCL, Yildiz FH.** 2019. Functional Specialization in *Vibrio cholerae* Diguanylate Cyclases: Distinct Modes of Motility Suppression and c-di-GMP Production. mBio **10**.
44. **Struempfer AW.** 2002. Adsorption characteristics of silver, lead, cadmium, zinc, and nickel on borosilicate glass, polyethylene, and polypropylene container surfaces. Anal Chem **45**:2251–2254.
45. **O'Toole GA, Pratt LA, Watnick PI, Newman DK, Weaver VB, Kolter R.** 1999. Genetic approaches to study of biofilms. Methods Enzymol **310**:91–109.
46. **Nakao R, Ramstedt M, Wai SN, Uhlin BE.** 2012. Enhanced Biofilm Formation by *Escherichia coli* LPS Mutants Defective in Hep Biosynthesis. PLOS ONE **7**:e51241.
47. **Heidelberg JF, Eisen JA, Nelson WC, Clayton RA, Gwinn ML, Dodson RJ, Haft DH, Hickey EK, Peterson JD, Umayam L, Gill SR, Nelson KE, Read TD, Tettelin H, Richardson D, Ermolaeva MD, Vamathevan J, Bass S, Qin H, Dragoi I, Sellers P, McDonald L, Utterback T, Fleishmann RD,**

- Nierman WC, White O, Salzberg SL, Smith HO, Colwell RR, Mekalanos JJ, Venter JC, Fraser CM.** 2000. DNA sequence of both chromosomes of the cholera pathogen *Vibrio cholerae*. *Nature* **406**:477–483.
48. **Joelsson A, Liu Z, Zhu J.** 2006. Genetic and Phenotypic Diversity of Quorum-Sensing Systems in Clinical and Environmental Isolates of *Vibrio cholerae*. *Infection and Immunity* **74**:1141–1147.
49. **Stutzmann S, Blokesch M, D'Orazio SEF.** 2016. Circulation of a Quorum-Sensing-Impaired Variant of *Vibrio cholerae* Strain C6706 Masks Important Phenotypes. *mSphere* **1**:e00098–16.
50. **Hensley MP, Gunasekera TS, Easton JA, Sigdel TK, Sugarbaker SA, Klingbeil L, Breece RM, Tierney DL, Crowder MW.** 2012. Characterization of Zn(II)-responsive ribosomal proteins YkgM and L31 in *E. coli*. *Journal of Inorganic Biochemistry* **111**:164–172.
51. **Sigdel TK, Easton JA, Crowder MW.** 2006. Transcriptional response of *Escherichia coli* to TPEN. *Journal of Bacteriology* **188**:6709–6713.
52. **Kallifidas D, Ben Pascoe, Owen GA, Strain-Damerell CM, Hong H-J, Paget MSB.** 2010. The Zinc-Responsive Regulator Zur Controls Expression of the Coelibactin Gene Cluster in *Streptomyces coelicolor*. *Journal of Bacteriology* **192**:608–611.
53. **Gaballa A, Wang T, Ye RW, Helmann JD.** 2002. Functional analysis of the *Bacillus subtilis* Zur regulon. *Journal of Bacteriology* **184**:6508–6514.
54. **Bütof L, Schmidt-Vogler C, Herzberg M, Große C, Nies DH, DiRita VJ.** 2017. The Components of the Unique Zur Regulon of *Cupriavidus metallidurans* Mediate Cytoplasmic Zinc Handling. *Journal of Bacteriology* **199**:e00372–17.
55. **Pawlik M-C, Hubert K, Joseph B, Claus H, Schoen C, Vogel U.** 2012. The zinc-responsive regulon of *Neisseria meningitidis* comprises seventeen genes under control of a Zur element. *Journal of Bacteriology* **194**:6594–6603.
56. **Neupane DP, Jacquez B, Sundararajan A, Ramaraj T, Schilkey FD, Yuki ET.** 2017. Zinc-Dependent Transcriptional Regulation in *Paracoccus denitrificans*. *Front Microbiol* **8**:123.
57. **Mazzon RR, Braz VS, da Silva Neto JF, do Valle Marques M.** 2014. Analysis of the *Caulobacter crescentus* Zur regulon reveals novel insights in zinc acquisition by TonB-dependent outer membrane proteins. *BMC Genomics* **15**:1–14.
58. **Moreau GB, Qin A, Mann BJ, Stock AM.** 2018. Zinc Acquisition

- Mechanisms Differ between Environmental and Virulent *Francisella* Species. *Journal of Bacteriology* **200**:e00587–17.
59. **Mortensen BL, Rathi S, Chazin WJ, Skaar EP.** 2014. *Acinetobacter baumannii* Response to Host-Mediated Zinc Limitation Requires the Transcriptional Regulator Zur. *Journal of Bacteriology* **196**:2616–2626.
 60. **Li Y, Qiu Y, Gao H, Guo Z, Han Y, Song Y, Du Z, Wang X, Zhou D, Yang R.** 2009. Characterization of Zur-dependent genes and direct Zur targets in *Yersinia pestis*. *BMC Microbiol* **9**:1–13.
 61. **Lim CK, Hassan KA, Penesyana A, Loper JE, Paulsen IT.** 2013. The effect of zinc limitation on the transcriptome of *Pseudomonas protegens* Pf05. *Environmental Microbiology* **15**:702–715.
 62. **Pederick VG, Eijkelkamp BA, Begg SL, Ween MP, McAllister LJ, Paton JC, McDevitt CA.** 2015. ZnuA and zinc homeostasis in *Pseudomonas aeruginosa*. *Scientific Reports* 2015 **5**:1–14.
 63. **Mastropasqua MC, D'Orazio M, Cerasi M, Pacello F, Gismondi A, Canini A, Canuti L, Consalvo A, Ciavardelli D, Chirullo B, Pasquali P, Battistoni A.** 2017. Growth of *Pseudomonas aeruginosa* in zinc poor environments is promoted by a nicotianamine-related metallophore. *Molecular Microbiology* **106**:543–561.
 64. **Latorre M, Low M, Gárate E, Reyes-Jara A, Murray BE, Cambiazo V, González M.** 2015. Interplay between copper and zinc homeostasis through the transcriptional regulator Zur in *Enterococcus faecalis*. *Metallomics* **7**:1137–1145.
 65. **Schröder J, Jochmann N, Rodionov DA, Tauch A.** 2010. The Zur regulon of *Corynebacterium glutamicum* ATCC 13032. *BMC Genomics* **11**:1–18.
 66. **Eckelt E, Jarek M, Frömke C, Meens J, Goethe R.** 2014. Identification of a lineage specific zinc responsive genomic island in *Mycobacterium avium* ssp. paratuberculosis. *BMC Genomics* **15**:1–15.
 67. **Owen GA, Pascoe B, Kallifidas D, Paget MSB.** 2007. Zinc-responsive regulation of alternative ribosomal protein genes in *Streptomyces coelicolor* involves zur and sigmaR. *Journal of Bacteriology* **189**:4078–4086.
 68. **Fong JCN, Syed KA, Klose KE, Yildiz FH.** 2010. Role of Vibrio polysaccharide (vps) genes in VPS production, biofilm formation and *Vibrio cholerae* pathogenesis. *Microbiology* **156**:2757–2769.
 69. **DiRita VJ.** 1992. Coordinate expression of virulence genes by ToxR in *Vibrio cholerae*. *Molecular Microbiology* **6**:451–458.

70. **DiRita VJ, Parsot C, Jander G, Mekalanos JJ.** 1991. Regulatory cascade controls virulence in *Vibrio cholerae*. Proc Natl Acad Sci USA **88**:5403–5407.
71. **Higgins DE, Nazareno E, DiRita VJ.** 1992. The virulence gene activator ToxT from *Vibrio cholerae* is a member of the AraC family of transcriptional activators. Journal of Bacteriology **174**:6974–6980.
72. **Weber GG, Klose KE.** 2011. The complexity of ToxT-dependent transcription in *Vibrio cholerae*. The Indian Journal of Medical Research **133**:201–206.
73. **Metzger LC, Blokesch M.** 2016. Regulation of competence-mediated horizontal gene transfer in the natural habitat of *Vibrio cholerae*. Current Opinion in Microbiology **30**:1–7.
74. **Yamamoto S, Mitobe J, Ishikawa T, Wai SN, Ohnishi M, Watanabe H, Izumiya H.** 2014. Regulation of natural competence by the orphan two-component system sensor kinase ChiS involves a non-canonical transmembrane regulator in *Vibrio cholerae*. Molecular Microbiology **91**:326–347.
75. **Dalia AB, Lazinski DW, Camilli A.** 2014. Identification of a membrane-bound transcriptional regulator that links chitin and natural competence in *Vibrio cholerae*. mBio **5**:e01028–13.
76. **Ud-Din AIMS, Roujeinikova A.** 2017. Methyl-accepting chemotaxis proteins: a core sensing element in prokaryotes and archaea. Cell Mol Life Sci **74**:3293–3303.
77. **Ringgaard S, Yang W, Alvarado A, Schirner K, Briegel A, DiRita VJ.** 2018. Chemotaxis Arrays in *Vibrio* Species and Their Intracellular Positioning by the ParC/ParP System. Journal of Bacteriology **200**:267–17.
78. **Alexander RP, Zhulin IB.** 2007. Evolutionary genomics reveals conserved structural determinants of signaling and adaptation in microbial chemoreceptors. Proc Natl Acad Sci USA **104**:2885–2890.
79. **Matthew D Coleman, Randal B Bass, Ryan S Mehan A, Falke JJ.** 2005. Conserved Glycine Residues in the Cytoplasmic Domain of the Aspartate Receptor Play Essential Roles in Kinase Coupling and On–Off Switching. Biochemistry **44**:7687–7695.
80. **Boin MA, Austin MJ, Häse CC.** 2004. Chemotaxis in *Vibrio cholerae*. FEMS Microbiology Letters **239**:1–8.
81. **Kanehisa M, Goto S, Kawashima S, Okuno Y, Hattori M.** 2004. The

- KEGG resource for deciphering the genome. *Nucleic Acids Res* **32**:D277–D280.
82. **Taylor BL**. 2007. Aer on the inside looking out: paradigm for a PAS–HAMP role in sensing oxygen, redox and energy. *Molecular Microbiology* **65**:1415–1424.
 83. **Boin MA, Häse CC**. 2007. Characterization of *Vibrio cholerae* aerotaxis. *FEMS Microbiology Letters* **276**:193–201.
 84. **Bibikov SI, Biran R, Rudd KE, Parkinson JS**. 1997. A signal transducer for aerotaxis in *Escherichia coli*. *Journal of Bacteriology* **179**:4075–4079.
 85. **Bibikov SI, Barnes LA, Gitin Y, Parkinson JS**. 2000. Domain organization and flavin adenine dinucleotide-binding determinants in the aerotaxis signal transducer Aer of *Escherichia coli*. *Proc Natl Acad Sci USA* **97**:5830–5835.
 86. **Xie Z, Ulrich LE, Zhulin IB, Alexandre G**. 2010. PAS domain containing chemoreceptor couples dynamic changes in metabolism with chemotaxis. *Proc Natl Acad Sci USA* **107**:2235–2240.
 87. **Harris HW, El-Naggar MY, Neilson KH**. 2012. *Shewanella oneidensis* MR-1 chemotaxis proteins and electron-transport chain components essential for congregation near insoluble electron acceptors. *Biochemical Society Transactions* **40**:1167–1177.
 88. **Cohen D, Melamed S, Millman A, Shulman G, Oppenheimer-Shaanan Y, Kacem A, Doron S, Amitai G, Sorek R**. 2019. Cyclic GMP–AMP signalling protects bacteria against viral infection. *Nature* **574**:691–695.
 89. **Severin GB, Hsueh BY, Elg CA, Dover JA, Rhoades CR, Wessel AJ, Ridenhour BJ, Top EM, Ravi J, Parent KN, Waters CM**. 2021. A Broadly Conserved Deoxycytidine Deaminase Protects Bacteria from Phage Infection. *bioRxiv* 2021.03.31.437871.
 90. **Taviani E, Grim CJ, Choi J, Chun J, Haley BJ, Hasan NA, Hug A, Colwell RR**. 2010. Discovery of novel *Vibrio cholerae* VSP-II genomic islands using comparative genomic analysis. *FEMS Microbiology Letters* **308**:130–137.
 91. **Sakib SN, Reddi G, Almagro-Moreno S, DiRita VJ**. 2018. Environmental Role of Pathogenic Traits in *Vibrio cholerae*. *Journal of Bacteriology* **200**:2123–17.
 92. **Pant A, Bag S, Saha B, Verma J, Kumar P, Banerjee S, Kumar B, Yashwant Kumar, Desigamani A, Suhrid Maiti, Tushar K Maiti, Sanjay K Banerjee, Rupak K Bhadra, Hemanta Koley, Dutta S, G Balakrish**

- Nair, Ramamurthy T, Das B.** 2020. Molecular insights into the genome dynamics and interactions between core and acquired genomes of *Vibrio cholerae*. Proc Natl Acad Sci USA **117**:23762–23773.
93. **Davis LM, Kakuda T, DiRita VJ.** 2009. A *Campylobacter jejuni* *znuA* Orthologue Is Essential for Growth in Low-Zinc Environments and Chick Colonization. Journal of Bacteriology **191**:1631–1640.
94. **Ammendola S, Pasquali P, Pistoia C, Petrucci P, Petrarca P, Rotilio G, Battistoni A.** 2007. High-Affinity Zn²⁺ Uptake System ZnuABC Is Required for Bacterial Zinc Homeostasis in Intracellular Environments and Contributes to the Virulence of *Salmonella enterica*. Infection and Immunity **75**:5867–5876.
95. **Campoy S, Jara M, Busquets N, de Rozas AMP, Badiola I, Barbé J.** 2002. Role of the High-Affinity Zinc Uptake *znuABC* System in *Salmonella enterica* Serovar Typhimurium Virulence. Infection and Immunity **70**:4721–4725.
96. **Bobrov AG, Kirillina O, Fosso MY, Fetherston JD, Miller MC, VanCleave TT, Burlison JA, Arnold WK, Lawrenz MB, Garneau-Tsodikova S, Perry RD.** 2017. Zinc transporters YbtX and ZnuABC are required for the virulence of *Yersinia pestis* in bubonic and pneumonic plague in mice. Metallomics **9**:757–772.
97. **Nielubowicz GR, Smith SN, Mobley HLT.** 2010. Zinc uptake contributes to motility and provides a competitive advantage to *Proteus mirabilis* during experimental urinary tract infection. Infection and Immunity **78**:2823–2833.
98. **Sabri M, Houle S, Dozois CM.** 2009. Roles of the extraintestinal pathogenic *Escherichia coli* ZnuACB and ZupT zinc transporters during urinary tract infection. Infection and Immunity **77**:1155–1164.
99. **Corbett D, Wang J, Schuler S, Lopez-Castejon G, Glenn S, Brough D, Andrew PW, Cavet JS, Roberts IS, Bäumlér AJ.** 2012. Two Zinc Uptake Systems Contribute to the Full Virulence of *Listeria monocytogenes* during Growth *In Vitro* and *In Vivo*. Infection and Immunity **80**:14–21.
100. **Hood MI, Mortensen BL, Moore JL, Zhang Y, Kehl-Fie TE, Sugitani N, Chazin WJ, Caprioli RM, Skaar EP.** 2012. Identification of an *Acinetobacter baumannii* Zinc Acquisition System that Facilitates Resistance to Calprotectin-mediated Zinc Sequestration. PLoS Pathog **8**:e1003068.
101. **Gielda LM, DiRita VJ.** 2012. Zinc competition among the intestinal microbiota. mBio **3**:e00171–12.
102. **Kamp HD, Patimalla-Dipali B, Lazinski DW, Wallace-Gadsden F,**

- Camilli A.** 2013. Gene Fitness Landscapes of *Vibrio cholerae* at Important Stages of Its Life Cycle. *PLoS Pathog* **9**:e1003800.
103. **Mueller RS, McDougald D, Cusumano D, Sodhi N, Kjelleberg S, Azam F, Bartlett DH.** 2007. *Vibrio cholerae* strains possess multiple strategies for abiotic and biotic surface colonization. *Journal of Bacteriology* **189**:5348–5360.
104. **Lai HC, Gygi D, Fraser GM, Hughes C.** 1998. A swarming-defective mutant of *Proteus mirabilis* lacking a putative cation-transporting membrane P-type ATPase. *Microbiology* **144**:1957–1961.
105. **Ammendola S, D'Amico Y, Chirullo B, Drumo R, Civardelli D, Pasquali P, Battistoni A.** 2016. Zinc is required to ensure the expression of flagella and the ability to form biofilms in *Salmonella enterica* sv Typhimurium. *Metallomics* **8**:1131–1140.
106. **Yeo J, Dippel AB, Wang XC, Hammond MC.** 2017. *In Vivo* Biochemistry: Single-Cell Dynamics of Cyclic Di-GMP in *Escherichia coli* in Response to Zinc Overload. *Biochemistry* **57**:108–116.
107. **Rebbapragada A, Johnson MS, Harding GP, Zuccarelli AJ, Fletcher HM, Zhulin IB, Taylor BL.** 1997. The Aer protein and the serine chemoreceptor Tsr independently sense intracellular energy levels and transduce oxygen, redox, and energy signals for *Escherichia coli* behavior. *Proc Natl Acad Sci USA* **94**:10541–10546.
108. **Alexandre G.** 2015. Chemotaxis Control of Transient Cell Aggregation. *Journal of Bacteriology* **197**:3230–3237.
109. **Bible AN, Stephens BB, Ortega DR, Xie Z, Alexandre G.** 2008. Function of a Chemotaxis-Like Signal Transduction Pathway in Modulating Motility, Cell Clumping, and Cell Length in the Alphaproteobacterium *Azospirillum brasilense*. *Journal of Bacteriology* **190**:6365–6375.
110. **Russell MH, Bible AN, Fang X, Gooding JR, Campagna SR, Gomelsky M, Alexandre G, Greenberg EP, Harwood CS.** 2013. Integration of the Second Messenger c-di-GMP into the Chemotactic Signaling Pathway. *mBio* **4**:1024–13.
111. **Harris HW, Sánchez-Andrea I, McLean JS, Salas EC, Tran W, El-Nagggar MY, Neilson KH.** 2018. Redox Sensing within the Genus *Shewanella*. *Front Microbiol* **8**.
112. **Collins KD, Andermann TM, Draper J, Sanders L, Williams SM, Araghi C, Ottemann KM.** 2016. The *Helicobacter pylori* CZB Cytoplasmic Chemoreceptor TlpD Forms an Autonomous Polar Chemotaxis Signaling

- Complex That Mediates a Tactic Response to Oxidative Stress. *Journal of Bacteriology* **198**:1563–1575.
113. **Collins KD, Hu S, Grasberger H, Kao JY, Ottemann KM.** 2018. Chemotaxis Allows Bacteria To Overcome Host-Generated Reactive Oxygen Species That Constrain Gland Colonization. *Infection and Immunity* **86**.
 114. **Butler SM, Camilli A.** 2005. Going against the grain: chemotaxis and infection in *Vibrio cholerae*. *Nat Rev Microbiol* **3**:611–620.
 115. **Butler SM, Camilli A.** 2004. Both chemotaxis and net motility greatly influence the infectivity of *Vibrio cholerae*. *Proc Natl Acad Sci USA* **101**:5018–5023.
 116. **Merrell DS, Butler SM, Qadri F, Dolganov NA, Alam A, Cohen MB, Calderwood SB, Schoolnik GK, Camilli A.** 2002. Host-induced epidemic spread of the cholera bacterium. *Nature* **417**:642–645.
 117. **Matilla MA, Krell T.** 2017. The effect of bacterial chemotaxis on host infection and pathogenicity. *FEMS Microbiol Rev* **42**.
 118. **Gibson DG, Young L, Chuang R-Y, Venter JC, Hutchison CA III, Smith HO.** 2009. Enzymatic assembly of DNA molecules up to several hundred kilobases. *Nat Methods* **6**:343–345.
 119. **Miller VL, DiRita VJ, Mekalanos JJ.** 1989. Identification of toxS, a regulatory gene whose product enhances toxR-mediated activation of the cholera toxin promoter. *Journal of Bacteriology* **171**:1288–1293.
 120. **Chiang SL, Rubin EJ.** 2002. Construction of a mariner-based transposon for epitope-tagging and genomic targeting. *Gene* **296**:179–185.
 121. **Altschul SF, Gish W, Miller W, Myers EW, Lipman DJ.** 1990. Basic local alignment search tool. *J Mol Biol* **215**:403–410.
 122. **Love MI, Huber W, Anders S.** 2014. Moderated estimation of fold change and dispersion for RNA-seq data with DESeq2. *Genome Biol* **15**:1–21.
 123. **Miller J.** 1972. *Experiments in molecular genetics*. Cold Spring Harbor Laboratory, Cold Spring Harbor, NY.
 124. **Zhang X, Bremer H.** 1995. Control of the *Escherichia coli* rrnB P1 promoter strength by ppGpp. *J Biol Chem* **270**:11181–11189.
 125. **Karimova G, Pidoux J, Ullmann A, Ladant D.** 1998. A bacterial two-hybrid system based on a reconstituted signal transduction pathway. *Proc Natl Acad Sci USA* **95**:5752–5756.

126. **Solovyev V, Salamov A.** 2011. Automatic annotation of microbial genomes and metagenomic sequences, pp. 61–78. *In* *Metagenomics and Its Application in Agriculture*.
127. **Larkin MA, Blackshields G, Brown NP, Chenna R, McGettigan PA, McWilliam H, Valentin F, Wallace IM, Wilm A, Lopez R, Thompson JD, Gibson TJ, Higgins DG.** 2007. Clustal W and Clustal X version 2.0. *Bioinformatics* **23**:2947–2948.

Supplementary information for:

***Vibrio cholerae*'s mysterious Seventh Pandemic island (VSP-II)
encodes novel Zur-regulated zinc starvation genes involved in
chemotaxis and cell congregation**

Shannon G. Murphy^{1,2}, Brianna A. Johnson^{1,3}, Camille M. Ledoux^{1,3}, Tobias Dörr^{1,2,3#}

¹ Weill Institute for Cell and Molecular Biology, Cornell University, Ithaca, NY 14853, USA

² Department of Microbiology, Cornell University, Ithaca NY 14853, USA

³ Cornell Institute of Host-Microbe Interactions and Disease, Cornell University, Ithaca NY 14853, USA

To whom correspondence should be addressed: Tobias Dörr, tdoerr@cornell.edu.

Supplementary Tables (available online)

Table S1. Summary of strains and oligos used in this study.

Table S2. Genes differentially expressed in Δzur relative to wild-type *V. cholerae*.

Table S3. Genes differentially expressed in a *V. cholerae* strain overexpressing VerA.

Supplementary Figures

Figure S1. Targeted genetic mutations exclude the involvement of a variety of genes in Δzur congregation in M9 minimal medium. Related to Fig 1 & 2.

Figure S2. Transposon insertions that prevented Δzur from aggregating in M9 minimal medium. Related to Fig 2.

Figure S3. Annotation of the *verA* promoter region. Related to Figure 3.

Figure S4. Genes differentially expressed in Δzur relative to wild-type *V. cholerae*. Related to Fig 3.

Figure S5. Zur-dependent regulation of the *vca1098* promoter. Related to Fig 3.

Figure S6. Construction of an *aerB* transcriptional reporter. Related to Fig 4.

Figure S7. AerB protein alignment with homologs from *V. cholerae*, *E. coli*, *A. brasilense*, and *S. oneidensis*. Related to Fig 5.

Figure S8. *V. cholerae* Δzur congregation requires oxygen. Related to Fig 5.

Figure S9. *V. cholerae* swarm assays with chemoreceptor mutants. Related to Fig 5.

Figure S10. Presence of VSP islands does not impact growth in zinc-chelated media.

Supplemental Movie 1. A *V. cholerae* N16961 Δ zur mutant congregates at the bottom of culture tubes. Δ zur was grown overnight shaking (200 rpm) in M9 minimal medium with glucose (0.2%) at 30°C.

Supplemental Table 1. Summary of strains and oligos used in this study. Strains used in this study are listed with unique identifiers (SGM-#). For *E. coli* donor strains, the primers or gene block used to construct each plasmid are listed in the “Oligos” column. Genetic changes introduced into *V. cholerae* were screened using the method indicated in the “confirmation” column: either via PCR using the indicated primers (SM-#), via purification on kanamycin plates, or via blue-white screening on X-gal plates.

Supplemental Table 2. Genes differentially expressed in Δ zur relative to wild-type *V. cholerae* N16961. Transcript abundances in Δ zur relative to wild-type was measured using RNA-seq (see Methods for details). Gene ID's and putative ontology (81) are shown for all significant (adjusted p-value < 0.05) differentially expressed (log 2-fold change > 1) genes. Positive values represent up-regulation and negative values represent down-regulation in Δ zur relative to the wild-type. Superscripts denote (a) a nearby canonical Zur box, (b) location on VSP-I or (c) location on VSP-II.

Supplemental Table 3. Genes differentially expressed in a *V. cholerae* strain overexpressing VerA. Transcript abundances in a strain overexpressing VerA (VC0513) relative to an empty-vector control were measured using RNA-seq (see Methods for details). Gene ID's and descriptions (81) are shown for all significant (adjusted p-value < 0.05) differentially expressed (log 2-fold change > 1) genes.

Figure S1. Targeted genetic mutations exclude the involvement of a variety of genes in Δzur congregation in M9 minimal medium.

(A-H) All strains were grown overnight in M9 minimal medium plus glucose (0.2%). All cultures were grown shaking (200 rpm), with the exception of static growth tested in panel (A). All cultures were grown in borosilicate glass tubes, with the exception of plastic tubes used in panel (B). Congregation was quantified by measuring the optical density (at 600 nm) of the culture supernatant before and after a brief vortex. The following mutants were tested in a Δzur background: (C) other putative Zur-regulatory targets (ABC-type transporter, $\Delta vca1098-vca1101$; che-III cluster, $\Delta vca1090-vca1097$), (D) chemotaxis genes ($cheA::STOP$, $\Delta cheY$, $\Delta cheZ$), (F) biofilm formation genes ($\Delta vspL$), type IV pili ($\Delta tcpA$, $\Delta mshA$, $\Delta pilA$, and $\Delta vc0502$), quorum sensing genes ($\Delta csqA$, $\Delta csqS$, Δtdh , $\Delta luxS$, or $\Delta luxQ$), (G) N16961 $hapR^{repaired}$, (H) the Vibrio Seventh Pandemic (VSP) island -I ($\Delta vc0175-vc0185$), regions of VSP-II (“ $\Delta VSP-II$ ”, $\Delta vc0491-vc0515$; $\Delta vc0490-vc0510$, $\Delta vc0511$, $\Delta vc0512$, $\Delta vc0513$ or $vc0513::STOP$, $\Delta vc0514$ or $vc0514::STOP$, $\Delta vc0515$ or $vc0515::STOP$, or $\Delta vc0516$). (E) Congregation was also measured in wild-type, Δzur , a rough mutant ($vc0225::STOP$), and a rough mutant harboring deletions for $\Delta fliC$, $\Delta motB$, or $\Delta vsp-II$. Data points represent biological replicates, error bars represent standard deviation, and asterisks denote statistical difference relative to the wild-type strain via (A,B,G) unpaired t-test or (C-F, H) Ordinary one-way ANOVA (****, $p < 0.0001$; ***, $p < 0.001$; *, $p < 0.05$).

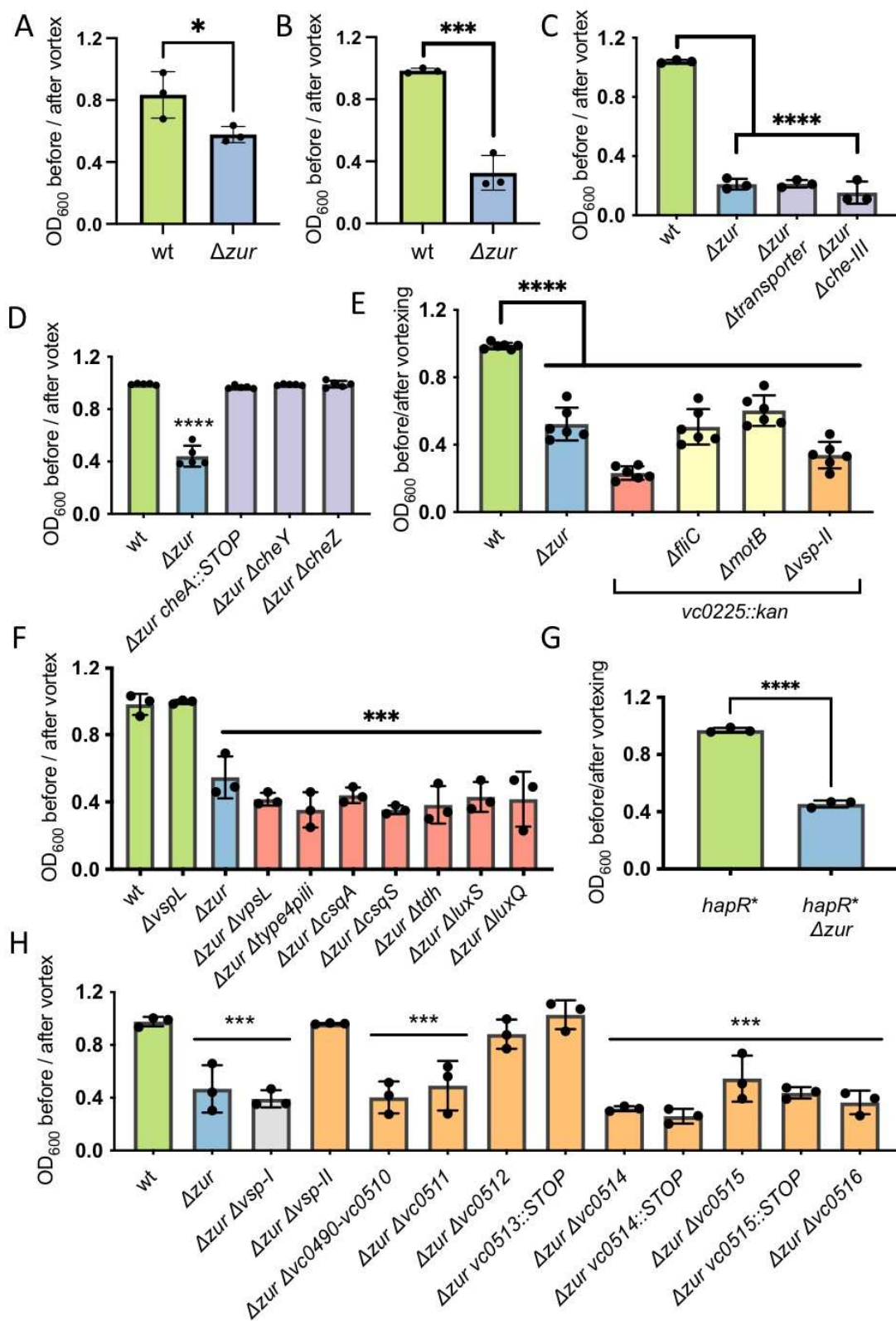


Figure S2. Transposon insertions that prevented Δzur from aggregating in M9 minimal medium.

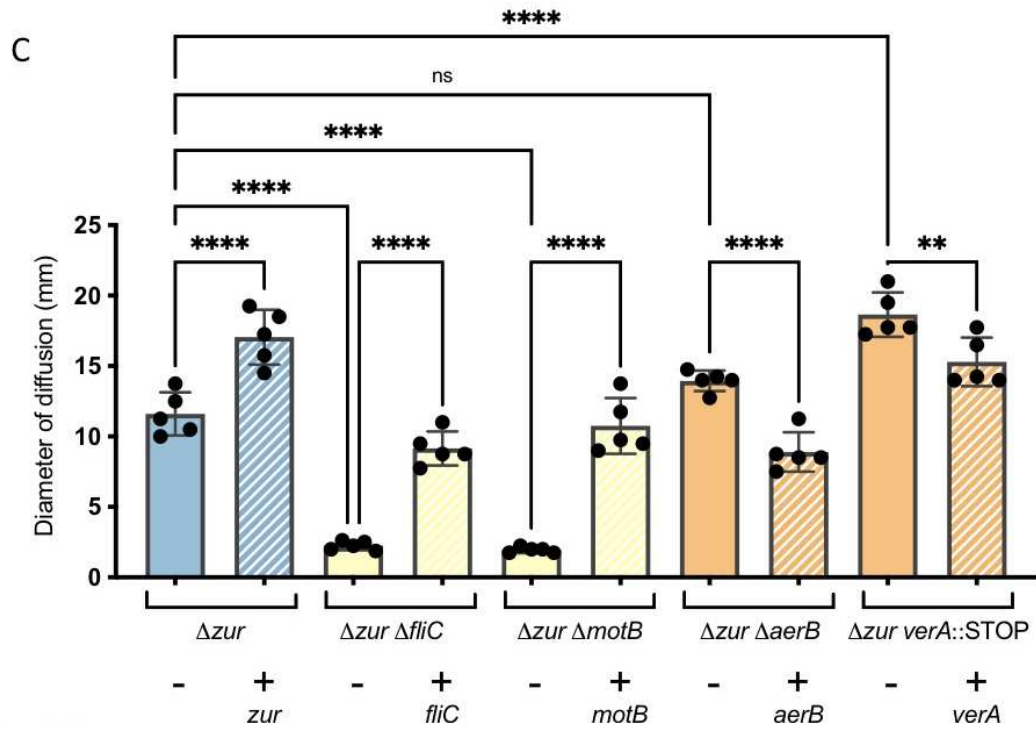
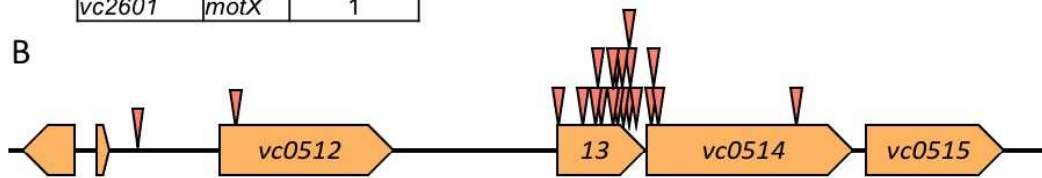
(A) Table indicating the number of transposon insertions within motility, chemotaxis, and VSP-II genes for each of the screens (without pre-selection, v.1; with pre-selection of motile mutants, v.2) described in Figure 2. (B) Approximate location of transposon insertions (triangles) determined by arbitrary PCR (45) and Sanger sequencing are shown. (C) Strains carrying either an empty vector (-) or complementation vector (+) were grown overnight in LB medium with kanamycin. Strains were washed thrice with M9 minimal medium. A sterile toothpick was used to inoculate cells into M9 soft agar (0.3%) containing glucose (0.2%), kanamycin, and inducer (IPTG, 500 μ M). The diameter of diffusion (mm) was measured following a 48-hr incubation at 30°C. Raw data points represent biological replicates, error bars represent standard deviation, and asterisks denote statistical difference via Ordinary one-way ANOVA test (****, $p < 0.0001$; **, $p < 0.01$; n.s., not significant).

A

Genes (motility)		# Insertions v.1
<i>vc0892</i>	<i>motA</i>	1
<i>vc2069</i>	<i>flhA</i>	2
<i>vc2120</i>	<i>flhB</i>	1
<i>vc2121</i>	<i>fliR</i>	2
<i>vc2130</i>	<i>fliI</i>	1
<i>vc2131</i>	<i>fliH</i>	2
<i>vc2132</i>	<i>fliG</i>	1
<i>vc2133</i>	<i>fliF</i>	2
<i>vc2134</i>	<i>fliE</i>	2
<i>vc2135</i>	<i>fliC</i>	2
<i>vc2137</i>	<i>fliA</i>	1
<i>vc2140</i>	<i>fliD</i>	1
<i>vc2190</i>	<i>flgL</i>	1
<i>vc2191</i>	<i>flgK</i>	2
<i>vc2203</i>	<i>flgA</i>	1
<i>vc2205</i>	<i>flgN</i>	1
<i>vc2601</i>	<i>motX</i>	1

Genes (chemotaxis)		# Insertions v.1
<i>vc2062</i>	<i>cheB-2</i>	1
<i>vc2063</i>	<i>cheA-2</i>	2
<i>vc2065</i>	<i>cheY-3</i>	2
<i>vc2201</i>	<i>cheR-2</i>	2

Genes (VSP-2)	# Insertions (screen v.1)	# Insertions (screen v.2)
intergenic	0	1
<i>vc0512</i>	1	0
<i>v0513</i>	1	14
<i>vc0514</i>	0	4



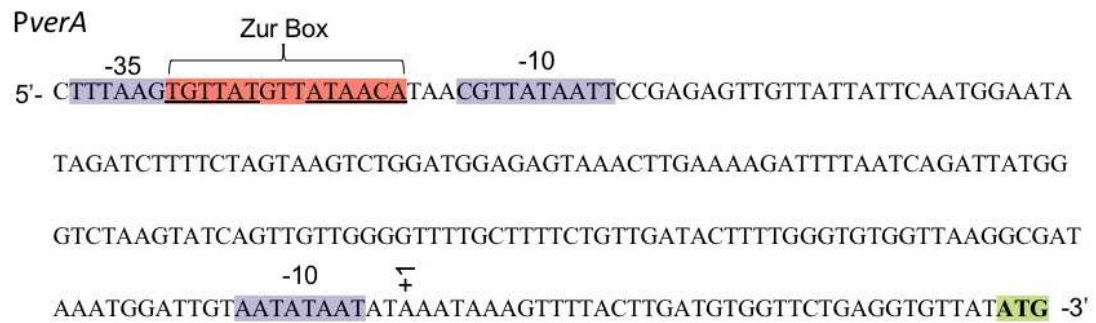


Figure S3. Annotation of the *verA* promoter region.

Diagram of the *verA* promoter regions annotated the following features: predicted Zur box (red), predicted -10 and -35 regions (purple) (126), suggested start codon (ATG, green).

Figure S4. Genes differentially expressed in Δzur relative to wild-type *V. cholerae* N16961.

(A-B) Volcano plots showing log 2-fold changes in gene expression in Δzur relative to wild-type; positive values represent up-regulation in Δzur and negative values represent down-regulation in Δzur . The y-axis denotes the negative log inverse of the p-value. Differentially expressed genes (log 2-fold change >1 , adjusted p-value < 0.05) are denoted in red and are labeled with gene identifiers. Panel (B) shows the subset of genes denoted in the blue box in Panel (A).

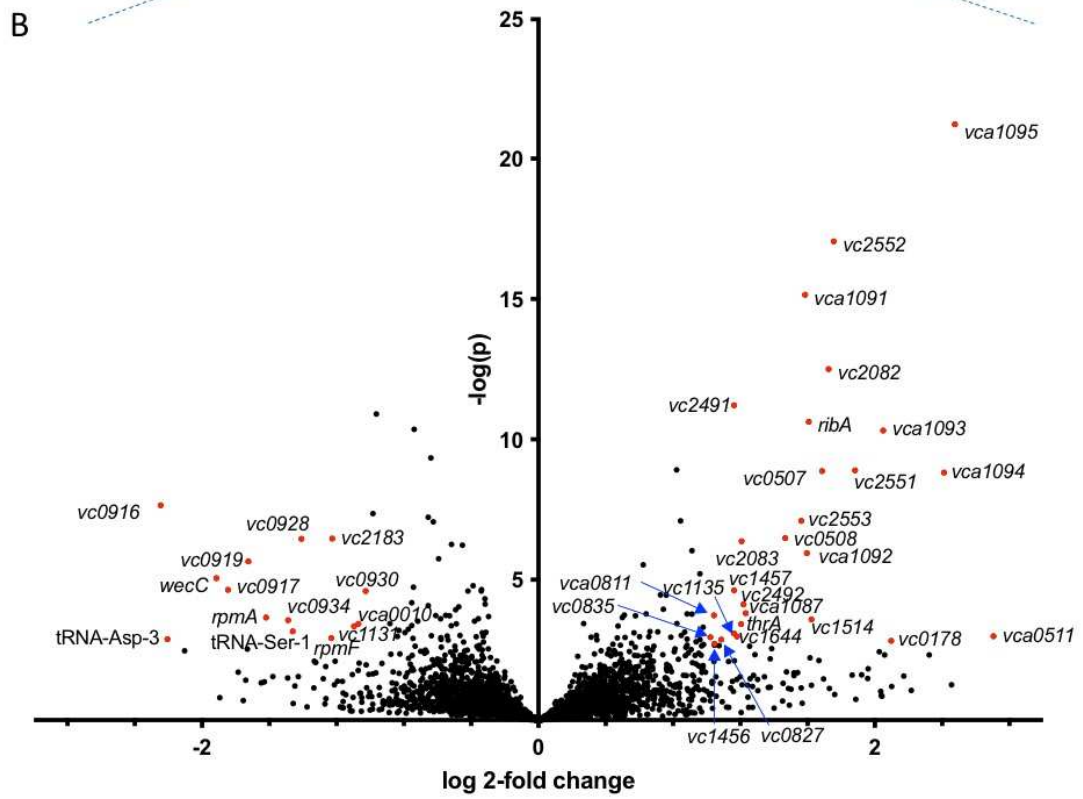
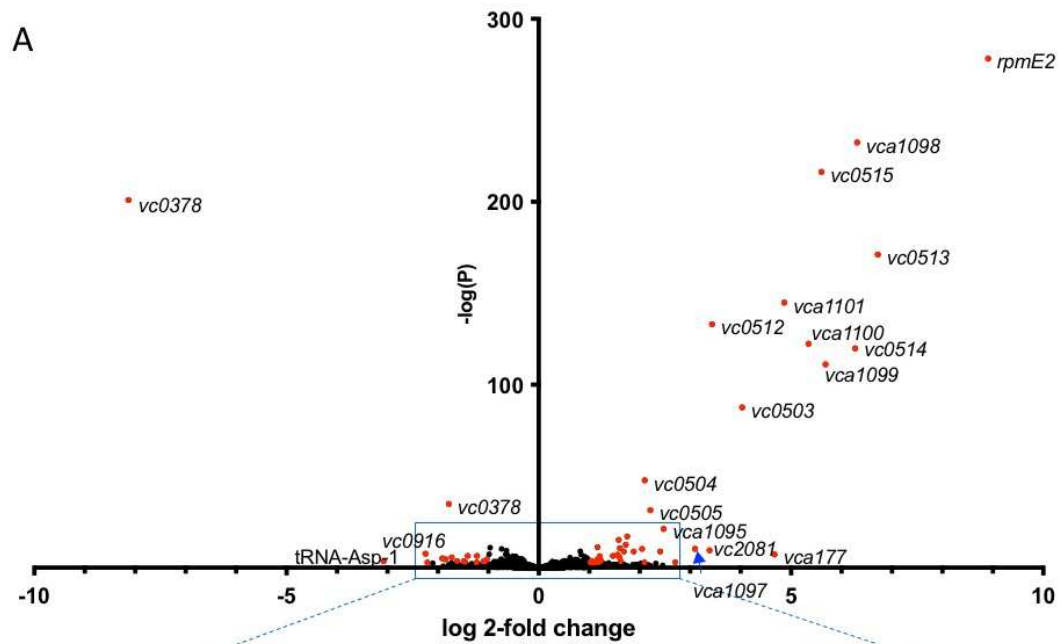


Figure S5. Zur-dependent regulation of the *vca1098* promoter.

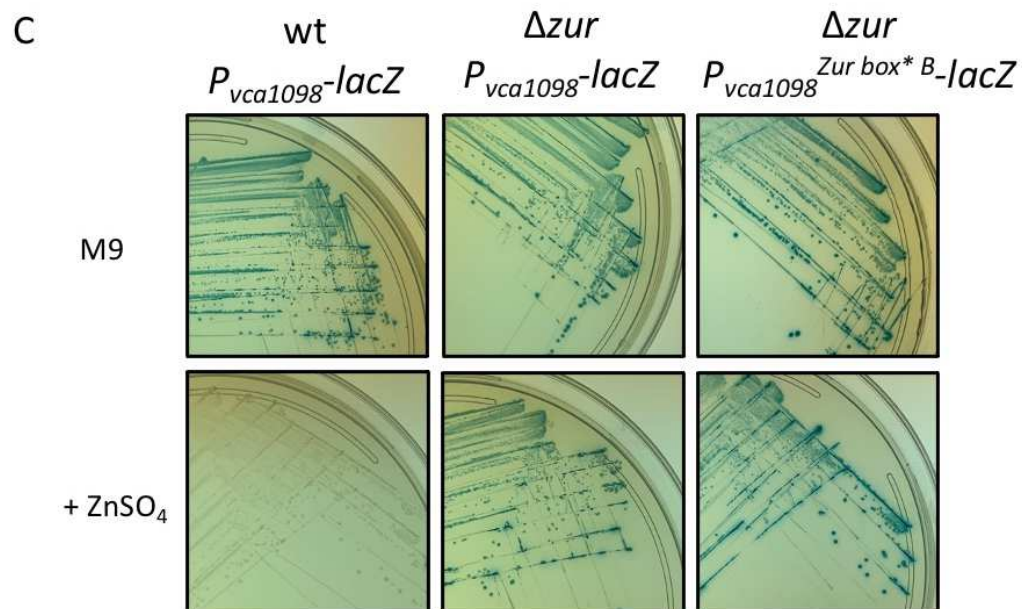
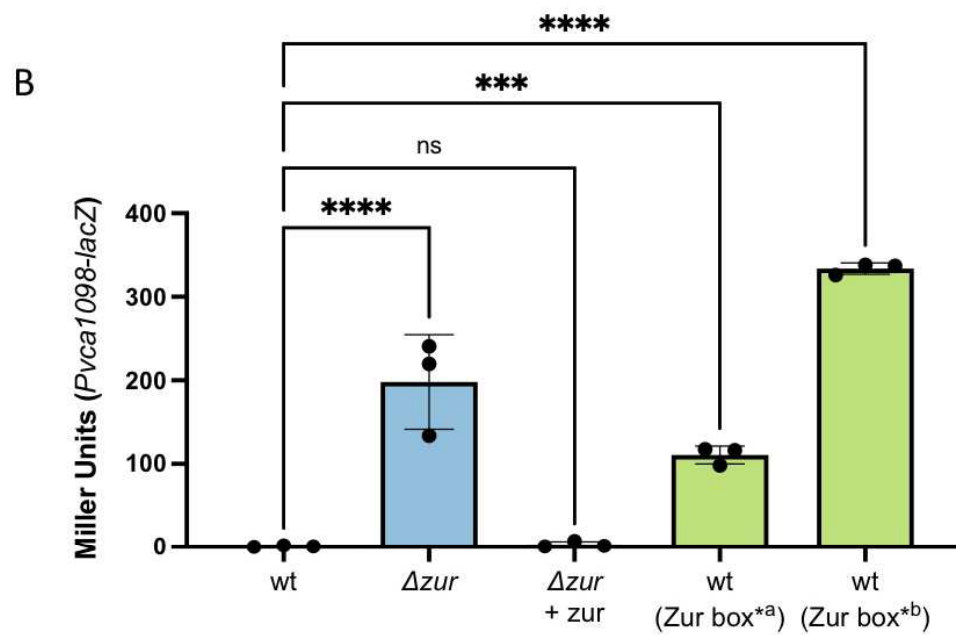
(A) Diagram of the *vca1098* promoter region annotated with the following features: predicted Zur box, red; predicted -10 region, purple (126); transcription start site, +1 (5'-RACE); predicted ribosome binding site (RBS), yellow; proposed start codon (ATG), green. Asterisks indicate Zur box nucleotides (region "a" or "b") that were altered in mutant reporters described below. (B) *vca1098* promoter *lacZ* transcriptional reporters ($P_{vca1098}$ -*lacZ*, solid bars) or mutated versions ($P_{vca1098}^{\text{Zur box}^* \text{ a or b}}$ -*lacZ*, striped bars) were inserted into a wild-type or Δzur background harboring a plasmid-borne, IPTG-inducible copy of *zur* (+) or empty vector control (-). Strains were grown overnight in LB and kanamycin, diluted 1:100 in fresh media containing inducer (IPTG, 400 μM), and grown for 3 hours at 37°C. Promoter activity (in Miller Units) was measured via β -galactosidase assays (See Methods and Materials). (C) Wild-type and Δzur strains carrying $P_{vca1098}$ -*lacZ* or mutant derivatives were streaked onto M9 minimal medium agar with glucose (0.2%), X-gal, and with or without added zinc (ZnSO_4 , 10 μM). Plates were incubated overnight at 30°C and then for an additional day at room temperature. *vca1098* promoter activity is indicated by a blue colony color.

A $P_{vca1098}$

ACACATATAGACATGATTTTTATTCTCATGCTTTAATTAAT **TGTTATGTTATAACA**ATTTTAATTAAGGACATTTTG**ATG**

-10 Zur box RBS Start

↑ a b
+ ** * ***



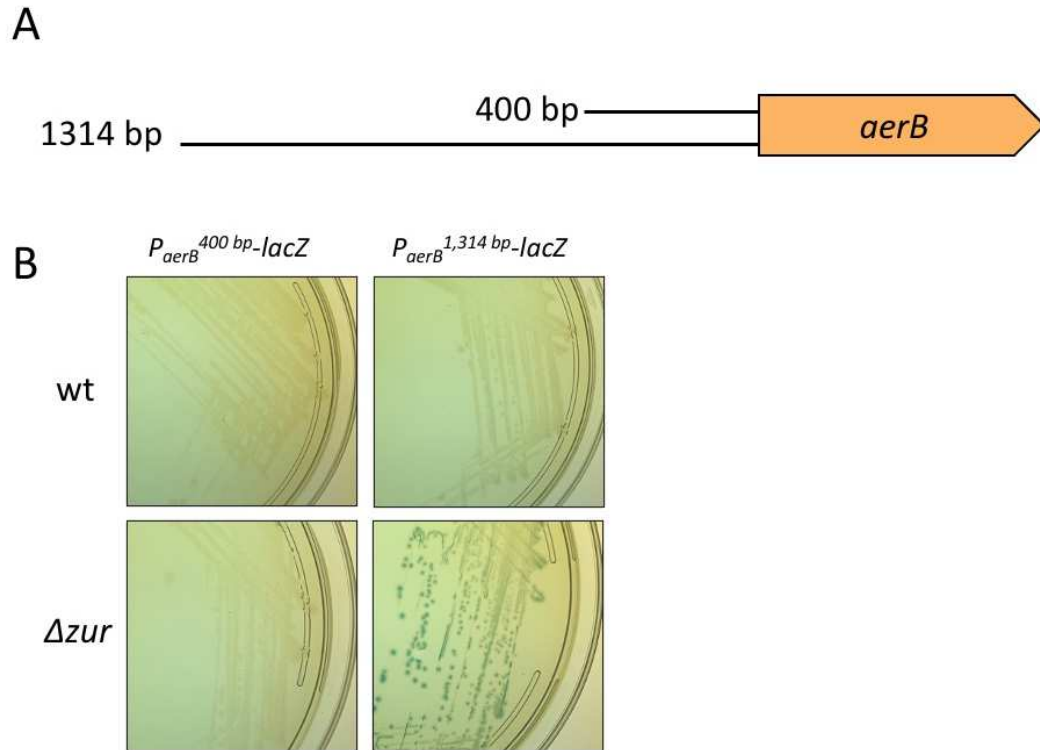


Figure S6. Construction of an *aerB* transcriptional reporter.

(A) Schematics for two attempted $P_{aerB}\text{-lacZ}$ reporters containing either 400 bp or 1,314 bp of the promoter region are shown. (B) The $P_{aerB}^{400 \text{ bp}}\text{-lacZ}$ and $P_{aerB}^{1,314 \text{ bp}}\text{-lacZ}$ reporters in a wild-type or Δzur background were struck onto LB X-gal plates and incubated overnight at 30°C and then for an additional day at room temperature. P_{aerB} expression is indicated by a blue colony color.

Figure S7. AerB protein alignment with homologs from *V. cholerae*, *E. coli*, *A. brasiliensis*, and *S. oneidensis*.

(A) Results of protein BLAST (121) and (B) Clustal Omega alignment (127) of AerB (VC0512) with homologs from *V. cholerae* (AerA/VCA0658), *E. coli* (Aer/B3072), *A. brasiliensis* (AerC/AKM58_23950), and *S. oneidensis* (SO_1385). Conserved ligand binding and MCP residues targeted for mutation are indicated by orange and pink arrows, respectively.

A	Gene	Score	Query cover	E-value	% Identity
	VCA0658 (AerA)	249	98%	7e-80	31%
	B3072 (Aer)	234	90%	2e-74	31%
	AMK58_23950 (AerC)	172	69%	8e-51	33%
	SO_1385	300	91%	3e-100	39%

B

AerC_AMK58_23950	-----	0
Aer_B3072	-----MSSHYPVTOQNTPLADDTLMSSTDLQSVITHANDTFVQVSGYT	44
AerB_VC0512	-----MESIMRKNLFPVTHGHNLELSSSTNLLSTTPDSHITVYVNPDFLKSIGFA	48
AerA_VCA0658	HYTFALIKITLQQAEMSAITPSAQQEVLVGDHDLVSTTDLKGVITVYVNDPTFCRIAGFQ	60
SO_1385	-----MSLS-NPSSRSKITHSNAEIRLTPQDELISSTNTRGITIIVYVQRFVAVSGYS	51
	↓ ↓	
AerC_AMK58_23950	-----MPPAFAANLNETTKDGRPEWGLVKNRSKNGDHYVVKANVTPIITE	44
Aer_B3072	LQELQGGPHNNVRHPDMPKAAFAADMWFTLKKGEFWSGIVKNRRKNGDHYVVRANAVPMVR	104
AerB_VC0512	EDELIGQPHNNVRHPDMPKAAFAADMWSTLKSGRSWMGLVKNRCKNGDHYVWAFAPMFIK	108
AerA_VCA0658	ADELLGKNHNIVRHSAFKAFAADMWHHLKQGHAWRGIVKNRCKSGGFYVVDAYVTPFIYQ	120
SO_1385	ADELIGHNNVRHPDMPKAAFAADMWHLKSGQSWRGIVKNRCKNGDHYVVDAYVSPFIPE	111
	* * * * . : * : * . * * : * * * * * . * . * * * . * : .	
AerC_AMK58_23950	KGVTVEVTSIRSKFSDAVAEAEIRIYAEIRAGRGQQVGLDGGIVRGGVWGLDGLASSI	104
Aer_B3072	EGKISGYSNIFRATDELAAYDEIIPRALNAERTSR-RIRKGL- - -YVRKGLKGLFLP	160
AerB_VC0512	NGKVVEYQSVRTKPEPSHFQAQAEKAYQLRNKKNILPKIRLGFHKLILLVWGLFASIA	168
AerA_VCA0658	QGOLTYQSVRKAERKVEIATKAYQALLAAEKAGKIKQFKLHTSLRYALLGALMSPA	180
SO_1385	NGTIVGYQSVRLQPAAYVSKATAYRKLHNKPIPKLMLQKRAVAVASV-----	164
	: * : * * * : : : * : : : : : :	
AerC_AMK58_23950	AGR-----IVATSGLLLTVMVLGWSLTSQSDSEAFAGLMLFGLLVAGVGTLS-VLGTV	158
Aer_B3072	LWRARGVMTLMFILLAAMLMFAAPVVTY-----ILCALVVL-LASACFEWQI-	208
AerB_VC0512	I-----VSLIYPSALMSILF--LTL-----LVGSITTLGITIYL-	199
AerA_VCA0658	L-----AHGFQAFQEWQ--W--LAS-----LLFA-GVL--GLLFRQELV	212
SO_1385	-----TGLLIGAFIHWG--W--GVT-----IAGA-ILMGLMLAIYDFEAF	198
	: : : :	
AerC_AMK58_23950	RRPLG-LVE-----THLDAIARGDLMTNVPSSGVA--EFARISQIRAVKAKNLSTQ	208
Aer_B3072	VRPIENVAHQALKVATGERNSVEH-----LNRSDDELGLTRAVGQGLMCRWLINDV----	260
AerB_VC0512	LVPKRLIQSYC--KDSNDPLSQVLYTGRSDEFQGL-----EFALRMAQAE-----	244
AerA_VCA0658	RTFQ-QLKQ--W--QNEYDSISRLIYSG-ADAFSVA-----DYHLKMASARI-----	253
SO_1385	RIPA-KLID--H--QTKYDSISRVIYAG-ADTSSL-----DFQLILLQAKM-----	239
	* : : . : : : : : : : : : :	
AerC_AMK58_23950	ERAERQRQAEERITALQSMAEVEREASHAVEQVALRTGGMAQDADAMATSAERVSINA	268
Aer_B3072	-----SSQVSSVRNGSETLA-----KGT	278
AerB_VC0512	-----SAVIGRIDASNQLNKFANDLHNI	269
AerA_VCA0658	-----RTLLGRMDSRPLGELANQLHHT	278
SO_1385	-----NGVLGRTOQDQANQLHAIADQLVVT	264
	: : : :	
AerC_AMK58_23950	QNVAASAEALANAQTVAAATELAASIREISAQIARSSAVTTRRA-----V-----	314
Aer_B3072	DELENTGQVVDVQVFTVATHWQMLAVKQASATASAADELSITASNAAYOGGGA-----	313
AerB_VC0512	EKNILHTEQAEQTEQVATINEMAATQEVATGAKHAANSSESANHITSGQQIVSQAS	329
AerA_VCA0658	QEVHQAQAQNSNIQAVTQATDAVESAERVSSTHSAHLIDQVQDHCAETKHSINVTH	338
SO_1385	BQTYASLDQEKQLEQLASAMEMSSTITEVAQNTQRTSINTAYELCLKSANNKANT	324
	: : : : : : : : : : : : : : : : :	
	↓	
AerC_AMK58_23950	-----ENGRTQGTIQSLSEAVGRIDEVVKLITDIASQTNLLALNATIEAARAGEAGK	367
Aer_B3072	-----MTTVIKTMDIADSTQRIGTITSLINDIAFQTNLLALNAEVAARAGEQGG	384
AerB_VC0512	QSTIELEHEVSQAKVHEHEEHSNDLSKVLVETRSIADQTNLLALNAEVAARAGEQGR	389
AerA_VCA0658	QNLQRLTAQASAAITLKLSDQAQVGLMTEIGGIAEQTNLLALNAEVAARAGEQGR	398
SO_1385	QKVEQLARVADAANANLLNQEAEERVASAMGEIDSTIAEQTNLLALNAEVAARAGEQGR	384
	. : : : : : * * * * * : : : : : * * * * * : : : : : * * * * * : :	
AerC_AMK58_23950	GFAVVAQEVKNLANQTSARSTEEITRLLAIEIQGVTSVAVGAVA-----	409
Aer_B3072	GFAVVAQEVRLASRSANAANDIRKLDASADKVSQSGQVHA-----AGR	430
AerB_VC0512	GFAVVAQEVRLAARTQQTMDIQRMDLQGRKLAVALVHEHSSQALLSVEQAQQAAD	449
AerA_VCA0658	GFAVVAQEVRLASRTQATQQTQTSIDTMLSTIEMRGDITASRDTQEQCAQDANTTLQ	458
SO_1385	GFAVVAQEVRLASRTQLSTNSISQVDMFSLMNAKEMEQSRQHAERCANDIQTSAE	444
	***** * * : : : : : * * : : : : : : : : * * * * * : : : : : * * * * * : :	
AerC_AMK58_23950	---EIGDTIGEIDQISSAIAAMEEQAAATQEIIRNVVETSNAQEVSVRIAAVSSDADQ	466
Aer_B3072	TMEDIQVQKNTVQLAQISHSLETLQADGLSSLTRADELMLITQKMAELV-----EE	483
AerB_VC0512	ALTGIGKRVSDITGMSVQMATAVDQSAVSDSEINHSISNIRMAADTVDNG-----KI	502
AerA_VCA0658	QLQDQVMSDMLRIVGEVASAAQHQRELTCEVNHQHSIASVATQNSAAT-----HT	511
SO_1385	NVNTIYQVSEIHTFAQNAVAADQROVVHEITNNIHFITQSSSENLAAT-----HQ	497
	: : : : . : : : * : : : : : : : : : : :	
AerC_AMK58_23950	TGSQASGVRRAGSDEVATSIDELRRVLVRYVVRTSTSDADRRRSRPRYRNEACGVVHGRDQ	526
Aer_B3072	SAQVSAVY----KIRASRLSDAVTILH-----	506
AerB_VC0512	NAKCAEGVY----AGLSNLSLQAGQFWRNK-----	529
AerA_VCA0658	VEQLAMAY----SGKVAEFGALSKQFAGK-----	536
SO_1385	IGDAANHL----KNAERKALGLRRAFQ-----	520
	. : : : : : :	
AerC_AMK58_23950	SGTLTDLSSNGGAMLSGIAGLVGDRGLRLDRFGLTVAFEVRAIDKTAIHVRFAESDVAL	586
Aer_B3072	-----	506
AerB_VC0512	-----	529
AerA_VCA0658	-----	536
SO_1385	-----	520

AerC_AMK58_23950	PRFRDFAQLTRGLQPVATAAA	608
Aer_B3072	-----	506
AerB_VC0512	-----	529
AerA_VCA0658	-----	536
SO_1385	-----	520

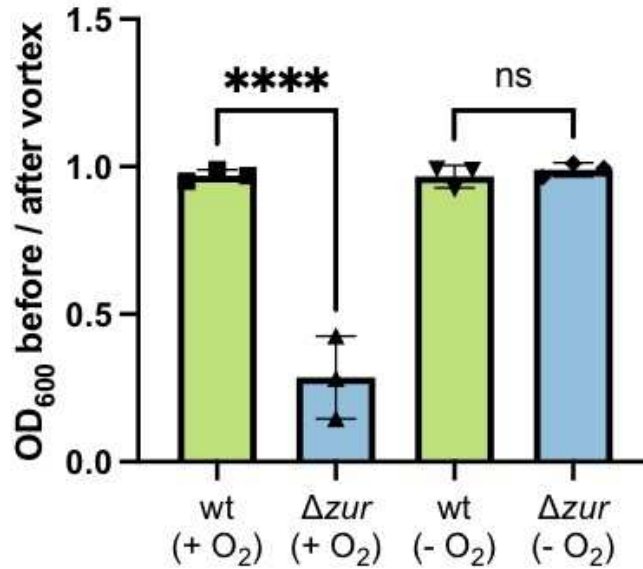


Figure S8. *V. cholerae* Δzur congregation requires oxygen.

Wild-type and Δzur were grown overnight in 5 mL M9 minimal medium plus glucose (0.5%) fermentatively (without a terminal electron acceptor) and cultured under aerobic (+ O₂) or anoxic (- O₂) conditions (see Methods for details). Tubes were grown shaking overnight at 30°C and congregation was quantified via spectrophotometry as described previously. All data points represent biological replicates, error bars represent standard deviation, and asterisks denote statistical difference via Ordinary one-way ANOVA test (****, $p < 0.0001$; n.s., not significant).

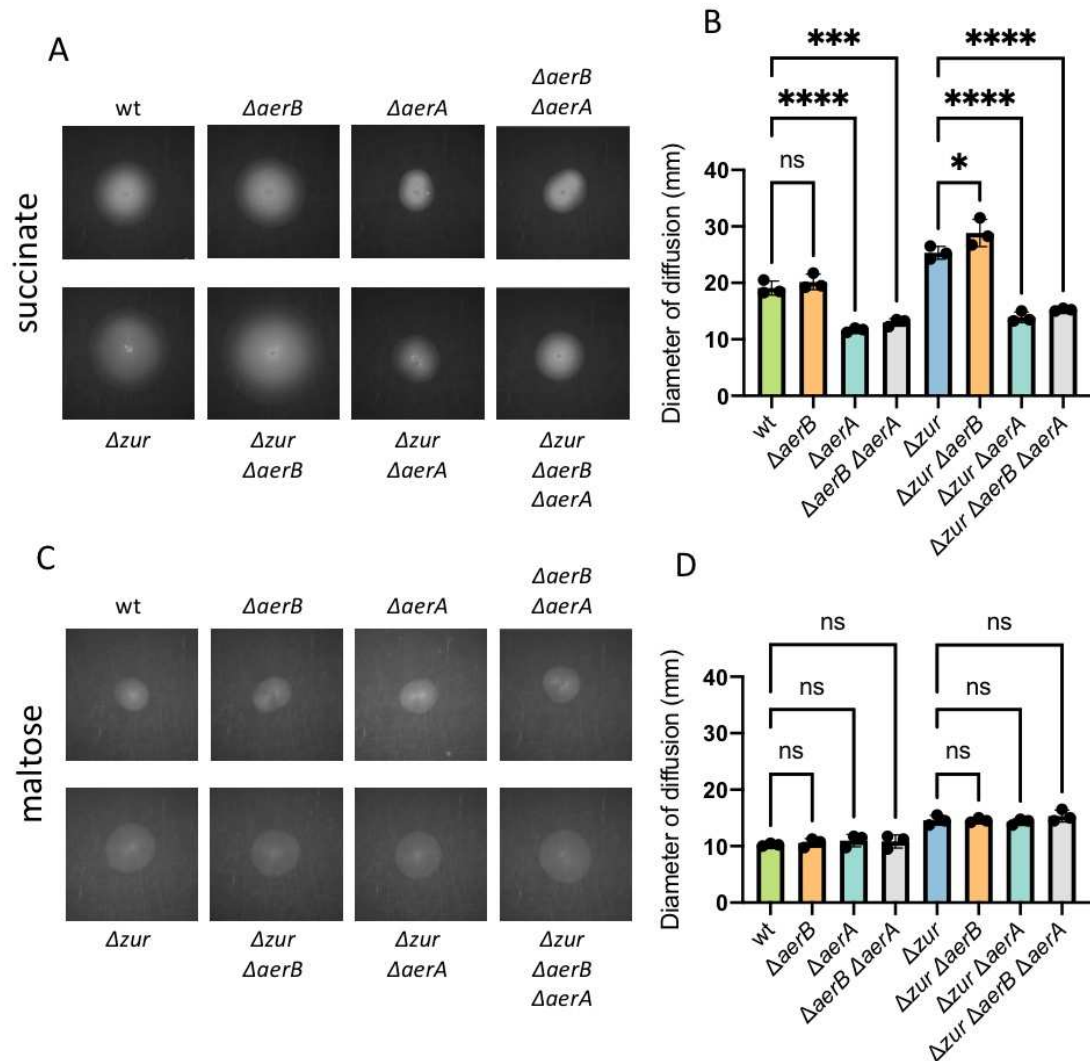


Figure S9. *V. cholerae* swarm assays with chemoreceptor mutants.

(A-D) The indicated strains were grown overnight in LB medium and washed thrice in M9 minimal medium lacking a carbon source. A sterile toothpick was used to inoculate cells into M9 soft agar (0.3%) with either (A-B) succinate (30 mM) or (C-D) maltose (0.1 mM) as a carbon source. The diameter of diffusion (mm) was measured following a 48-h incubation at 30°C and representative swarms are shown (A,C). Note: Data for $\Delta z u r$, $\Delta z u r \Delta a e r B$, $\Delta z u r \Delta a e r A$, and $\Delta z u r \Delta a e r A \Delta a e r B$ are the same as shown in Fig. 5 and are shown here for comparison with a wild-type background. All data points represent biological replicates, error bars represent standard deviation, and asterisks denote statistical difference via Ordinary one-way ANOVA test (****, $p < 0.0001$; ***, $p < 0.001$, *, $p < 0.05$, and n.s., not significant).

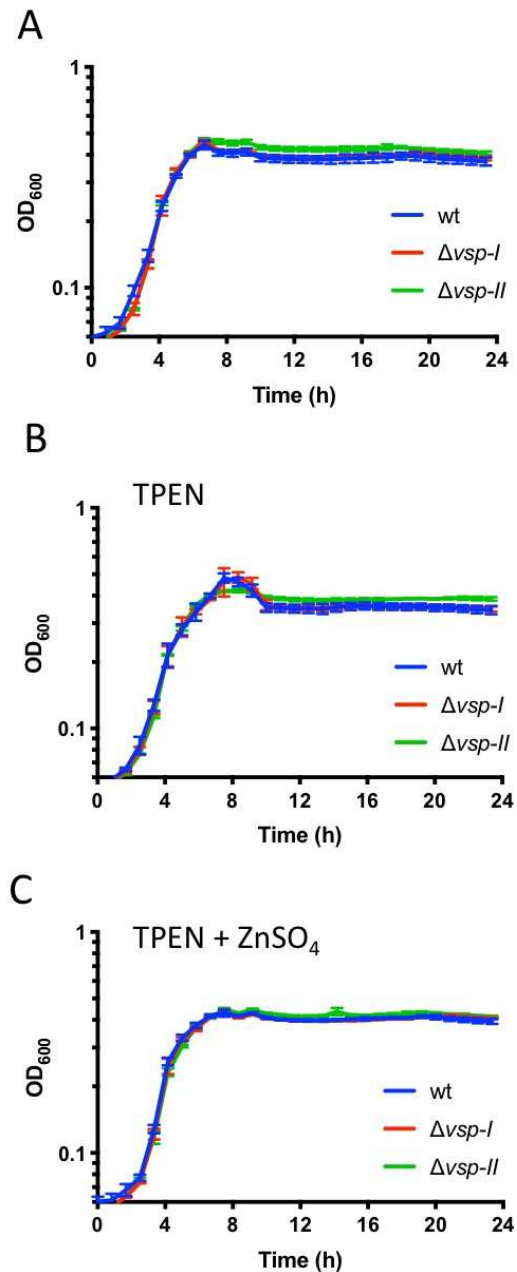


Figure S10. Presence of VSP islands does not impact growth in zinc-chelated medium.

Wild-type, $\Delta vsp-I$, and $\Delta vsp-II$ were grown overnight in M9 minimal medium with glucose (0.2%) at 30°C. Cultures were washed twice and diluted 1:100 into (A) fresh M9 minimal medium glucose (0.2%), (B) plus the zinc-specific chelator TPEN (250 nM), or (C) plus TPEN and exogenous zinc ($ZnSO_4$, 1 μM). Growth at 30°C of each 200- μl culture in a 100-well plate was monitored by optical density at 600 nm (OD_{600}) on a Bioscreen C plate reader (Growth Curves America).

Chapter 4. Concluding Remarks and Future Directions

CONCLUDING REMARKS

Vibrio cholerae's VSP-II island, a mysterious genomic element that is associated with the seventh cholera pandemic, largely evaded characterization due to a lack of knowledge of the stimuli that favor its expression. In this work, we discover that many VSP-II genes are regulated by the Zur-dependent zinc starvation response. These novel Zur targets were initially identified via mutagenic screens seeking to explain two, unusual observations: (a) medium-dependent transcription of a cell wall hydrolase and (b) congregation of the *zur* mutant in liquid culture. Characterizations of these Zur-regulated, island-encoded genes lend insight into El Tor's unique adaptations to zinc-starved environments.

In chapter 2, we found that the cell wall endopeptidase, ShyB, retains activity in the presence of metal chelators *in vitro*. This finding is congruent the idea that seemingly redundant cell wall enzymes may actually function as “specialists” that maintain cell wall integrity under a specific set of growth conditions (i.e. during metal limitation) (1). Using bioinformatics, we predicted that Zur-regulated cell wall enzymes may be present in other Gram-negative bacteria; indeed, others have reported similar findings in the human pathogen *Acinetobacter baumannii* (2) and the plant pathogen *Erwinia amylovora* (3). In both cases, these Zur-regulated peptidases enhanced bacterial virulence within their respective hosts, suggesting a role for specialized cell wall hydrolases during pathogenesis.

In chapter 3, we characterized the Zur-regulated VerA, which activates transcription of other VSP-II encoded genes and thereby expands the regulatory effects of Zur. One of VerA's targets, AerB, is an energy-sensing receptor that mediates cell

congregation and oxygen-dependent chemotaxis. These results raise the intriguing possibility that this VSP-II component allows El Tor to escape redox stress in zinc-starved environments.

Taken together, the presence of zinc starvation genes on VSP-II implies that this island may enhance bacterial fitness in low-zinc environments. Such contributions appear to be more complex than facilitating growth in zinc-starved media and may instead alter movement within zinc-starved microenvironments (in the case of VerA/AerB) or provide benefit under a combination of environmental stresses (in the case of ShyB). Future endeavors, discussed below, will continue to explore the function of VSP-II in order to understand its presence in the El Tor seventh pandemic strain.

FUTURE DIRECTIONS

We discovered segments of VSP-II that are novel components of the Zur-regulated zinc starvation response. These findings suggest a role for VSP-II in zinc-starved environments; however, we have not yet assessed the role of these island components in a zinc-limited vertebrate host. Future work will measure fitness of VSP-II mutants in a mouse infection model to determine the island's contributions to host colonization and pathogenicity.

Additionally, the stimuli that favor expression of the other VSP-II genes remain unknown. Future exploratory efforts will attempt to identify such regulators via transcriptional reporters and genetic screens (e.g., transposon mutagenesis to identify repressors, open reading frame overexpression systems to identify activators). A more comprehensive understanding of how VSP-II is genetically regulated may advance our understanding of VSP-II as either a pathogenicity or environmental persistence island.

REFERENCES

1. **Mueller EA, Levin PA, Garsin DA.** 2020. Bacterial Cell Wall Quality Control during Environmental Stress. *mBio* **11**:59.
2. **Lonergan ZR, Nairn BL, Wang J, Hsu Y-P, Hesse LE, Beavers WN, Chazin WJ, Trinidad JC, VanNieuwenhze MS, Giedroc DP, Skaar EP.** 2019. An *Acinetobacter baumannii*, Zinc-Regulated Peptidase Maintains Cell Wall Integrity during Immune-Mediated Nutrient Sequestration. *Cell Reports* **26**:2009–2018.e6.
3. **Roshni R Kharadi GWS.** 2020. Cyclic-di-GMP Regulates Autoaggregation Through the Putative Peptidoglycan Hydrolase, EagA, and Regulates Transcription of the *znuABC* Zinc Uptake Gene Cluster in *Erwinia amylovora*. *Front Microbiol* **11**:5867.